# ROLL FORCE, TORQUE AND SPREAD IN HOT ROLLING STEEL BARS FROM SQUARE TO DIAMOND CROSS SECTION

by

AMIR NASSER SOURESRAFIL

M.Sc.

A Thesis submitted for the Degree
of Doctor of Philosophy in the
University of London

and

The Diploma of Imperial College

July 1970

## ACKNOWLEDGEMENTS

The author wishes to express his sincere thanks to Professor J. M. Alexander for his guidance and much helpful advice throughout the work. He acknowledges the technical assistance given by the staff of the Metal Working Laboratory, in particular Mr. Jack H. Pooley, Chief Technician, for his assistance in the experimental work.

The author is grateful to British Iron and Steel Research Institute for providing the specimen material and the Ministry of Overseas Development for awarding the fellowship that enabled him to carry out this work.

# LIST of CONTENTS

| | | Page |
|---|---|---|
| | Title | 1 |
| | Acknowledgements | 2 |
| | List of Contents | 3 |
| | List of symbols | 7 |
| | Abstact | 8 |
| | CHAPTER 1 | |
| | Introduction | 10 |
| | CHAPTER 2 INSTRUMENTATION | |
| 2.1.1 | Rolling Mill | 14 |
| 2.1.2 | The Rolls | 14 |
| 2.1.3 | Guides | 15 |
| 2.2 | The Heating Furnace | 16 |
| 2.3 | Measuring Equipment | 16 |
| 2.3.1 | load Measurement | 17 |
| 2.3.2 | Roll Torque Measurement | 18 |
| 2.3.3 | Ultra Violet Recorder | 18 |
| 2.3.4 | The Electrical Circuits | 19 |
| 2.3.5 | Length Measuring Instrument | 20 |
| 2.4 | Specimen Material | 20 |
| | CHAPTER 3 EXPERIMENTAL METHOD | |
| 3.1 | Introduction | 21 |
| 3.2 | Length Measurements | 22 |
| 3.3.1 | Load and Torque Measurements | 25 |
| 3.3.2 | Load Cell Calibration | 25 |

3.3.2 Torque Cell Calibration 26

3.4.1 Scale Control 27

3.4.2 Control of the Furnace Atmosphere 28

3.4.3 Temperature at the Box Interior 31

3.5.1 Temperature of Rolling 31

3.5.2 Electrical Circuit for Cooling Curves 34

3.5.3 Experimental Cooling Curves 36

3.5.4 Theoretical Cooling Curves 37

3.5.5 Heat Loss to the Rolls 40

3.6 Summary and Conclusions 44

CHAPTER FOUR

SPREAD CALCULATIONS IN SQUARE-DIAMOND PASS

4.1 Introduction 46

4.2 Some Early Spread Formulae for Flat Rolling 47

4.2.1 Siebel's Formula 47

4.2.2 Ekelund's Formula 48

4.3 Recent Formulae of Spread 49

4.3.1 Wusatowski's Formula 49

4.3.2 Hill's Formula 50

4.3.3 Sparling's Formula 52

4.3.4 Tselikov's Formula 52

4.4 Spread in Square Diamond Pass 55

4.4.1 Observations on Surface Deformation of the Square Bars in Diamond Pass 57

| | | Page |
|---|---|---|
| 4.4.2 | Interior Deformation of the Square Bar Diagonal | 59 |
| 4.5.1 | New Spread Formula | 60 |
| 4.5.2 | Some Comments on the New Spread Formula | 64 |
| 4.5.3 | Comparison with the Experimental Results | 65 |
| 4.5.4 | Draft vs. Spread Measurements | 66 |
| 4.6.1 | Prediction of the Correct Size of the Bar to Fill the Pass Geometry | 68 |
| 4.6.2 | Small Variations of Diamond Angle $\alpha$ | 70 |
| 4.7.1 | Effective Reduction of the Pass | 70 |
| 4.8.1 | Reduction vs. Draft, Experimental Verification of New Spread Formula | 72 |
| 4.9.1 | Summary and Conclusions | 81 |
| 4.10 | Sample Calculations | 82 |

CHAPTER FIVE

ROLL FORCE AND TORQUE CALCULATIONS

| | | |
|---|---|---|
| 5.1 | Introduction and Background | 85 |
| 5.2 | General Analysis | 92 |
| 5.3.1 | New Load Formula | 96 |
| 5.3.2 | New Torque Formula | 98 |
| 5.3.3 | Strain Rate Formula | 100 |
| 5.3.4 | Yield Stress in Compression | 103 |
| 5.4 | Experimental Data | 105 |
| 5.5 | General Note | 107 |

6. APPENDIX 108

I Computor Program for Calculation of Elongation

II Computor Program for Calculation of Non-Linear Differential Equation of the Thermal Cooling

7. References 120

8. Drawings and Figures 126

9. Experimental Data for Spread 180

10. Experimental Data for Load and Torque 193

## LIST of SYMBOLS

| | |
|---|---|
| $G$ | Roll Torque per Unit Width for Both Rolls |
| $G_t$ | Total Measured Roll Torque for Both Rolls |
| $H_1$ | Square Bar Diagonal Length, Perpendicular to the the Rolls Axis, at Entry to Pass |
| $H_2$ | Square Bar Diagonal at Exit from Pass |
| $k$ | Shear Yield Stress |
| $k$ | Mean Shear Yield Stress in the Pass |
| $\mathbb{L}_o$ | Length of Arc of Contact |
| $P$ | Roll Force per Unit Width |
| $r$ | Pass Reduction $\frac{H_1-H_2}{H_1}$ |
| $R$ | Roll Radius at the $120^o$ Corner in the Diamond Pass |
| $R_m$ | Average Roll Radius of the Diamond Pass |
| $S$ | Spread $W_2-W_1$ |
| $S_x$ | Spread at Distance x fom Plane of Entry |
| $V_n$ | Peripheral Speed of the Rolls |
| $W_1$ | Squre Bar Diagonal Length, Parallel to the Rolls Axis, at Entry to Pass |
| $W_2$ | Square Bar Diagonal at Exit from Pass |
| $\delta$ | Draft $H_1-H_2$ |
| $\delta_x$ | Draft at Distance x from Plane of Entry |
| $\bar{\lambda}$ | Average Strain Rate in the Flat Rolling |
| $\bar{\lambda}_m$ | Average Strain Rate in the Diamond Pass |

# ABSTRACT

A series of experiments have been carried out for prediction of load, torque and spread in square diamond rolling process. More than 250 bars of different size 1/4, 3/8, 1/2 and 5/8 have been rolled in diamond passes, in a 4" diameter roll, under carefully controlled conditions of scale free surface and uniform temperature. A new formula has been found for diagonal spread of square bars in diamond pass. The formula is in good agreement with the experimental data. Using this formula, the calculations of the following quantities have been made possible.

a) The correct size of a square bar to fill a given dimensional pass

b) The correct dimensions of a diamond pass for a given bar size, so that no overfilling or underfilling occurs in the pass.

c) Total reduction of the pass.

In contrast to previous methods of applying flat rolling spread formulae for calculations of spread in square diamond rolling, the new formula is applied directly and is simple to use.

J. M. Alexander and H. Ford Flat rolling formula based on the slip line field solution is modified and adopted for predictions of load and torque in square diamond rolling. The new formula is equally simple to apply. This formula, used in conjunction with the Cook-McRum data for shear yield stress in plane strain, shows good agreement with the experimental data.

# CHAPTER ONE

## INTRODUCTION

The early history of the use of the rolling mill to impart mechanical work is not known. It is possible that rolling mills have their origin in ancient mills which were used for extracting sugar from sugar canes. Ox-driven mills were used in Egypt for this purpose, the rolls for this application being made from wood.

The first drawings of a rolling mill for metal working were made by the famous artist and engineer, Leonardo da Vinci, in 1498. It is reported that he rolled flat sheets of precious metal on a hand-operated two-roll mill (FIG. 1.1). In England John Payne was the first to be granted a patent in 1728 for a rolling mill in which the two rolls were to be grooved (FIG 1.2), but it is not known whether this mill was ever built. In 1783 Henry Cort made one of the basic advances in the history of section rolling, he introduced grooved "cogging" rolls and eliminated all hammering at that stage. The cogged bar was then re-rolled to a suitable section between further grooved rolls. This was the foundation of modern methods of section rolling and since then much thought and ingenuity has been given to the construction of more efficient rolling mills.

Today, with the ever-increasing demand for different sections, one of the chief departments of any modern steel plant is the rolling department. Almost all the steel that is produced in the steel making department passes through the rolling department, only a small portion being used for making castings and forgings.

Tremendous advances in the engineering field coupled with the development of powerful drives, high speed reversing mills plus a whole system of mechanised and automated controls and many other features, has availed the mass production of sections by the rolling process. With the use of these expensive experiments and the desire for high yield and low cost per ton on a highly accurate product, it is important to have the best pass design, and to have a thorough knowledge of the effect of various factors in the rolling mechanics.

The early development of the rolling mill was based on individual experience and craft. No analytical frame existed from which to draw any conclusions. The analytical approach starts with the pioneer work of Siebel, Von Karman, and Ekelund in the early 1920's. Since then various investigators have put forward different approaches to the mechanics of the flat rolling process. From the existing literature an accurate prediction of the load and power in flat rolling is possible under a variety of working conditions; cold rolling with and without lubricants, hot rolling, rolling with back tension, with rough or smooth rolls and so on. From all this, conclusions may be drawn for general questions of rolling mill operation and design, for example:

What size roll diameter is optimal for certain bloom or billet size? What effects may application of lubricants have on the power consumption? Is it wrothwhile to attempt a reduction in friction? In a given case of rolling what reduction is preferable? And so on.

At present, the mechanics of rolling flat material is well explored and the general effect of the different factors is quite predictable by theoretical as well as experimental relations. Section rolling, on the other hand, has not lent itself to complete theoretical and experimental analysis. Some attempts have been made to apply flat rolling theories but the results are not always conclusive.

In this work one particular geometry of section rolling, namely square-diamond, has been investigated. This is one type of breakdown pass commonly used for rolling stock of comparatively small cross section. A typical sequence of square-diamond and diamond-square reduces a square section to a smaller square size. The initial square section is rolled into a diamond geometry with some reduction in area, then the diamond is turned through $90^{\circ}$ and rolled onto a square pass, which reduces it to a smaller square. With this type of pass geometrically accurate square sections are obtained, and it is also good for the mechanical properties of the steel to be worked from all four sides. The common temperature range used in hot rolling steel, from $900^{\circ}C$ to $1200^{\circ}C$, is covered in this investigation. Square bars, size 1/4", 3/8", 1/2" and 5/8", are rolled in diamond passes cut in 4" diameter rolls for about 30% area reduction. Load, torque and spread have all been found predictable by simple and easy formula.

# CHAPTER TWO

## INSTRUMENTATION AND EQUIPMENT

This chapter and chapter three are concerned with the instrumentation and the experimental method. These are basic to a better understanding of the chapters four and five, which deal with calculations of spread, load and torque. A brief description of the instruments used in the experiments will be given here.

### 2.1.1 Rolling Mill

This is a small two high rolling mill, manufactured by W.H.A. Robertson and Sons Ltd. A constant speed D.C. motor, 7 b.h.p. at 1500 r.p.m., provides the power source. The power is transmitted through a pinion box with a 50 to 1 reduction ratio, with 4" diameter rolls. This gives a peripheral roll speed of 30 ft/min. A screw down mechanism can raise the upper roll to a maximum of 0.5 inch roll gap.

### 2.1.2 The Rolls

The rolls are made of EN25 steel hardened and tempered to condition X. The barrel length is 6", with necks fitted with needle bearings and the square ends coupled with drive spindles. Fig. (2.1) shows the general dimensions of the rolls.

Five diamond passes, $120^{\circ}$, are cut in the rolls in which five different size square bars, 1/4", 5/16", 3/8", 1/2" and 5/8", were rolled. Thus a wide range of roll radius to stock size ratio is obtained. This ratio is one of the parameters affecting the spread. Fig. (2.2) shows the dimensions of the pass. See (3) and (16) for design considerations.

### 2.1.3 Guide

For correct guidance of the bars into the pass and preventing the bars from being overturned, a guide as shown in Fig. (2.3) was made and installed on the mill in front of the rolls. Since the guide was adjustable, the centres of the openings in the guide could be lined up with the centres of the corresponding diamond passes. In this way the bars were correctly entered into the pass; in fact very few bars were overturned.

## 2.2 The Heating Furnace

The heating furnace was a 5 K.w. electric box furnace manufactured by Gallenkamp. The maximum operating temperature of the furnace is 1500° and the temperature was continually shown by an indicator. The heating elements were arranged in both sides of the furnace to provide uniform heating. The furnace temperature could be preset and automatically maintained at the desired level. Since the samples were heated in a protective atmosphere in a stainless steel box inside the furnace, alumel-chromel thermocouples were inserted inside the stainless steel box and the voltage was read on a digital voltmeter to 0.01 millivolt accuracy. In this way the temperature of the furnace and the box interior were continually monirored Fig. (2.6).

## 2.3 Measuring Equipment

Experimental data is obtained through measurement of the different parameters of the process. The instruments and techniques used in measurement are very important if the correct conclusions are to be drawn from the data. In this series of experiments, measurements of load, torque, spread and elongation of the rolled bar were necessary. A description of the instruments used for these measurements will be given here.

### 2.3.1 Load Measurement

The separating force on the rolls was measured by two cylindrical load cells, positioned between the upper roll chocks and screw downs of the mill. They were secured in place by fitting circular bumps on the chocks into circular recesses in the bottoms of the load cells. The load cells were designed and manufactured by "Industrial Transducers Ltd". They are of the same general principle described by R.B. Sims (17). The four $2000\,\Omega$ strain gauges are fixed to the surface of the cylinder and connected to form a temperature compensating wheatstone bridge, the gauges also being protected from humidity by a sealing compound. Loading of the cells produces an out-of-balance current across the bridge. This out-of balance current is calibrated for the applied load, the calibration curves being given in the next chapter. The out-of-balance current was directly fed into one channel of a multi channel ultra violet recorder, and the deflection of the galvanometer beam was calibrated for the loads.

### 2.3.2 Roll Torque Measurement

The torque was measured by the common method discussed by R.B. Sims (18). Four 2000 $\Omega$ strain gauges are mounted on opposite sides of the driving spindle at $45^{\circ}$ to the axis and connected to form a self compensating wheatstone bridge. This arrangement ensures that the bridge would not be affected by either axial thrust or bending, as gauges on opposite sides cancel out these effects. The bridge, therefore, can only be affected by the applied torque. The supply voltage was fed to the bridge by insulated brass slip rings through flexible pick-up copper wires. The copper wires were extended over the slip rings and connected to tension springs at each end for better contact and flexibility.

### 2.3.3 Ultra Violet Recorder

The out-of-balance currents from the load and torque cells were fed into a ten channel ultra violet recorder, manufactured by Southern Instruments Ltd. Four channels having SMI/Y galvanometers were used to make the load and torque recordings (two channels for the upper and lower spindle torque cells, and two chanels for the left and right load cells). Galvanometers have a sensitivity of 0.0007 mA/cm and were also manufactured by Southern Instruments Ltd. The ultra violet light beam reflected from galvanometer mirror makes recordings of the mirror deflections on an oscilloscript paper, which unrolls at a constant speed. The recorder had a 150 mm. full deflection scale Fig. (2.6).

By changing the bridge voltage, the out-of-balance output could be varied, and consequently, the galvanometer deflection. This arrangement provides a choice of different sensitivities. In fact 8, 10 and 12 volts were chosen as the bridge input voltages. The recorder had twelve recording speeds, ranging from 0.15 inch/sec to 100 in/sec. The normal speed used in load and torque recordings was 0.5 in/sec.

### 2.3.4 The Electrical Circuits

Electrical circuits for load and torque cells are shown on Fig. (2.4) and Fig. (2.5). The circuits are typical bridge circuits. Two variable resistances, 10 K$\Omega$ and 100 K$\Omega$ are used for coarse and fine adjustments of the bridge. Initially, the bridge is balanced and no current flows through the galvanometers in the recorder. A microammeter indicates any current passing to the galvanometer. The power source was a stabilised power pack manufactured by Weir. Electronics Ltd. All the four circuits (two load cells and two torque cells) were fed from the same power source.

### 2.3.5 Length Measuring Instruments

Length measurements were made by a Universal measuring machine, manufactured by Société Génévoise d'Instruments de Physique. The highest accuracy of this machine, guaranteed by the manufacturer, is 0.00004 inch, which is suitable for most laboratory purposes. This machine has been described in a research note by J. M. Alexander and R. C. Brewer (14).

## 2.4 Specimen Material

The material used in the experiments was low carbon bright draw mild steel of the following composition:
C = 0.14%, Mn = 0.55%, Si = 0.132%, P = 0.010%, S = 0.055%
The steel bars were not of the same cast, but a chemical analysis of the fifteen random samples showed a 0.0025% standard deviation for carbon content and 0.003% standard deviation for magnesium content.

# CHAPTER THREE

# EXPERIMENTAL METHOD

## 3.1 Introduction

Every experimental investigation in science and engineering consists of careful observation of the obtained data, for conclusion of useful results, or confirmation of preconceived theories. Thus the basic part of the whole process is the data. If the data is not conclusive, naturally no useful conclusions can be drawn, or if the data is not accurate, erroneous conclusions may render the investigations irrelevant and useless. Sufficiently conclusive or accurate data is not always easy to obtain. There are usually sources of error, some of which may not be possible to eliminate entirely, or the instrumentation may not have adequate accuracy.

For the current investigations, the instrumentation was discussed briefly in the previous chapter. These instruments were used to measure the following quantities as data: dimensions of the deformed bar after rolling, load, and torque. In the following sections the technique and method for making these measurements are discussed. The two main sources of scatter, which may well render the data inconclusive, are surface scale variations and temperature variations.

Since the experiments involved rolling different sizes of square bars in their corresponding passes, it was expected that there would be a more rapid rate of cooling for the smaller bars with a larger temperature drop for the same duration of rolling test. On the other hand since the experiments covered 900°C, 1000°C, 1100°C and 1200°C temperature ranges, scale variations were also expected. These two error-introducing factors were controlled as will be discussed in this chapter.

## 3.2 Length Measurements

The length measurements in the experiments consisted of:

(a) Measurements of gauge lengths along the bar before and after rolling, in order to determine the amount of elongation.

(b) Measurement of each bar's diagonals, before and after rolling, in order to measure draft and spread of the diagonal lengths.

As for part (a), the Universal measuring Instrument described in Chapter two, section 2.3.5 was used for all the measurements.

Impressing the gauge length marking on the bar was made by two different methods.

First a 1/8 inch thick jig plate with guide holes at 1", 2", 3" and 4" spacing was used, to provide a uniform pattern of markings. Markings were impressed by a 1/8" cylindrical centre punch with a conical end. The centre punch was guided through the holes in the jig plate and care was taken to have uniform markings However, the centre punch markings were somewhat deformed in the rolling process, as they were squeezed under the rolls. This method introduced some error in the elongation measurements and calculations. A second method was found to give better results with less error and subsequently adopted for all the markings. The square bars were turned in a lathe and the markings were cut on the four corners of the square bars at 1", 2", 3" and 4" spacings. The cuts were effected by a sharp V-shaped tool. Forward advancement of the tool, that is towards the centre of the bar, was set at 0.010".

The tool's travel, that is along the bar length, was controlled at 1", 2", 3" and 4" standard stops. With this method two of the markings, namely those on the diagonal plane parallel to the roll axis, will remain undisturbed but slightly elongated. This elongation does not change the general V shape of the marking. In some tests, the bars after rolling were slightly curved to one side and in those cases the average measurement of both sides was taken as the actual length.

As for the measurements in (b), regular micrometers with an accuracy of $\pm$ 0.0001 in. were used. It is easier to make diagonal measurements by micrometer. It was found that not all the square bars were perfect squares, some diagonals being as much as 5% different from the nominal size. This could introduce some error on the spread and draft measurements, if the nominal size of the bar were accepted as the basis. Therefore the diagonal lengths of every test bar were measured before rolling, and diagonals were identified to ensure correct positioning of the bar when entering the pass.

### 3.3.1 Load and Torque Measurements

As mentioned in chapter two the load was measured by two load cells in conjunction with a Wheatstone bridge circuit and ultra-violet recorder. Similarly torque was measured with a pair of strain gauges in conjunction with the bridge circuit and the recorder. This method correlates galvanometer deflection with the applied load or torque. The key to making correct measurements is the calibration curves. Therefore the entire system, from the load and torque cells to the ultra violet recorder was calibrated under conditions similar to the working conditions.

### 3.3.2 Load Cell Calibration

The load cells were calibrated separately on a five range 100T Avery testing machine. The 10 ton range was selected for the calibration, as the maximum load on either load cell never exceeded six tons. The load cells were placed on a steel block similar to the bearing block of the rolls, and a short 1" diameter steel rod, similar to the screw down end of the mill, was placed on top of them. This arrangement ensured that conditions during the calibration and the tests were similar.

Recordings of galvanometer deflection were taken for 500 Kg load increments up to nine tons, and then the load cells were unloaded by the same 500 Kg steps, the deflections being recorded again. This process was repeated twice. Three different input voltages were used, 8, 10 and 12 volts. Galvanometer deflection corresponds to the input signal, and the input signal in turn corresponds to the input voltage. For the small bars 12 volts input voltage was applied in order to obtain a larger deflection of the galvanometer to give a more accurate estimate of the load. Calibration curves are shown in Fig. (3.1) and Fig. (3.2) for the left hand and right hand load cells.

### 3.3.3 Torque Cell Calibration

The torque cells were calibrated in an Avery Torsion Machine. Each torque cell was calibrated separately. The same precautions were taken to ensure similarity between test conditions and calibration conditions. Special adapters were used to simulate the square end of the rolls and the pinion shaft. Mill couplings were used to connect each torque cell spindle to the torsion head and the machine face.

Recordings of galvanometer deflection were taken for 500 lb-in torque increments up to 4500 lb-in This was the maximum value of the measured torque. The torque was then released at the same 500 lb-in steps and recordings again taken. Again, three input voltages were used, namely 8, 10 and 12 volts. The input of 12 volts was used for the small bars. Calibration curves are shown in Fig. (3.3) and Fig. (3.4) for the upper and lower spindles.

### 3.4.1 Scale Control

In so far as the load, torque and spread factors are concerned in the hot rolling process, one of the main parameters is the superficial scale on the ingoing hot bar. It is well understood that scale acts as a poor lubricant. It influences the coefficient of friction and therefore the frictional forces which causes inhomogeneity of deformation. Mode of deformation together with strain rate determines the yield stress which in turn sets the limit of load and torque and it may effect the spread as well. Whitton and Ford (19) have experimentally determined the coefficient of friction in the lubricated cold rolling process for a number of lubricants. Decreases of the frictional coefficient, with the application of different lubricants, were noted in their work.

In the hot rolling process, whilst scale has the effect of a lubricant, its extent is related to the heating time and oxidising atmosphere of the furnace. The effects of different degrees of surface scale on spread in hot rolling have been observed by Skelton (20). If the superficial scale on the hot bars is not uniform, it would be expected to lead to erratic measurements of various factors, such as load, torque and spread. So, in order to eliminate one source of scatter in hot rolling experiments, surface scale on the bars should be kept uniform or its formation be prevented.

The only way to achieve this is by careful control of the furnace atmosphere. In this investigation the best effective method was found to be as follows:-

### 3.4.2 Control of the Furnace Atmosphere

The usual technique for controlling the atmosphere is to fill the heating chamber of the furnace with some non-oxidising gas, or to heat in a vacuum. The former method was adopted since it gave a low cost of test and operation; plus facility and quickness of handling the bars in a regular electric heating furnace.

The heating electric furnace, described in section 2.2.1, was a Gallenkamp Model with a heating chamber of 7 x 7 x 12 inch dimensions. Oxygen free nitrogen from large size pressure bottles was used to provide the non-oxidising atmosphere. The furnace was not airtight, so a constant flow of nitrogen had to be maintained. Filling the entire volume of the heating chamber required a considerable amount of nitrogen flow, and yet scaling was not prevented effectively. In order to cut down on the amount of nitrogen flow, and have an effective control of the scaling, the bars were heated in a stainless steel box inside the heating chamber, and the box interior was flushed with nitrogen through 3/16" stainless steel tubing. The rectangular box, 2" by 6" and 10" long, was placed in the heating chamber as shown in Fig. (3.5). The front part of the box was open for easy access to the interior and it could be blocked with a 3/8" thick cover plate to seal the box. Two fire brick stands with V shaped cuts, as shown in Fig. (3.5), were positioned along the box and the square bars were placed in the V cuts. With this arrangement the hot bars never stuck together and were quite separated, plus the fact, that, since the bars rested only at two locations on the fire bricks, it was very easy to slide them out with a tong for rolling in a mill just a few feet away.

In actual experiments, the sequence of operation consisted of opening the furnace and removing the cover plate whilst a second operator removed the hot bar for insertion into the pass. The average time for transferring the hot bar from the box interior to the pass was about 2,75 seconds (see the next section). The nitrogen was supplied into the box through a 3/16" bore stainless steel tube, entering the heating chamber from the front side and passing through a V shaped cut in the bottom of the coverplate. The nitrogen tube was bent to form a rectangular coil inside the box and small holes were drilled along the coil at 3" spacing, the end of the coil being blocked off. Thus a uniform spray of nitrogen entered the box and filled it completely, providing a non-oxodising atmosphere.

### 3.4.3 Temperature at the Box Interior

The temperature of the heating chamber was monitored through the temperature indicator of the furnace. But the interior of the box, as a result of the constant nitrogen flow, could have a lower temperature. To determine the actual temperature, Alumel-Chromel thermocouples were placed inside the box and the potential difference was momitored by a digital voltmeter capable of reading 0.01 of a millivolt. In the thermal sense this means a temperature of $0.2^{\circ}C$, which is accurate enough.

Except for the terminal hot junction of the thermo-couples which was exposed to the interior atmosphere of the box, the rest of the thermocouple wires inside the furnace were protected by ceramic shielding, and the ceramic itself was protected inside a stainless steel tube.

### 3.5.1 The Temperature of Rolling General Remarks

The experiments were carried out at four different temperatures, $900^{\circ}$, $1000^{\circ}$, $1100^{\circ}$ and $1200^{\circ}$ centigrade. At each temperature 1/4", 3/8", 1/2" and 5/8" square bars were rolled in corresponding diamond passes. Bars of each size were rolled for different roll gap settings from fully open to touching rolls, in order to study the gradual change of spread and draft on the diagonal planes. To have consistent results the average rolling temperature, for each series of experiments should be maintained constant.

The control of the temperature inside the furnace is easy and reliable. As mentioned before, the furnace temperature indicator, and thermocouples inside the protective stainless steel box, with the digital voltmeter, monitored the interior temperature constantly. However the average rolling temperature is lower than the furnace temperature, as it is impossible for the hot bars to enter the pass instantly, after leaving the furnace. In the actual experiments the bars had to be removed from the furnace by a pair of tongs, transported to the rolling mill and put into the pass through guide rollers. This procedure involves a certain amount of heat loss to the colder surroundings, thus causing a temperature drop in the bar.

In general the temperature of the square bars emerging from the furnace and going through the pass changed due to:

(1) Loss of heat to the surroundings by radiation

(2) Loss of heat by convection

(3) Conduction of the heat to the rolls and guides

(4) Acquisition of heat resulting from the energy expended on plastic deformation of the metal.

Of all these, radiation is the most important factor, since at temperatures higher than 200°C to 300°C, cooling is primarily by radiation. Convective loss while present is not so important, but convective loss is increased by movement of the bar. The conduction of heat to the rolls and guide, although generally known to be insignificant due to the short duration of the time of contact between rolls and bar, was investigated experimentally. Temperature rise due to the work of plastic deformation is negligible, furthermore it is compensated for by heat conduction to the rolls.

Heavy sections of slab or billets, having a large heat capacity, retain a relatively constant temperature during the rolling process, or experience only a small temperature drop. However, since the current experiments were carried out on small square sections, 1/4" x 1/4" up to 5/8" x 5/8", it was considered necessary to have a better knowledge of the actual temperature drop. As will be discussed in the next section, by using the ultra violet recorder set a circuit was set up to record the actual cooling curves of each bar size, both in the air and whilst going through the rolls.

### 3.5.2 Electrical Circuit for Cooling Curves

The Ultra Violet Recorder was put into a simple circuit to record the cooling curves in the air and in the rolling process.

Considering the galvanometer sensitivity of 0.0007 mA/cm, the the osilloscript paper width of 15 cm, the maximun current through the galvanometer had to be limited to:

$$0.0007 \times 15 = 0.0105 \text{ mA}$$

At 1200°C an e.m.f. of about 48.9 millivolts is generated by Alumel-chromel thermocouples (44). If this is directly applied to the recorder's galvanometer which has a resistance of 44 ohms a current of 48.9/44 = 1,102 mA is produced, which would give excessive deflection of the light beam (much larger than 15 cm, which is the maximum recordable length and is achieved by 0.0105 mA only). Because of this, the circuit shown in Fig. (3.6) was set up to cut down the current flow to the galvanometer.

A stable standard cell of 1.5 volt was used with a potential divider having 1/10, 1/100, 1/1000, 1/10000 and 1/100000 multiplier steps. The polarity of this dry cell-potential divider circuit, was connected opposed to the polarity of the thermocouples. In this way the combined potential difference to be applied to the galvanometer was adjusted to be about 5 to 7 millivolts, according to the temperature range. Two resistances of 390 and 600 ohms were put in parallel and in series with the recorder's galvanometer. With this arrangement, for a temperature drop of 125°C to 175°C (or 5 to 7 millivolt drop), full deflection of the light beam (15 cm) occurred, and more accurate cooling curves were obtained, Since the whole operation of removing the hot bar from the furnace and putting it through the rolls took not more than four seconds, cooling curves for a duration of six seconds were good enough for practical purposes.

### 3.5.3 Experimental Cooling Curves

Cooling curves for each bar size were obtained in the following way: The Alumel-chromel thermocouples were connected to each bar and the bars were then placed into the furnace and the temperature monitored to the desired value. Initially when the temperature of the square bar reached the desired value, the recorder's deflection was adjusted to about 15 cm (maximum). This was done by adjusting the counter e.m.f. of the dry cell through the potential divider box. The potential divider could alter the voltage in 0.015 mV steps. The speed of the recording paper was set at 0.5 in/sec, thus every inch of the paper was equivalent to about two seconds. Then the recording paper was turned on and the hot bar removed from the furnace. As the bar continued cooling in air, the thermic potential difference dropped until it reached the counter e.m.f. of the dry cell, thus the combined potential difference became zero and the galvanometer light beam returns to its initial zero setting. Further cooling deflected the light beam in the opposite direction which was outside the recordable range; at this stage the circuit was always cut off. While the light beam was returning to the zero position the recording paper unrolled at a constant speed of 0.5in/sec, the two motions being perpendicular. Thus the light beam traced the exact cooling curve of the bar. Fig. (3.7) through Fig. (3.10) show typical cooling curves obtained for 1/4" to 5/8" square bars. In Fig. (3.7) the furnace temperature was 984°C. Handling inside the furnace caused a temperature drop of 14°C, but in the majority of experiments the temperature drop inside the furnace was not more than 10°C. Fig. (3.8) and Fig. (3.10) show the cooling curves of 3/8" and 5/8" square bars at different temperatures. Cooling curves of 1/4" square bar at about 1100°C and 1200°C are shown in Fig. (3.11) and Fig. (3.12). These curves are exact, and account for the combined effect of radiation and convection in the air.

### 3.5.4 Theoretical Cooling Curves

Using a simple theoretical analysis an expression for the cooling curves can be obtained in the form of a relation between time and temperature. Heat is dissipated by radiation and convection. In Fig. (3.19) an element of length dx is considered for a temperature drop dT during a short duration dt, the heat balance equation being:-

$$-(1^2 \cdot dx)(\rho \cdot c) \cdot dT =$$

$$[4 \cdot 1 \cdot dx \cdot \varepsilon \cdot \sigma \cdot (T^4 - T_o^4) + 4 \cdot 1 \cdot dx \cdot h\,(T - T_o)]dt \qquad (3.1)$$

in which h is the surface coefficient of heat convection, $\varepsilon$ an emissivity factor which is taken equal to 0.73 (45) and $\sigma$ is the Boltzman-Plank coefficient. The minus sign on the left hand side is inserted because whilst the temperature is decreasing, the time t is increasing. This relation is developed to give the following differential equation of the temperature:-

$$\frac{dT}{dt} = \frac{4 \cdot \varepsilon \cdot \sigma}{1 \cdot \rho \cdot c} T^4 + \frac{4 \cdot h}{1 \cdot \rho \cdot c} T - \left(\frac{4 \cdot \varepsilon \cdot \sigma}{1 \cdot \rho \cdot c} T_o^{\,4} + \frac{4 \cdot h}{1 \cdot \rho \cdot c} T_o\right) \qquad (3.2)$$

Equation (3.2) is a first order non-linear differential equation with constant coefficients of the form

$$\frac{dT}{dt} = C_1 T^4 + C_2 T + C_3 \qquad (3.3)$$

This equation is complete with the initial boundary condition that at t = o the temperature of the bar is specified. By using a simple finite difference method assuming time intervals of 1/20 second and a known initial temperature, this equation can easily be solved by the digital computor, so that temperature vs. time can be tabulated.

The Boltzman - Plank coefficient is a constant $\sigma = 1.355 \times 10^{-12}$, but h is increased with movement of the bar in the air. h was determined so as to give the best possible agreement with the exact experimental cooling curves. The values of h in c.g.s. units are as follows:

| | | | | |
|---|---|---|---|---|
| For 1/4" | Bar | h | = | 0.0013 $cal/cm^2 - c^o$ sec |
| For 3/8" | Bar | h | = | 0.0016 " |
| For 1/2" | Bar | h | = | 0.0022 " |
| For 5/8" | Bar | h | = | 0.0028 " |

Tabulated values for the theoretical cooling curves are given at the end of this chapter, the calculation being done by means of the University of London CDC 6600 Computer. Equation (3.3) can be written in the following form

$$\frac{T_{i+1} - T_i}{\Delta_t} = c_1 T_i^4 + c_2 T_i + c_3$$

$$T_{i+1} = T_i + \Delta_t [c_1 T_i^4 + c_2 T_i + c_3] \qquad (3.4)$$

$T_i$ is temperature at the time t, $T_{i+1}$ is temperature at the time t + $\Delta_t$ and so on. Thus starting from an initial temperature (i.e. the furnace temperature) step-by-step calculations give the temperature at every instant. Initial values were chosen as 970°C, 1105°C, 1220°C, and 1350°C. The corresponding curves are shown in Fig. (3.14) and Fig. (3.17).

### 3.5.5 Heat Loss to the Rolls

The cooling curves obtained experimentally and analytically, give a good measure of the temperature drop during handling in the furnace and in the air. A knowledge of the heat conduction to the rolls and the resulting temperature drop was also desirable.

In view of the small heat capacity of 1/4" square bars, a considerable heat flow to the rolls could cause a large temperature drop which if not accounted for could introduce errors. The length of the 1/4" square bar in contact with the rolls is , as It will be seen in chapter four, that for 1/4" bar the optimal draft δ is 0.1156 (δ = 0.1156) and the average pass radius R = 1,828", so $\sqrt{1.828 \cdot 0.1156} = 0.466$ in.

At the constant peripheral speed of the rolls (30 f.p.m. or 6 in/sec), each section of the square bar will be in contact with rolls for t = 6/0.466 or 1/13 seconds. Although this is a very short time, a knowledge of the temperature drop in the rolls is useful. An analytical approach was not attempted but with the existing instruments this problem could be solved by an experi mental method, as follows:-

An infra-red pyrometer could be used to give an indication of the temperature before and after rolling, but exact and accurate measurement of the temperature would not be possible by this method. The bars after removal from the furnace, were transported rapidly to the mill and put through the rolls. Tracking the hot bar with an infra-red pyrometer from the furnace to the rolls and out of the rolls is difficult and unreliable, plus the fact that the emissivity of the hot bar has to be known at every stage of the process in order to make correct estimates of the temperature.

In view of these difficulties, the same electrical circuit with the ultra violet recorder and the thermocouples was used to obtain exact recording of the cooling curves during the entire operation, from handling inside the furnace to exit from the rolling mill.

The experimental difficulty was mainly in holding the thermocouples against the bar during the rolling process. Because of the intense metal deformation in the rolls, the thermocouples would be disconnected from the hot bar or would be loosened and the cooling curves would become unstable and show lower temperatures than the actual ones Fig. (3.11). This problem was overcome by inserting the thermocouple in fine holes drilled on the corners of the horizontal diagonal plane of the bars Fig. (3.18) and secured in place by closing the hole by a slight tap of a centre punch. This method of fixing thermocouples is often called "peaning".

Since the horizontal diagonal is a plane of symmetry, and plastically deforming material is compressed from the top and bottom halves, this plane only spreads and therefore remains flat. Thus thermocouples in this region do not undergo severe deformation and there is a good chance of holding them securely on the bar, during passage through the rolls. To make sure that the thermocouples had not been loosened during the rolling process, the curves were compared with simple cooling curves obtained in air cooling of the hot bars, as mentioned in section 5.5.3. The result is shown on Fig. (3.12) and Fig. (3.13) for 1/4" and 3/8" square bars. These two were the smallest sizes used in the experiments and any significant heat flow to the rolls would appear as a sharp temperature drop after leaving the rolls. By feeding the load cell out of the balance onto another channel of the U.V. recorder, exact timing of the operation was recorded. Rapid cooling starts when the bar is out of the furnace, the moment of entry into the rolls is indicated by the recorder's beam deflection; and exit from the rolls is also indicated by the recorder's beam deflection Fig. (3.11) and Fig. (3.13).

## 3.6 Summary and Conclusions

The set of cooling curves in Fig. (3.7) through Fig. (3.17) clearly show the temperature drop at each stage of the experiments.

The temperature drop inside the furnace from the moment the furnace is opened to the moment when the bar is just out of the furnace is not more than 10°C.

Heat flow to the rolls is negligible and for $\frac{1}{4}$" square bar is not more than 5 to 10°C. For the large sizes it is negligible and compensated by plastic work.

By far the main cause of temperature drop is general air cooling which is effected through radiation and convection. The theoretical differential equation in section 3.5.4 is good enough to account for temperature drop vs. time, provided h is known on an average basis.

The bar enters the pass about 2.75 seconds after being out of the furnace, the time spent in the pass being about 1.5 seconds. Thus the average time for the bar from the furnace to the rolled stage is about 3.5 seconds. On this basis it was found that different bars could not be rolled from the same temperature and expected to have the same mean rolling temperature. The smaller size bars have a sharper cooling curve than the larger sizes. They should be heated to a higher initial temperature. Table (3.1) shows the furnace temperature required for each bar size to give average rolling temperatures of 900°C, 1000°C, 1100°C and 1200°C.

| | | 900°C | 1000°C | 1100°C | 1200°C |
|---|---|---|---|---|---|
| 1/4 | → | 990 | 1105 | 1220 | 1350 |
| 3/8 | → | 970 | 1082 | 1196 | 1320 |
| 1/2 | → | 955 | 1065 | 1175 | 1295 |
| 5/8 | → | 950 | 1058 | 1166 | 1275 |

Table 3-1

# CHAPTER FOUR

## Spread Formula

### 4.1 Introduction

When metals are compressed between rolls, they flow in the direction of least resistance, there is not only longitudinal flow but also some flow in the lateral direction: this lateral flow of metal is called "spread". In general spread can have two kinds of effects:- in some types of rolling it has a reducing effect on the amount of elongation; in which too much spread diminishes the limit of attainable reduction, in some other rolling processes spread is important to achieve a required geometry, as in most section rolling.

In the case of flat stock passing through plain cylindrical rolls, spread is free, unrestricted and has a minor effect on elongation. In closed passes where spread is restricted the ingoing bar must be smaller in width than the pass, because over-filling means excessive wear, and side thrusts on the collars are harmful. On the other hand if the spread is not sufficient to fill the pass, either the required geometry is not obtained or the pass is not of optimal size. For these reasons a reasonable knowledge of the spread is desirable.

The extent of spread as opposed to elongation in a pass has been and still is a matter of research, Researchers in the rolling field have been devoted to this problem as early as the beginning of theoretical formulations of the rolling theory itself (Eklund 1927) Most of the research on spread has been concerned with flat rolling, and it is appropriate to give here a short description of early work.

## 4.2 Some Early Spread Formulae for Flat Rolling

### 4.2.1 Siebel's Formula

This formula was formulated for values of $\frac{w_1}{h_1} > 1$ and takes account of temperature and $w_1/\sqrt{R\delta}$ variations. The formula is:

$$w_2 - w_1 = m.C.R.\frac{\delta^2}{h_1} \qquad (4.1)$$

where:

$C = 0.35$ for temperatures above $1000^{\circ}C$

$C = 0.35$ to $0.40$ for temperatures below $1000^{\circ}C$

m is a correction factor to account for the width of the material, its value varying according to the table below:

| $w_1/\sqrt{R\delta}$ | 1 to 7 | 8 | 10 | 12 | 14 | 16 | 18 | 20 |
|---|---|---|---|---|---|---|---|---|
| m | 1 | 0.92 | 0.75 | 0.60 | 0.45 | 0.30 | 0.15 | 0 |

For $w_1/\sqrt{R\delta} > 20$ the spread is zero.

This formula has been superseded and is not in use any more.

### 4.2.2 Ekelund Formula

The Eklund formula takes into account most of the parameters affecting spread,[1,2] except for the quality or composition of the steel. The formula is too complicated to use, but there are monographs for calculations as well as a slide rule by A.V. Mogiljansky. Since the Ekelund formula does not account for the quality of the steel, in practice it has been found to overestimate spread in carbon steels and to underestimate the spread in alloy steels, which spread is more due to their high strain hardenability and lower annealing properties, (This enhances a higher resistance to metal flow in the longitudinal direction, because of higher strain in this direction as opposed to the lateral direction).

The Ekelund formula is written as:-

$$w_2^2 - w_1^2 = 2[4\delta - 2\ln(\frac{w_2}{w_1})(h_1 + h_2)](\sqrt{R\delta})(\frac{1.6\mu\sqrt{R\delta} - 1.2\mu}{h_1 + h_2}) \qquad (4.2)$$

$\mu$ is the coefficient of friction and for steel rolls is given as a function of temperature by the equation:-

$$\mu = 0.55 - 0.0005(T - 1000)$$

where T is the rolling temperature in degrees centigrade.

## 4.3 Recent Formulae for Spread

Among recent formulae which are more commonly used are those of Wusatowski, Hill, and Sparling. The suitable range of application of these formulae has been investigated by J.M. Alexander and A. Halmi,[4] and a formula suitable for a wide range of rolling conditions has been derived[4]. Another recent formula is by Tselikov[10] which like Hill's formula has a theoretical basis. A brief description of these formulae is given here.

### 4.3.1 Wusatowski's Formula[5]

This formula is the result of many experiments by Wusatowski and has the following form:

$$\frac{w_2}{w_1} = a.b.c.d.\left(\frac{h_2}{h_1}\right)^{e^{-1,987\left[\frac{w_1}{h_1}\right]\left[\frac{h_1}{R}\right]^{0.556}}} \qquad (4.3)$$

a, b, c and d are factors to account for, steel composition, rolling temperature, rolling speed and roll material respectively. These coefficients are all given in Wusatowski's original paper(5), and they are very close to unity. Wusatowski later revised this formula, changing 1,987 and 0.556 to 1,269 and 0.9676 respectively(6).

### 4.3.2 Hill's Formula

Unlike Wusatowski's purely empirical formula, Hill's formula is derived from a consideration of the Levy-Mises stress-strain relations for plastic flow. An average state of stress in flat rolling is assumed as follows:- a normal roll pressure s, a lateral compressive stress ms (m is a factor $o < m < \frac{1}{2}$), and the longitudinal forces at the entry and exit planes zero. The Levy-Mises stress-strain relations for the two dimensional case are

$$\epsilon_{xx} = \frac{2}{3}\,\delta\lambda\,[P_{xx} - \tfrac{1}{2}P_{yy}]$$

$$\epsilon_{yy} = \frac{2}{3}\,\delta\lambda\,[P_{yy} - \tfrac{1}{2}P_{xx}]$$

(Using the notation given by Ford and Alexander) $P_{xx}$ and $P_{yy}$ correspond to s and ms respectively Fig. (4.1). In the case of plane strain, spread is absent ($\epsilon_{yy} = o$) and this establishes $m = \frac{1}{2}$; similarly if there is unrestricted flow in the lateral direction (the case of plane stress) $m = o$.

$$\delta\epsilon_{xx} = \frac{dw}{w_1} = \frac{2}{3}\,\delta\,\lambda\,(ms - \tfrac{1}{2}s)$$

$$\delta\epsilon_{yy} = \frac{dh}{h_1} = \frac{2}{3}\,\delta\,\lambda\,(s - \tfrac{1}{2}ms)$$

a formula for spread is easily found from these equations to be:-

$$-\frac{dw}{w_1} \Big/ \frac{dh}{h_1} = \frac{1 - 2m}{2 - m} = P \qquad o < P < \tfrac{1}{2}$$

This is integrated to give $\dfrac{\ln\,({}^{w}2/w_1)}{\ln\,({}^{h}1/h_2)} = P.$

Considering the rapid decrease of strain ratio P with $\frac{w_1}{\sqrt{R\delta}}$ Hill originally suggested $P = \frac{1}{2}\,e^{-\lambda\left(\frac{w_1}{\sqrt{R\delta}}\right)}$ with $\lambda = \frac{1}{2}$ a constant. (McRum has shown that $\lambda = 0.525$ gives better agreement with experimental results). Thus Hill's formula is

$$\frac{\ln\,({}^{w}2/w_1)}{\ln\,({}^{h}1/h_2)} = \tfrac{1}{2}\,e^{-\frac{1}{2}\left(\frac{w_1}{\sqrt{R\delta}}\right)} \qquad (4.4)$$

### 4.3.3 Sparling's Formula

Sparling's formula is similar in form to Hill's formula but Sparling's introduced correction factors to account for various rolling conditions.. Sparling's formula is

$$\frac{\ln(w_2/w_1)}{\ln(h_1/h_2)} = 0.981\, e^{-0.6735\{2.935(\frac{w_1^{0.9}}{R^{0.55} h_1^{0.1} \delta^{0.25}})\}^{a.b.f.g.j}}$$

where a, b, f, g, j account for roll condition, bar surface conditions, composition of the rolled material, temperature of rolling and mean strain rate during rolling. The coefficient 0.981 as the maximum strain ratio contradicts Hill's upper value of 0.5, but Sparling has mentioned[9] that according to experimental results the strain ratio does exceed 0.5.

### 4.3.4 Tselikov's Spread Formula[10]

Tselikov's formula calculates the width of the strip all along the zone of deformation; so that at the exit plane the maximum width and the total spread is obtainable. The basic assumptions in Tselikov's theoretical treatment of the problem are as follows:-

a) Only some arbitrary zones at the edges of the strip tend to spread, depending on the ratio $w_1/\sqrt{R\delta}$; the central portion of the strip undergoes plane strain deformation in the direction of rolling (Fig. 4.2).

b) The normal pressure at the edges is less than 2K ($s < 2K$), so that a condition of dry friction could exist on the edges ($\tau = 2\mu K$).

c) Longitudinal and lateral frictional forces in the edge zone are equal $\tau_x = \tau_z$ (z is the lateral direction).

With these assumptions and some approximations Tselikov derives the following formula for the width of the strip in the deforming zone.

$$w_x - w_1 = \left(1-\frac{\delta}{2\mu}\right)\frac{4h_1h_2}{\delta^2}\left[y\left(0.5\frac{h_1}{h_2}y-1\right)\ln y - 0.25\frac{h_1}{h_2}(y^2-1) + y - 1\right] \tag{4.6}$$

where

$w_x$ – width of the strip at a distance x from the exit plane Fig (4.3)

$$y = \frac{h_2 + \frac{\delta x}{l}}{h_1}$$

$l = \sqrt{R\delta}$ = length of the arc of contact

The spread formula at the exit plane is modified to

$$w_2 - w_1 = 0.5\ C_w \cdot C_\sigma \left(\sqrt{R\delta} - \frac{\delta}{2\mu}\right) \ln \frac{h_1}{h_2}$$

where $C_w$ is a factor to account for the variations of $\left(\frac{w_1}{\sqrt{\sqrt{R\delta}}}\right)$ and is given by the following formula

$$C_w = 1{,}34\left(\frac{w_1}{\sqrt{R\delta}} - 0.15\right) e^{0.15 - \frac{w_1}{\sqrt{R\delta}}} + 0.5 \qquad (4.7)$$

but subsequent work has revised this formula to

$$C_w = 4(1-r)\left(\frac{w_1}{\sqrt{R\delta}} - 0.15\right) e^{1{,}5\left(0.15 - \frac{w_1}{\sqrt{R\delta}}\right)} + r$$

where r is reduction in the pass.

$C_\sigma$ is a factor to account for back tension (Tselikov has also found that back tension has a negligible effect on the spread); it is given by the following formula:-

$$C_\sigma = 1 - \frac{2\sigma_o}{Y}$$

where:

- $\sigma_o$ is the back tension stress
- Y is the yield stress in uniaxial tension or compression.

If there is no back tension, $C_\sigma = 1$.

## 4.4 Spread in Square-Diamond Passes

Although there are many spread formulae for hot rolling of strip, there is no independent formula to account for the hot rolling of sections. Almost all approaches consist of sub-dividing the section into flat elements and then applying one of the existing spread formulae for strip rolling. A.E. Lendl (12) has used Ekelund's formula for this purpose. As also indicated by R.B. Sim (11) calculations on this basis are not accurate enough.

Two of the main factors affecting the spread are friction and inhomogeneity of deformation. The effect of friction has been discussed by many investigators (41); in all metal forming processes, including rolling, friction controls not only the stress distribution but also the degree of inhomogeneity of deformation: inhomogeneity arises also from the geometry of deformation; for example when a metal is plastically stretched in tension, it is found to be uniformly worked. This mode of deformation is homogenous. In many other metal forming processes including rolling and extrusion; some parts of the section are much more heavily deformed than others, This is the mode of 'inhomogenous deformation'. In the case of cold strip rolling, deformation is essentially homogenous and the dominant factor of spread is friction, but in the case of rolling billets or rectangllar bars with high R/h ratios inhomogeneity of deformation occurs. Spread in this case is affected both by friction and inhomogeneity, furthermore for high ratios of R/h, characteristic of section and billet rolling, some investigators (13) have concluded that spread takes place mainly due to transition of side surfaces into the contact surfaces, and not due to contact slip in the transverse direction. In Square-Diamond rolling the inclined surfaces of the diamond pass restrict lateral flow of the metal, thus setting up higher transverse frictional forces as compared with flat rolling. This process contributes to inhomogeneity of deformation; furthermore square bars in diamond passes are rolled at varying values of R/h from the central diagonal plane to the corners of the pass. Similarly the length of the arc of contact $\sqrt{R.\delta}$ is varying at each point of the roll's contact with the material, from the centre to the corners. In the central part the R/h ratio is small similar to the rolling of thick material, whereas in the corners R/h is large similar to the rolling of thin material. Considering the non-uniformity of deformation and the transverse frictional forces on the inclined surfaces of the pass, it becomes clear that the metal flow in a Square-Diamond pass is quite different from plane-strain flow, On this account a direct application of formulae for spread in flat rolling to Square-Diamond passes is bound to have some margin of error.

### 4.4.1 Observations on the Surface Deformation of Square Bars in Diamond Passes

To investigate conditions of lateral spread, in particular to see whether spread is the result of the side surfaces turning into contact surfaces or lateral stretching, longitudinal grid coordinates were inscribed on the surfaces of lead square bars. A universal measuring instrument equipped with a tracelet mechanism was used to inscribe all the grid lines, this instrument has been described previously by Alexander and Brewer in a research note (14). The manufacturer (Société Génévoise d'Instrument de physique) have guaranteed an accuracy of 0,000040 inches. The grid lines were inscribed at 0.025 inch spacing. The bars were held secure in a V block jig under the travelling microscope of the instrument and the horizontal distance between the grid lines, $d_1$, Fig. (4.4) was measured before rolling. The square lead bars were then part rolled and removed from the mill. The continuation of the grid lines from the undeformed part into the deformed contact area was observed. If any grid line on the bar surface could be traced into the deformed contact area, between the planes of entry and exit then the question of superficial lateral movement of material and therefore sticking or slipping in the lateral direction could be clarified.

In most of the tests traces of the longitudinal grid lines disappeared on the contact zone, or due to the curvature of the rolled lead bar accurate measurements for quantitative results were not possible. Before inscribing the grid lines the square lead bars were dipped into blue marking solution, so that the grid lines then appeared more distinct and in the contact zone some blue paint was impressed into the lead giving a better picture of the grid deformation. In a good many tests, however, the blue colour was rubbed off by the rolls. The general observation from these series of tests is that the longitudinal grid lines spread slightly on the beginning of contact with the rolls, and then inside the contact area the condition of sticking friction prevails as there is no further spread observed.

### 4.4.2 Interior Deformation of the Square Bar DIAGONAL

The interior deformation in diamond passes is non-homogeneous and complex. The velocity changes from that of the roll's peripheral speed in the contact area to higher or lower values in the interior. However, from considerations of symmetry, the diagonals of the square bar in the pass should undergo plane strain deformation. Again tellurium lead was used and the molten lead was cast into a right triangular shaped mould 12" long fig. (4.5). The mould itself was kept hot by a gas flame underneath, to prevent formation of air pockets, to maintain a slow cooling rate, and to ensure smooth surfaces of the cast bars. The cast bar was then screwed down in a V block jig and the base shaved down to size by a fly cutter tool in a milling machine at 0.001 inch steps in the final runs. Thus a triangular prism with smooth surfaces and mirror polished base was obtained. A grid coordinate system of 0.025 spacing was inscribed on the base plane. Two pieces of these prismatic bars joined together provides a $\frac{1}{2}$ inch square bar with a grid inscribed on the interior coordinate diagonal plane. Araldite was used to join the two halves, and to secure them in the pass it was found necessary to put intermittent soft solder seams along the corner lines fig. (4.7). These bars were part rolled with the plane of the grid vertical, removed from the mill, and separated open with great care. Fig. (4.23)is a photograph of the distorted grid, which is very similar to the plane strain case. Attempts to obtain similar distorted grids on vertical planes parallel to the vertical diagonal plane failed, because of separation generally occured in the pass and the distorted grid surface did not remain plane. This was apparently because deformation is not plane in those sections. Thus the only two planes in the deformation zone remaining plane surfaces are the diagonal planes of the bar. In accordance with flat rolling terminology, contraction and expansion of diagonal lengths will be called draft and spread in the following sections. In fact since other sections have no clear deformation pattern as yet, all the measurements and calculations for spread will be based on these lengths.

### 4.5.1 New Spread Formula

Plastic deformation of the bar starts as it comes into contact with the rolls and as it moves further into the pass the plastic zone of deformation progressively expands and the bar undergoes a reduction in area as well as a change in the geometry from square to diamond. Changes of geometry brought about by the pass configuration cause shortening of the vertical diagonal length along with downward, forward and lateral movement of the material in the interior of the bar. Meanwhile, because of lateral movement of the material, the horizontal diagonal length is increased. These changes are referred to as draft and spread, analogous to plane strain deformation. As mentioned previously the two diagonal planes are the only ones to remain plane. If deformation in the pass is homogeneous then a thin segment of the square bar entering the pass would undergo a geometry change from flat square to flat diamond (somewhat thicker) fig.(4.8a), and diagonal lengths would be decreasing and spreading concurrently all along the zone of contact from the entry to the exit plane. The actual deformation is more complex and there are velocity variations both along the stream-lines and all over the section. At the boundaries, because of the sticking conditions; the velocity of the material is equal to the peripheral speed of the rolls. The overall velocity picture if far from being uniform therefore the ingoing square segment may have a hypothetical shape as shown in Fig. (4.8b) at the exit plane.

It would be difficult to describe these changes of geometry mathematically, as material proceeds through the rolls. The flow equations are three-dimensional and subject to mixed boundary conditions (velocity and frictional forces), (see section 5.2). They are too complicated for analytical treatment but there is no doubt that concurrent decreasing and spreading of the diagonals occurs along the deformation zone, irrespective of the precise deformation mode.

If the basic factors having an influence on the deformation and plastic flow of the material in the pass (such as pass geometry, frictional forces, temperature, composition of the material and rolling speed (15),) are kept the same in various experiments, then the values of diagonal spread and draft should be substantially identical, although the deformation may be inhomogeneous. In actual practice keeping all these factors the same during different experiemtns is a definite impossibility. However, by careful experiments it is possible to minimize the variations. Thus a carefully derived relation between spread and draft which takes into account all the relevant parameters should be universally valid.

A new formula is derived to account for spread all along the arc of contact, from the entry plane to the exit plane. The formula is expressed in terms of dimensionless variables of the rolling process expressing the geometry of the pass and the bar size. At each intermediate plane, between the entry and the exit plane, corresponding values of draft and spread are tied together by this formula. At the exit plane the maximum spread is calculated, which is important in determining the correct size of an ingoing bar to fill the pass completely.

The new formula is expressed as

$$W_x = W_1 \left[\frac{H_1}{H_1 - \delta_x}\right] e^{-\alpha (R/H_1)^{\beta} \left(\frac{W_1}{\sqrt{R\delta_x}}\right)^{\gamma}} \qquad (4.8)$$

where $W_x$ and $\delta_x$ are width and draft of the diagonal length at some intermediate plane at distance x from the plane of entry Fig. (4.9a), and $\alpha$, $\beta$ and $\gamma$ are constants which were found to be:

$$\alpha = 1{,}441 \qquad \beta = 0.10 \qquad \gamma = 1{,}072$$

At the exit plane $\delta_x$ will have its maximum value, $\delta$, and $W_x$ its maximum value $W_2$, thus

$$W_2 = W_1 \left[\frac{H_1}{H_1 - \delta}\right]^{e^{-\alpha(R/H_1)^{\beta}\left(\frac{W_1}{\sqrt{R\delta}}\right)^{\gamma}}} \quad (4.9)$$

similarly the final spread of the exit plane is expressed as:

$$S = W_2 - W_1 = W_1 \left[\left(\frac{H_1}{H_1 - \delta}\right)^{e^{-\alpha(R/H_1)^{\beta}\left(\frac{W_1}{\sqrt{R\delta}}\right)^{\gamma}}} - 1\right] \quad (4.10)$$

For intermediate planes

$$S_x = W_1 \left[\left(\frac{H_1}{H_1 - \delta_x}\right)^{e^{-\alpha(R/H_1)^{\beta}\left(\frac{W_1}{\sqrt{R\delta_x}}\right)^{\gamma}}} - 1\right] \quad (4.11)$$

4.5.2 <u>Some Comments on the New Spread Formula</u>

The general form of the formula is very similar to previous formulae derived for flat rolling by Hill (8), Sparling (9) and Alexander and Helmi (4). This formula can be rearranged to give the spread coefficient for any intermediate plane as follows:-

$$Sw_x = \frac{\ln W_x/W_1}{\ln H_1/H_x} = e^{-\alpha\left(\frac{R}{H_1}\right)^{\beta}\left(\frac{W_1}{\sqrt{R\delta_x}}\right)^{\gamma}} \quad (4.12)$$

or for the exit plane, which is of the main interest

$$S_w = \frac{\ln {W_2/W_1}}{\ln {H_1/H_2}} = e^{-\alpha(\frac{R}{H_1})^{\beta}(\frac{W_1}{R\delta})^{\gamma}} \qquad (4.13)$$

The main dimensionless groups influencing the spread are $R/_{H_1}$ and $({W_1}/_{\sqrt{R\delta_x}})$, both of which have been found previously in flat rolling spread formula. Because $(R/_H)$ has a small power $\beta$ =0.10, its effect is small, and $W_1/\sqrt{R\delta_x}$ is by far the more important factor. $\delta_x$ is progressively increasing from zero to its highest value at the exit plane $\delta$, and $W_1$ and R have definite values for any given bar and pass geometry.

### 4.5.3 Comparison with the Experimental Results

This formula is compared with experimental data on Fig.(4.10) to Fig.(4.13). On these figures the range of R/H is from 2.07 to 5.52 and the temperature range is 900°, 1000°, 1100° and 1200 centigrade. For each case the standard deviation is given in the Table below. As can be seen, the standard deviation never exceeds 0,0034 which is 6% of the calculated spread value.

| SIZE | STANDARD DEVIATION 900°C | 1000°C | 1100°C | 1200°C |
|---|---|---|---|---|
| $\frac{1}{4}$ | 0.0027 | 0.0031 | 0.0041 | |
| $\frac{3}{8}$ | 0.0023 | 0.0026 | 0.0030 | |
| $\frac{1}{2}$ | 0.0017 | 0.0017 | 0.0021 | |
| $\frac{5}{8}$ | 0.0025 | 0.0034 | 0.0030 | 0.0056 |

Table 4-1

### 4.5.4 Draft vs. Spread Measurements

Accurate measurements of the corresponding values of draft and spread on the same intermediate plane is difficult and cannot be achieved without errors, besides the square bars would have to be part rolled and then removed from the mill for subsequent measurements. Although this method may be possible for cold rolling process, at elevated temperatures such as 1000° or 1100°C part rolling and removal from the mill is not practicable. The values of $\delta_x$ and $W_x$ were obtained directly in a practical method, as follows. The rolls were separated initially so that the square bar could slide through the diamond pass as shown in Fig.(4.14). Form this position the rolls were screwed down step by step to the fully closed position. A square bar was rolled in at each step and after quenching diagonal lengths were measured by a micrometer and compared with the original lengths. In this way the spread and draft were obtained. In the experiments eight steps were chosen between a fully open and a fully closed gap. The values ($\delta_1$, $S_1$), ($\delta_2$, $S_2$) ... ($\delta_8$, $S_8$) should constitute points on a draft as spread curve in the deforming zone. Fig.(4.15) shows the deforming cross sections at each stage through the deformation zone. If the roll gap is closed deformation is from a complete square to a complete diamond, so closing the roll gap step by step should be approximately equivalent to stopping the progressive deformation from square to diamond at intermediate stages. Draft and Spread measurements for each step should therefore correspond to some intermediate plane in the deforming zone. The envelope curve of all these points ($\delta_1$ $S_1$) . . . . ($\delta_n$, $S_n$) should not differ greatly from the curve of $\delta_x$ vs. $S_x$ in the deformation zone. Experimental points on Fig.(4.10) to Fig.(4.13) were all obtained on this basis.

### 4.6.1 Prediction of Correct Size of the Bar to Fill the Pass Geometry

The horizontal diagonal of the bar going through the rolls progressively spreads to its maximum value at the exit plane. If the deforming bar is to fill the pass completely, that is to become a complete diamond, then for $\alpha = 120^o$ or $\tan\alpha = \sqrt{3}$

$$W_2 = \sqrt{3}\ H_2 \tag{4.14}$$

(4.14) could be worked out as follows

$$W_2 - W_1 = \sqrt{3}\ H_2 - W_1$$

Since $W_1 = H_1$ are diagonals of the square bar and

$$S = \sqrt{3}\ H_2 - H_1 + \sqrt{3}\ H_1 - \sqrt{3}\ H_1$$

$$S = \sqrt{3}\ (H_1 - H_2) + H_1(\sqrt{3} - 1)$$

or

$$S = -\sqrt{3}\ \delta + H_1(\sqrt{3} - 1) \tag{4.15}$$

(4.15) on a coordinate system S vs. $\delta$ is a straight line with a slope of $-\sqrt{3}$, but physically it is only valid when $W_2 = \sqrt{3}\ H_2$, meaning only when the pass is completely filled.

The spread formula for the section X (4.11) was expressed as

$$S_x = W_1 \left[ \left(\frac{H_1}{H_1 - \delta_x}\right) e^{-\alpha (R/H_1)^{\beta} \left(\frac{W_1}{R\delta_x}\right)^{\gamma}} - 1 \right]$$

This is of a parabolic form as shown in Fig.(4.10) to Fig.(4.13). Equations (4.15) and (4.10) if plotted on the same S vs. δ coordinates have the general form shown in Fig. (4.16), and the intersection point I gives the values of δ and S corresponding to a complete diamond shape at the exit plane. Since

$$\delta = H_1 - H_2 \qquad (4.16)$$

if the size of the bar is known ($H_1$ known) then $H_2$ (the smaller diagonal of the diamond pass) is found and the other dimensions of the pass follow from the simple geometrical relationship

$$W_2 = \sqrt{3}\, H_2$$

If the pass is already available ($H_2$ is known) then $H_1$ is easily found from Equation (4.16) that the correct bar size to fill the existing pass can be obtained.

### 4.6.2 Small Variations of Diamond Angle $\alpha$

Equation (4.15) was derived for $120^{o}$ diamond pass. In practical square-diamond rolling the angle may be less or more, the common range of application being between $110^{o}$ to $125^{o}$. In general, equation (4.15) can be written

$$S = -\tan\alpha.\ \delta + H_1 (\tan\alpha - 1) \qquad (4.17)$$

but the spread in diamond passes has been reported to depend on the angle $\alpha$ (A.W. McCrum BISRA report MW/A/14/55) so the spread (equation (4.11)) may need to be revalued for any angle other than $120^{o}$. However, if $\alpha$ is within 2 or 3 degrees of $120^{o}$, that is from $117^{o}$ to $123^{o}$, equation (4.11) could be used in conjunction with (4. 17) to calculate the draft $\delta$ for filling the pass.

### 4.7.1 Effective Reduction of the Pass

Once the correct size of the daimond pass diagonals for complete filling is obtained, it is a simple matter to calculate the bar elongation. If the initial area of the square bar is $A_1$ and the final area of the outgoing diamond is $A_2$ then

$$A_1 = \frac{H_1^{\ 2}}{2} \quad \text{and} \quad A_2 = \frac{W_2 \,.\, H_2}{2}$$

If the gauge length on the bar is $l_1$ before rolling and $l_2$ after rolling, then because of constancy of the volume

$$l_1 A_1 = l_2 A_2$$

or

$$\frac{l_2}{l_1} = \frac{A_1}{A_2}$$

In terms of natural strain:

$$\ln \frac{l_2}{l_1} = \ln \frac{A_1}{A_2}$$

The elongation and reduction per cent would then become

$$e = 100 \frac{l_2 - l_1}{l_1} = 100 \frac{A_1 - A_2}{A_2} \quad \text{(elongation)}$$

and

$$r = 100 \frac{A_1 - A_2}{A_1} \quad \text{(area reduction)}$$

refering to equations (4.16) and (4.14)

$$r = 100 \left(1 - \frac{W_2 H_2}{H_1^{\,2}}\right)$$

or

$$r = 100 \left(1 - \sqrt{3} \left(\frac{H_2}{H_1}\right)^2\right) \tag{4.18}$$

### 4.8.1 Reduction Vs. Draft, Experimental Verification of Spread Formula

Quantities which are measurable with good accuracy are the diagonal lengths and the gauge lengths inscribed on the bars. From these quantities, measured before and after rolling, actual values of spread, draft and elongation (or area reduction) of the bar can be determined. Every workable theory predicting variations of these factors should be in close agreement with the experimental results. In fig. (4.10) to (4.13) the correlation between the experimental points and the spread curve, equation (4.11), for different temperatures and sizes was shown. Now the spread formula (4.11) is used to calculate the elongation of the bar, for each roll gap setting and the results will be compared with the experimental results.

From the geometry of the square bar and diamond pass, the excess area to be rolled forward is at the top and bottom corners of the bar's vertical diagonal, Fig. (4.17). This area, a b c d and $a^1$ $b^1$ $c^1$ $d^1$ can be expressed in terms of $\delta$. If this area is denoted by $A_R$ then

$$A_R = \frac{\sqrt{3}}{2(\sqrt{3} - 1)} \delta^2 \qquad (4.19)$$

where $\delta$ varies from zero at the entry plane to $H_1 - H_2$ at the exit plane.

Relative to the coordinate system x and y shown in Fig. 4.17 the equations of the diamond contour line and the square bar will be

$$y = \sqrt{3} \quad (x - \delta/2)$$

$$y = x \qquad\qquad bc = \frac{\delta}{2}$$

solving these equations yields the coordinate of the point a

$$x_a = \frac{\sqrt{3}}{\sqrt{3} - 1} \cdot \frac{\delta}{2} \qquad\qquad y_A = \frac{\sqrt{3}}{\sqrt{3} - 1} \cdot \frac{\delta}{2}$$

$$A_R = 2 \cdot bc \cdot y_A$$

$$\therefore$$

$$A_R = \frac{\sqrt{3}}{2(\sqrt{3} - 1)} \cdot \delta^2$$

If the rolls are not touching and rolling is carried out with a certain roll gap setting, or if the square bar is undersize for the pass and cannot fill the pass completely, then formula (4.18) cannot be used to determine the elongation of the bar, it is obvious that the outcoming bar will not be a complete diamond. From the practical point of view no square-diamond rolling is done under these conditions, but the purpose here is to verify the spread formula and to allow comparison between theoretical and experimental values of the bar elongation.

To evaluate the elongation; two cases will be considered: First a hypothetical case where the entire excess area a b c d and $a^1$ $b^1$ $c^1$ $d^1$ is displaced forward by the rolls and spread is zero. In this case, it is an easy task to evaluate the pass reduction. If the original area of the bar is $A_1$, $l_1$ and $l_2$ the gauge lengths before and after the rolling, and $A_R$ the excess area from equation (4.19) then constancy of volume requires

$$l_1 A_1 = l_2 (A_1 - A_R)$$

$$\frac{l_2}{l_1} = \frac{A_1}{A_1 - A_R}$$

$$\frac{l_2 - l_1}{l_1} = \frac{A_R}{A_1 - A_R}$$

since $E_t = \dfrac{l_2 - l_1}{l_1} \times 100$ (elongation per cent)

$$E_t = \frac{\dfrac{\sqrt{3}}{2(\sqrt{3} - 1)}\,\delta^2}{\dfrac{H_1^{\,2}}{2} - \dfrac{\sqrt{3}}{2(\sqrt{3} - 1)}\,\delta^2}$$

$$E_t = \frac{(\delta/H_1)^2}{\sqrt{\dfrac{3 - 1}{\sqrt{3}}} - (\delta/H_1)^2}\ 100 \qquad (4.20)$$

or in terms of the natural strains

$$\ln \frac{l_2}{l_1} = \ln \frac{A_1}{A_1 - A_R}$$

$$e_t = 100 \cdot \ln \frac{l_2}{l_1}$$

$$\therefore \quad e_t = 100 \cdot \ln \frac{\dfrac{H_1^{\,2}}{2}}{\dfrac{H_1^{\,2}}{2} - \dfrac{\sqrt{3}}{2(\sqrt{3} - 1)}\,\delta^2}$$

$$e_t = 100 \ln \frac{1}{1 - \frac{\sqrt{3}}{\sqrt{3} - 1} \left(\delta/H_1\right)^2} \tag{4.21}$$

Equations (4.20) and (4.21) express the bar elongation for the hypothetical case of no spread

In the actual rolling process spread is always present so that the real reduction in the pass is always smaller than $E_t$ or $e_t$.

Due to lateral flow, the material spent for elongation becomes less, thus reducing the elongation of the bar. A fraction of $A_R$, the total excess area displaced by the rolls, flows in lateral direction, if this is denoted by $A_S$, then, from constancy of volume:

$$l_1 A_1 = l_2 (A_1 - A_R + A_S)$$

$$\frac{l_2}{l_1} = \frac{A_1}{A_1 - A_R + A_S}$$

$$\therefore \quad \frac{l_2 - l_1}{l_1} = \frac{A_R - A_S}{A_1 - A_R + A_S}$$

$$E = 100 \frac{l_2 - l_1}{l_1} \quad \text{(elongation per cent)}$$

then
$$E = \frac{100}{\frac{A_1}{A_R - A_S} - 1} \quad (4.22)$$

or in terms of the natural strain

$$\ln \frac{l_2}{l_1} = \ln \frac{A_1}{A_1 - A_R + A_S}$$

if
$$e = 100 \ln \frac{l_2}{l_1}$$

$$\therefore \quad e = 100 \ln \left( \frac{1}{1 - \frac{A_R - A_S}{A_1}} \right) \quad (4.23)$$

Formula (4.22) and (4.23) can easily be calculated for each roll gap setting provided $A_S$ is known. To derive $A_S$ it is necessary to know the lateral flow of the material in the pass. It was mentioned before that except for the diagonal planes deformations of the other sections and areas of the bar are not plane strain and not known as yet. However a simplified form can be assumed. Assuming sticking conditions at the roll, a parabolic distribution of the lateral flow should be close enough to the actual lateral flow profile, and at the same time provide an analytical curve suitable for algebraic manipulation.

Each section of the bar spreads cumulatively from the entry plane to the exit plane, so that if for a plane at distance x from the entry plane the spread is equal to $S_x$, then at a plane distanced $x + \delta x$, the spread would be $S_x + \delta S_x$. The geometrical intersection of the pass contours and the bar surface is $AA^1$ as shown in Fig.(4.18), but due to spread $S_x$, the incremental lateral flow at this section, x, would be distributed over $BB^1$ Fig.(4.18). Now the incremental value of $A_S$, at the section x, can be derived

$$\delta A_S = \frac{2}{3} \cdot \delta S_x \cdot BB^1$$

The length of $AA^1$ can again be calculated from considerations of geometry (For $\alpha = 120^o$)

$$AA^1 = H_1 - \frac{\sqrt{3}}{\sqrt{3} - 1} \delta$$

$BB^1$ can be derived from $AA^1$ Fig.(4.19) again from geometrical considerations:-

$$\frac{S_x/_2}{\text{Sin } 15} = \frac{1}{\text{Sin } 135}$$

$$1 = \frac{S_x}{2} \frac{\text{Sin } 135}{\text{Sin } 15}$$

$$2\ AH = 2 . 1 . \text{Cos } 60 = 1$$

$$2\ AH = 1 = \frac{S_x}{2} \frac{\text{Sin } 45}{\text{Sin}(45 - 30)}$$

$$2\ AH = \frac{S_x}{2} \frac{\sqrt{2/2}}{\sqrt{\frac{2}{2}} . \sqrt{\frac{3}{2}} - \sqrt{\frac{2}{2}} . \frac{1}{2}}$$

$\therefore$

$$2\ AH = \frac{S_x}{\sqrt{3} - 1}$$

therefore

$$BB^1 = H_1 - \frac{\sqrt{3}}{\sqrt{3} - 1} \delta_x - \frac{S_x}{\sqrt{3} - 1} \tag{4.24}$$

and

$$\delta A_S = \frac{2}{3}(H_1 - \frac{\sqrt{3}}{\sqrt{3} - 1} \cdot \delta_x - \frac{S_x}{\sqrt{3} - 1}) \cdot \delta S_x \tag{4.25}$$

The integral of the $\delta A_S$ from the plane of entry (zero spread) to the total spread for each roll gap setting gives $A_S$, thus

$$A_S = \frac{2}{3} \int_o^{S_x} (H_1 - \frac{\sqrt{3}}{\sqrt{3} - 1} \delta_x - \frac{S_x}{\sqrt{3} - 1}) \, d S_x$$

Since $S_x$ is expressed in terms of $\delta_x$ according to the spread formula (4.11), this integral can be evaluated as follows:

$$A_S = \frac{2}{3} \int_0^{S_x} \left(H_1 - \frac{\sqrt{3}}{\sqrt{3} - 1} \delta_x\right) dS_x - \frac{S_x^{\ 2}}{3(\sqrt{3} - 1)}$$

$$A_s = \frac{2}{3} \int_0^{\delta_x} \left(H_1 - \frac{\sqrt{3}}{\sqrt{3} - 1} \delta_x\right) \frac{dS_x}{d\delta_x} \cdot d\delta_x - \frac{S_x^{\ 2}}{3(\sqrt{3} - 1)}$$

and

$$A_S = \left(H_1 - \frac{\sqrt{3}}{\sqrt{3} - 1} \delta_x\right) . S_x + \frac{\sqrt{3}}{\sqrt{3} - 1} \int_0^{\delta_x} S_x \, d\delta_x - \frac{S_x^{\ 2}}{3(\sqrt{3} - 1)} \qquad (4.26)$$

For each roll gap setting corresponding values of $\delta_x$ and $S_x$ of the bar can be measured directly by a micrometer, the integral term can be calculated numerically by using the spread formula for $S_x$ thus $A_S$ is obtainable at each step. If the spread formula (4.11) is used $A_S$ can be calculated from $\delta_x = 0$ to any final value of $\delta$ the draft at the exit plane.

Having calculated $A_S$ for each roll gap setting using equation (4.22) or (4.23), theoretical prediction of the bar elongation; on the basis of the new spread formula (4.11) is obtained. If this prediction agrees well with the experimental measurements, then the new Formula for $S_x$ vs. $\delta_x$ is judged to be valid.

In view of the small figures involved, this calculation was done using the CDC 6600 computer unit. The results are plotted on Fig. (4.20) to Fig. (4.22) by a calcomp plotter. Experimental data for 1/4", 3/8", 1/2", 5/8" square bar has been shown on the same graphs. Considering the approximate nature of the parabolic lateral flow assumption and sensitivity of the calculations and scale of the graphs, in which small values are involved and could increase the computational relative error, the agreement is very good, indicating the soundness of the new spread formula.

### 4.9.1 Summary and Conclusions

A new formula has been found to predict spread in square-diamond rolling, this formula is direct and there is no need to apply flat rolling spread formulae to flat elements of the section. This formula combined with simple geometrical relations allows estimation of the correct size of an ingoing bar to fill a certain pass, or it is possible to find the optimal dimensions of a diamond pass for a certain bar size. Reduction of the pass is simply calculated, Comparison of data for different temperatures of rolling in this type of pass indicates that for low carbon steels spread is not sensitive to temperature variations.

The basic technique used in obtaining experimental curves of draft-spread inside the deforming zone could be applied under various conditions, such as various frictional conditions or different diamond angle or in any particular pass. The corresponding curves should be of the same general form in respect to the dimensionless variables, but the constant powers $\alpha$, $\beta$, $\gamma$ may need modification.

## 4.10 Sample Calculations

Supposing it is desired to find the dimensions of a diamond pass for the optimal reduction of a 1" x 1" square bar in a rolling mill with 7" diameter rolls: Equation (4.10) and (4.15) solved together provide the optimal value of $\delta$

$$S = W_1 \left[ \left(\frac{H_1}{H_1 - \delta}\right)^{e^{-\alpha (R/H_1)^{\beta} \left(\frac{W_1}{\sqrt{R\delta}}\right)^{\gamma}}} - 1 \right] \qquad (4.10)$$

$$S = -\sqrt{3}\,\delta + H_1 . (\sqrt{3} - 1) \tag{4.15}$$

With the exception of R, which was the smallest radius of the pass (radius at the wide corner of a diamond pass) every other parameter is known. So in the first approximation we may take $R = \frac{D}{2} = 3.5''$

then:

$$R = 3.5$$

$$H_1 = 1{,}4142$$

$$W_1 = 1{,}4142$$

and the optimal value of draft and corresponding spread will be:

$$\delta = 0.5220$$

$$S = 0.1184$$

Then the approximate geometry of the diamond pass will be

$$a = 1{,}4142 + 0{,}1184 = 1{,}5326$$

$$b = 1{,}4142 - 0{,}5220 = 0.8922$$

Now the correct value of R can be derived for a second calculation

$$R = 3.5 - \frac{b}{2}$$

$$R = 3,5 - .446$$

$$R = 3,0539$$

with the value of R the correct values of draft and spread are found

$$\delta = 0,528$$

$$S = 0,1201$$

in this case correction of R does not seem to have a significant effect so the final dimensions of the pass will be:

$$a = 1,5343$$

$$b = 0,8862$$

Thus the area reduction will be:

$$r = \frac{A_1 - A_2}{A_1} = \frac{1 - 1,5343 \times 0.4431}{1} = 32\%$$

# CHAPTER FIVE

## Roll Force and Torque Calculations

### 5.1 Introduction and Background

The start and development of rolling theories for estimation of load and torque has been mainly for the flat rolling process. Occasional attempts have been made to apply flat rolling theories to section and profile rolling. Pioneer work on the analytical treatment starts with Siebel (21) and Von Karman (22), as early as 1924. Prior to this date rolling mill design was considered a craft and a question of experience rather than of engineering science. No analytical basis existed for the determination of rolling mill dimensions.

Von Karman (22), starting from basic assumption of homogeneous deformation, in which initially plane cross sections remain plane during rolling, and sliding friction exists between the rolls and the rolled material, derived and solved the basic differential equation of the process. Karman's basic equation is the equilibrium condition of the forces acting on vertical segment of the material in the plastically deforming zone, fig.(5.1)

$$\frac{df}{d\phi} = DS \sin \phi \pm D\mu S \cos \phi \qquad (5.1)$$

+ and - refer to the exit and entry side of the rolls respectively. On this equation f(Ø) and S(Ø) are unknowns, thus a second relation is necessary between S(Ø) and f(Ø), Karmen used the yield criterion of Von Mises for plane strain and derived an expression for S(Ø). In this approach since deformation is presumed to be homogeneous the problem becomes statically determinate. Karman's theory has proved to be a very good starting point for subsequent development of the theory. In fact in cold rolling with smooth rolls ( where the frictional coefficient is less than 0.1), the Karman theory is quite practical.

Siebel (21) roughly assumed that the vertical pressure on the rolls, all along the arc of contact, is equal to the yield stress in plane compression.

The Mechanics of flat rolling is made more clear by later investigations. N. Sobolevski (1933) expressed the view that the metal being rolled does not necessarily slip along the surface of the rolls, in the case of rolling thick strip with a small arc of contact (i.e. small rolls), There are grounds to believe that slip is absent. Sobolevski put forward practical arguments against slipping friction in (1935, 1936), (24).

Orowan (1943), (25) was the first to present a solution based on the hypothesis of sticking friction. He has provided means for calculating results with mixed sticking and slipping friction. Orowantried to do away with as many approximate assumptions as possible. Although using Karman's basic equilibrium equation (5.1), he discarded the assumption of homogeneous deformation. This he did by assuming that deformation resembled compression between rough inclined platens, and by using the Prandtl-Nadai stress distribution in a plastic wedge compressed between non-parallel plates (26). With this assumption he calculated f the horizontal force in the equilibrium equation, (5.1). Orowan's theory although used as a standard for comparing different rolling theories has not been generally applied to mill design calculations because of the time needed to complete the calculations for each pass.

Bland and Ford applying simple assumptions have solved equation (5.1) for the case of cold rolling (slipping friction), with considerable simplicity and yet the deviation from Orowan's exact method is less than 2% (27).

R. B. Sims (28) (1954), assuming the condition of sticking friction along the entire arc of contact - this is the case of hot rolling, where frictional coefficient is high - and other simplifying assumptions such as

$$\sin\theta = \tan\theta = \theta \quad \cos\theta = 1 \quad 1 - \cos\theta = \frac{\theta^2}{2}$$

solved Karman's equilibrium equation.

Sims's method has been investigated experimentally by Stewartson (29), and agreement with the theory is shown to be very good. Sims's method of calculating was later modified by Cook and McRum (30). This, combined with their measurement of yield stress at high temperature and different strain-rates for a number of materials, has provided a graphical method for roll force and torque calculations. This general technique is called the B.I.S.R.A. method and its correctness under actual production conditions has been investigated by R. B. Sims and Wright (1962) (31).
So far all these methods have used Von Karman's basic equilibrium equation, in which, as mentioned before deformations do not enter into the calculations.
According to a basic theorem due to Hencky (1923), in

the case of plane strain, the stress distribution can be determined without any knowledge of the corresponding deformation. Prandtl's solution of the problem of a compressed plastic slab was subsequent to this theorem, so even Orowan's original solution of the rolling problem does not account for deformations. Exact solution of the rolling problem is a formidable task and it was not attempted until geometrical representation of the equations for plane strain flow of a plastic-rigid solid (the slip line field) was presented in 1953 by W. Prager (32).

In the slip line field approach, which is applicable to rigid plastic material, every solution satisfies equilibrium condtiions, the yield criteria and flow equations, this is achieved through construction of a stress plane and velocity plane (hodograph) for the plastically deforming zone. In so far as the velocities of the rigid zone are made compatible with the boundary conditions, and the stresses in the rigid zone may remain undetermined, slip line field solutions are all upper bound solutions, i.e. over-estimating the yield load. In this case any solution is incomplete and only a partial solution to any given problem. If the stress field is extended into the rigid zone, and shown to be in statical equilibrium with the deforming zone, then, as this is a "statically admissable stress field" the solution becomes at the same time a lower bound. In this case the solution becomes complete and the exact load is determined (for the rigid plastic material assumed).

Shortly after Prager's geometrical representation, J.M. Alexander (33) proposed a partial solution for hot rolling with the assumption of complete sticking condition along the arc of contact. This solution is only for one given set of conditions (Roll radius R = 15", strip thickness $h_1$ = 0.259", exit thickness $h_2$ = 0.173), and yet because of statically indeterminate nature of the problem, it is necessary to proceed by continually modifying the solution until the velocity and stress planes are simultaneously satisfied. The complete solution to this problem was obtained by Alexander and Ford (34), in which the stress field is extended into the rigid zones without violating the yield criterion while the rate of energy dissipation is shown to be positive. The only draw-back of this theory was its limitation to one set of conditions. Determination of the additional solutions for presumed geometries was very time consuming. Alexander and Ford have overcome this limitation by presenting a simplified form of the slip line field, in which the entry slip line is straight and the exit slip line is made into a circular arc (35). In its present form, in conjunction with mean field stress against strain rate at various temperatures, this theory is a viable tool for simple load and torque calculations.

Another method which may be applied to rolling problems is the upper bound technique, in which an admissible velocity field is assumed, and from that the energy of plastic deformation derived. This approach has been used by Avitzur (34) and (37). The upper bound method is also applicable to rigid perfectly plastic solids (i.e. no work hardening or rate effects), in fact velocity discontinuities are admissible with such solids. This method is useful only to obtain approximate solutions. while in cases where the slip line field solution is complete, such as hot rolling, the solution is exact.

The general conclusion is that the best theoretical model of plastic deformation in hot rolling is provided by slip line field theory. The solution in this case is exact and in the mathematical sense superior to the methods described previously.

## 5.2 General Analysis

As previously described in Chapter 4, for square-diamond rolling the non-homogeneous nature of the deformation and lateral flow of the material in the pass, renders any exact calculations difficult. Methods of plane strain can no longer be applied here directly. Generally exact calculations of the yield load, and there on power requirement, for any plastic forming process, involves the solution of the following equations:

$$\begin{aligned}
&(1) \quad \frac{\partial \sigma_x}{\partial_x} + \frac{\partial \tau_{xy}}{\partial_y} + \frac{\partial \tau_{xz}}{\partial_z} = 0 \\
&(2) \quad \frac{\partial \tau_{yx}}{\partial_x} + \frac{\partial \sigma_y}{\partial_y} + \frac{\partial \tau_{yz}}{\partial_z} = 0 \\
&(3) \quad \frac{\partial \tau_{zx}}{\partial_x} + \frac{\partial \tau_{zy}}{\partial_y} + \frac{\partial \sigma_z}{\partial_z} = 0
\end{aligned} \quad \left. \vphantom{\begin{aligned} a \\ b \\ c \end{aligned}} \right) \text{ equilibrium}$$

$$(4) \quad \frac{\partial u}{\partial x} = \lambda(2\sigma_x - \sigma_y - \sigma_z)$$

$$(5) \quad \frac{\partial v}{\partial y} = \lambda(2\sigma_y - \sigma_x - \sigma_z)$$

$$(6) \quad \frac{\partial w}{\partial z} = \lambda(2\sigma_z - \sigma_x - \sigma_y)$$

$$(7) \quad \frac{\partial u}{\partial y} + \frac{\partial v}{\partial x} = 6\lambda\ \tau_{xy}$$

$$(8) \quad \frac{\partial v}{\partial z} + \frac{\partial w}{\partial y} = 6\lambda\ \tau_{yz}$$

$$(9) \quad \frac{\partial u}{\partial z} + \frac{\partial w}{\partial x} = 6\lambda\ \tau_{zx}$$

$$(10) \quad (\sigma_x - \sigma_y)^2 + (\sigma_y - \sigma_z)^2 + (\sigma_z - \sigma_x)^2 + 6\tau_{xy}^{\ 2} + 6\tau_{yz}^{\ 2} + 6\tau_{zx}^{\ 2} = 6K^2$$

equation (10) is the yield criteria. These equations should all be valid for every small element cut off from the rest of the material, in fact they are derived from the equilibrium, flow and yield of a microscopic element. In practice every forming problem is subject to boundary conditions whether force or velocity, and particular geometry of the deformations. These restrictions make the problem statically indererminate. Equations (1) to (10) have been solved for a few cases.

Hill (38) found the solution for extrusion of a plastic material from a cylindrical die which narrows in the radial direction. Brovman and Genzelev (39) have found the solution for extrusion from a square die, in which the sides approach one another at a constant rate. The method of solution is semi-inverse, in which some of the unknowns like u, v, $\tau_{xy}$ are presumed, then on this basis the remainder of the unknowns can be calculated. It is obvious that assumptions of u, v, or $\tau_{xy}$ as known values is not arbitrary, they are observed to be compatible with the boundary conditions and the nature of the problem with intuition and physical insight. In plane strain cases, field type solutions such as the slip line field, have incorporated all these equations into an ingenious technique with the result of much relative simplification; and yet finding complete slip line field solutions requires great intuition. Such techniques are not available in three-dimensional cases, thus direct solution of equations (1) to (10) is necessary for any complete solutions.

In the case of square-diamond deformation; from the spread formula given in Chapter 4 it is easily observed that although inclined surfaces of the pass restrict the amount of spread, yet there is a definite departure from plane strain deformation. Unfortunately since the mechanics of deformation in this type of pass are not known, no reasonable assumptions of velocity or shear stress distribution can be made to facilitate the solution of equations (1) to (10). The exact solution is an almost hopelessly difficult problem, however for practical calculations it is possible to modify some plane strain formula. This approach has been adopted here.

## 5.3 New Formula

As discussed in section 5.1, the slip line field solutions for hot rolling by Alexander and Ford constitute an exact solution; in which considerations of deformations are inclusive while other formulae based on Karman's equilibrium equation are not exact. However experimental comparison between the results of Alexander and Ford and R.B. Sims's analysis (which is commonly used) shows good agreement (35). For practical calculation of load or torque the Alexander and Ford formula is much simpler and even hand calculations with sufficient accuracy are possible. Being exact and simple to apply this formula is shown to give a simple method for load and torque calculation for the square-diamond rolling process.

### 5.3.1 Load Formula

The original formula, giving load per unit width of the strip in hot rolling is expressed as

$$\frac{P}{k} = L \left(1{,}571 + \frac{L}{h_1 + h_2}\right) \qquad (5.2)$$

referring to Fig.(5.2) L, $h_1$ and $h_2$ are variables of x as measured from the diagonal, so

$$\delta_x = h_{1x} - h_{2x} = (h_1 - h_2)\left(1 - \frac{2x}{\overline{w}}\right) \qquad (5.3)$$

where $\overline{w} = \dfrac{2w_2 + w_1}{3}$

is the average width of the bar

$$L_x = \sqrt{R_x(h_{1x} - h_{2x})} = \sqrt{R_x(h_1 - h_2)\left(1 - \frac{2x}{\overline{w}}\right)} \qquad (5.4)$$

$R_x$ is the radius of the rolls at the distance x, relative to the roll radius variation of $R_x$ is not very much. Calculations would be easier if an average $R_x$ is taken. Since $\alpha = 120^o$ then $Tg\ \alpha = \sqrt{3}$

$$R_x = R(1 + \frac{x}{\sqrt{3}}) \quad (5.5)$$

$$R_m = \frac{2}{\overline{w}} R \int_o^{\frac{\overline{w}}{2}} (1 + \frac{x}{\sqrt{3}})\, dx$$

$$R_m = R + \frac{\overline{w}}{4\sqrt{3}} \quad (5.6)$$

(R is the smallest radius of the pass).

Now for the width $\delta x$ the load is $\delta P$ and equation (5.2) is expressed as:

$$\frac{\delta P}{\overline{k}} = \sqrt{R_m(h_1 - h_2)(1 - \frac{2x}{w})} \quad [1,571 + \frac{\sqrt{R_m(h_1 - h_2)(1 - \frac{2x}{w})}}{(h_1 + h_2)(1 - \frac{2x}{w})}]\ \delta x$$

if $L_o = R_m(h_1 - h_2)$ then

$$\frac{\delta P}{\overline{k}} = L_o\ [1,571 \sqrt{(1 - \frac{2x}{w})} + \frac{L_o}{h_1 + h_2}]\ \delta x$$

and the total load will be

$$\frac{P_t}{\overline{k}} = 2 \int_o^{\frac{\overline{w}}{2}} L_o\, [1,571( 1 - \frac{2x}{w}) + \frac{L_o}{h_1 + h_2}]\ dx$$

$$\frac{P_t}{\overline{k}} = 2\ L_o\ [1,571 \cdot \frac{w}{3} + \frac{w\ L_o}{2(h_1 + h_2)}]$$

or $$\frac{P_t}{\bar{k}} = L_o \, [1{,}57 \cdot \frac{2}{3} \dot{w} + \frac{w \, L_o}{h_1 + h_2}]$$

and the load per unit width of the bar will be

$$\frac{P}{\bar{k}} = \frac{P_t}{\bar{w} \, \bar{k}} \tag{5.7}$$

$$\frac{P}{\bar{k}} = L_o \, [1{,}0474 + \frac{L_o}{h_1 + h_2}] \tag{5.8}$$

This formula is as simple as (5.2) for flat rolling except for the constant value of 1,571 which is replaced by 1,0474.

### 5.3.2 Torque Formula

The original formula of Alexander and Ford giving Torque per unit width of the strip in hot rolling is expressed as

$$\frac{G}{\bar{k}} = L_o^2 \, [1{,}571 + \frac{2L_o}{3} \frac{h_1 + 2h_2}{(h_2 + h_2)^2}] \tag{5.9}$$

refering to figure (5.2) L, $h_1$, $h_2$ are again functions of x so that at the distance x

$$\frac{Gx}{\bar{k}} = L_x{}^2 [1{,}571 + \frac{2L_x}{3} \frac{h_{1x} + 2h_{2x}}{(h_{1x} + h_{2x})^2}]$$

Quantities $L_x$, $h_{1x}$, $h_{2x}$ are functions of x according to equation (5.3) to (5.5) in the previous section. The torque per unit width can be derived in a similar manner, for the width δx the torques will be $\delta G_x$

$$\frac{\delta Gx}{\overline{k}} = R_m(h_1-h_2)(1-\frac{2x}{w})[1,571 + \frac{2\sqrt{R_m(h_1-h_2)(1-\frac{2x}{w})}}{3} \cdot \frac{(h_1+2h_2)(1-\frac{2x}{w})}{(h_1+h_2)^2(1-\frac{2x}{\overline{w}})^2}] \; dx$$

as before the total torque can be calculated;

$$\frac{G_t}{\overline{k}} = 2\int_0^{\frac{\overline{w}}{2}} L_o^2 \; 1,571(1-\frac{2x}{\overline{w}}) + \frac{2L_o}{3}\frac{h_1+2h_2}{(h_1+h_2)^2}\sqrt{(1-\frac{2x}{\overline{w}})} \quad dx$$

and

$$\frac{G_t}{\overline{k}} = L_o^2[1.571 \cdot \frac{\overline{w}}{2} + \frac{2}{3} L_o \frac{h_1 + 2h_2}{(h_1 + h_2)^2} \cdot \frac{2\overline{w}}{3}]$$

again

$$\frac{G}{\overline{k}} = \frac{G_t}{\overline{wk}} \quad \text{torque per unit width} \tag{5.10}$$

and torque per unit width for square diamond pass will be:

$$\frac{G}{\bar{k}} = L_o^2 \left[ \frac{1,571}{2} + \frac{4}{9} L_o \frac{h_1 + 2h_2}{(h_1 + h_2)^2} \right] \tag{5.11}$$

Torque formula has the same simple expression except for the constants $\frac{1,571}{2}$ and $\frac{4}{9}$. Equations (5.8) and (5.11) are simple to use, provided $R_m$, $h_1$, $h_2$ and $\bar{k}$ are known. Except for $\bar{k}$ these values are calculated in conjunction with the spread formula derived in the previous chapter, a sample calculation is given in section (4.10)

$\bar{k}$ is in general a function of strain rate and strain hardening, but in the case of hot rolling the effect of strain hardening is compensated by thermal softening, which continually annihilates the strain hardening, thus hardening cannot accumulate. So for hot rolling the important factor for determining $\bar{k}$ is the strain rate which is dependent on the rolling speed.

### 5.3.3 Strain Rate

It is necessary to define a mean value of the strain rate in the pass in order to choose the correct stress-strain data for estimating the value of $\bar{k}$.

There are three formulae to account for flat rolling mean strain rate. The first one proposed by Orowan and Pascoe (40) in 1946 is

$$\bar{\lambda} = \frac{V_N}{\sqrt{Rh_1}} \sqrt{r} \quad [\frac{1 - \frac{3}{4}r}{1 - r}] \tag{5.12}$$

the second formula put forward by R.B. Sims (28), (1954) is

$$\bar{\lambda} = \frac{V_N}{\sqrt{Rh_1}} \frac{1}{\sqrt{r}} \quad \ln \frac{1}{1 - r} \tag{5.13}$$

the third formula has been put forward by Alexander and Ford (1964), this formula in the exact form is expressed as

$$\bar{\lambda} = \frac{V_N}{\sqrt{Rh_1}} \sqrt{r} \quad [\frac{4 - 3r}{(2 - r)^2}] \tag{5.14}$$

and in approximate form is expressed as

$$\bar{\lambda} = \frac{V_N}{\sqrt{Rh_1}} \sqrt{r} \quad [1 + \frac{r}{4}] \tag{5.14a}$$

both of the formulae prososed by Orowan - Pascoe and R.B. Sims give higher values of strain rate in comparison with the Alexander - Ford formula (35). However, as stated by El-Kalay and Sparling (41) Sims's formula is based on the angular velocity of the rolls and not the angular velocity of the metal in the pass, becuase of backward and forward slip the angular velocity of the metal is different from the rolls. So Sims's formula for mean strain rate is not considered to be sufficiently accurate for medium and large reductions.

For square-diamond passes the mean strain rate will be calculated on the basis of the Alexander and Ford formula. Refering to fig.(5.2) the respective variable quantities at the distance x from diagonal will be

$$V_n = \frac{2\pi R_m N}{60}$$

$$L_x = \sqrt{R_m(h_1 - h_2)(1 - \frac{2x}{\overline{w}})}$$

$$r_x = \frac{h_1 - h_2}{h_1} \cdot \frac{(1 - \frac{2x}{w})}{(1 - \frac{2x}{w})} \quad \therefore r_x = \frac{h_1 - h_2}{h_1}$$

and the mean strain rate for the square-diamond pass will be

$$\overline{\lambda}_m = \frac{2}{\overline{w}} \int_o^{\frac{\overline{w}}{2}} \frac{V_N}{\sqrt{R_m h_1 (1 - \frac{2x}{\overline{w}})}} \sqrt{r} \; [\frac{4 - 3r}{(2 - r)^2}]dx$$

and

$$\bar{\lambda}_m = \frac{V_n}{\sqrt{R_m h_1}} \sqrt{r} \left[\frac{4 - 3r}{(2 - r)^2}\right] . \frac{2}{\bar{w}} . \int_o^{\frac{\bar{w}}{2}} (1 - \frac{2x}{\bar{w}})^{-\frac{1}{2}} dx$$

$\therefore$

$$\bar{\lambda}_m = \frac{2V_n}{\sqrt{R_m h_1}} \sqrt{r} \left[\frac{4 - 3r}{(2 - r)^2}\right] \qquad (5.15)$$

equation (5.15) is the same as (5.14) except for a coefficient of 2.

### 5.3.4 Yield Stress in Compression

In every metal forming operation calculations of load and torque require a knowledge of the yield strength of the material. For cold working processes, the experimental determination of appropriate yield stress-strain curves is a reasonably easy task, and data for a wide range of ferrous and non-ferrous material is available. In hot rolling the situation is complicated owing to the fact that yield strength is affected by temperature as well as strain rate. In every meaningful stress-strain curve these two factors should be considered and taken care of. P.M. Cook (42) using a high speed compression-test machine equipped with a Cam plastometer - as described by Orowan (43) - for maintaining a constant rate of strain, has provided stress-strain data for a range of different types of steel at the temperature and deformation rates applicable to the hot rolling process (20).

Cook's results are based on 25 mm. high 18 or 12 mm. diameter cylindrical specimens in free compression tests. Cook applied molten glass to minimize friction at the interfaces of the compression platens and the specimen in order to obtain homogeneous free compression. In square-diamond rolling, the compressing mode is closer to plane strain, rather than free compression. For plane strain compression therefore, Cook and McRum (30), using the true stress (Y)/natural strain ($\varepsilon$), data obtained in cam plastometer by Cook, have calculated and plotted two sets of curves, for calculations of load and torque in flat rolling. Graphs of a parameter, $J_P = \bar{k} \left(\frac{1 + r}{1 - r}\right)^{\frac{1}{2}}$ are given in terms of strain rate and reduction , for fifteen different steel qualities at 900°C, 1000°C, 1100°C and 1200°C. From this parameter, $\bar{k}$ can be calculated $\bar{k} = J_P \left(\frac{1 - r}{1 + r}\right)^{\frac{1}{2}}$, which is the mean compressive yield in plane strain, at the given conditions of temperature, strain rate and reduction of the pass. Similar graphs, $J_G$, are introduced for derivation of mean compressive yield in plane strain for calculations of torque in flat rolling. For experimental data the values of $\bar{k}$ were derived only from $J_p$ graphs.

If the true stress (Y)/natural strain ($\epsilon$) data obtained by Cook (42) is used for calculations of $\bar{k}$, it should be remembered that since this data is for uniaxial compression, to make it useful for plane strain comditions the equivalent stress and strain should be considered, that is, the stress scale should be multiplied by $2/\sqrt{3}$ and strain scale should be multiplied by $\sqrt{3}/2$.

## 5.4 Experimental Data

If the load and torque formulae (5.8) and (5.11) are divided by $h_1$ and $h_1^2$ respectively, two dimensionless terms $\frac{P}{\bar{k}h_1}$ and $\frac{G}{\bar{k}h_1^2}$ will be obtained. By rearranging the right hand side of the equation we will have:

$$\frac{P}{\bar{k}h_1} = \frac{L_o}{h_1}\left[1,0474 + \frac{L_o}{h_1 + h_2}\right]$$

or

$$\frac{P}{\bar{k}h_1} = 1,0474\sqrt{\frac{R_m \cdot r}{h_1}} + \frac{R_m \cdot r}{h_1(2-r)} \tag{5.16}$$

and similarly the torque equation will be

$$\frac{G}{\bar{k}h_1^{\,2}} = \left[ \frac{1,571}{2} + \left(\frac{4}{9}\right) \frac{3 - 2r}{(2 - r)^2} \sqrt{\frac{R_m r}{h_1}} \right] \frac{R_m . r}{h_1} \qquad (5.17)$$

From (5.16) and (5.17) it is clear that the two geometric parameters of the process are $R_m/h_1$ and $r = \frac{h_1 - h_2}{h_1}$

$R_m/h_1$ accounts for the relative size of the rolls and the bar and it remains constant for each bar size. From chapter 4, r has an optimal value for each bar size to fill the diamond geometry, thus the bar size and the roll radius are sufficient for calculating the terms $\frac{P}{\bar{k}h_1}$ and $\frac{G}{\bar{k}h_1^{\,2}}$, from which, knowing $\bar{k}$, load and torque per unit width are calculated. On figures (5.3) to (5.10) experimental data is shown together with theoretical $\frac{P}{\bar{k}h_1}$ and $\frac{G}{\bar{k}h_1^{\,2}}$ versus for each bar size. The terminal point I on each curve constitutes the optimal r for which the diamond geometry is completely filled. From equations (4.10) and (4.15) in chapter 4, using average value of radius from equation (5.6), optimal values of r, are easily calculated

for 1/4 square bar r = 0.3461

for 3/8 square bar r = 0.3578

for 1/2 square bar r = 0.3684

for 5/8 square bar r = 0.3765

The experimental data, which was obtained for increasing values of r, by progressive closing of the roll gap, shows convergence to the terminal point I, which is the actual operating point of the square diamond rolling.

5.5 General Note

Conclusions of chapter four and chapter five provide an easy method for finding the dimensions of a diamond pass and determination of the load and torque.

a) Optimal draft $\delta = h_1 - h_2$, for a certain bar size and roll radius can be calculated form the solution of (4.10) and (4.15). The solution is easily effected by a simple computer program or plotting the equations on graph paper. The values of $\delta$ and spread thus obtained, determine the diagonals of the diamond pass

$$a = w_1 + S$$

$$b = h_1 - \delta$$

b) With the known values of $r = \frac{\delta}{h_1}$, roll radius and the final spread, equations (5.8) - (5.11) or (5.16) - (5.17) enable load and torque per unit width to be calculated. $\overline{k}$ can be determined from Cook and McRum (30).

## Further Discussion and Conclusions

The formula of spread in chapter four (4-10), is in close agreement with the experimental data obtained under effective control of the superficial scale. The scale was always kept at a low level. However in the normal operation of the rolling mill, scale is present and its effects on the spread must be accounted for.

It is well understood that scale acts as a poor and variable lubricant, but in general it has a reducing effect on the frictional coefficient which in turn reduces the frictional forces. Roll pressure and frictional forces determine the stress distribution and therefore strains in the plastically deforming zone. Unfortunately so far there has not been a reliable method of assessing a realistic effective coefficient of friction with hot scaled materials.

There are some empirical formulas in which spread is shown to be related to the coefficient of friction. The formula by one author (16)Fedosov,quoting from B. Bakhtinov, gives an empirical formula of the form:

$$s = 1.15 \, \frac{\delta}{2h_1} \left( \sqrt{R\delta} - \frac{\delta}{f} \right)$$

for spread in the hot rolling of bars. From this formula it is clear that spread and friction both decrease or increase together. R. C. Skelton (20) in a series

of rolling experiments with heavily and lightly scaled bars has found that heavily scaled bars have a smaller lateral spread than lightly scaled bars.
In the case of square-diamond rolling, as the inclined walls of the pass restrict the lateral spread it is probable that the difference between the amount of spread for heavily and lightly scaled square bars is not as large as when there is free and unrestricted lateral spread. However, in view of the general observations by R. C. Skelton and B. Bakhtinov, it can be stated that for the average conditions of rolling practice, the new formula (4-10) can be considered as providing a maximal value of spread and can therefore be used as an upper bound.

From careful observation of the experimental data for load and torque (fig. 5-3 to fig. 5-10) it is revealed that while experimental data is converging to the terminal point I, which corresponds with filling the diamond pass, the experimental data for load falls some 20% lower than predicted by the theory (point I). It may also be observed that the experimental data for 5/8 in. square bar (Fig. 5-6) has the largest margin of difference.

As the theoretical and experimental background of the equations (5-2) and (5-9) from which the equation (5-8) and (5-11) are derived has been well explored, the discrepancy must have been caused from some uncontrolled mechanical source rather than a flaw in the basic theory. The discrepancy can be arising from the following sources.

a) Due to mill spring (elastic stretch of the bearing mounts) the experimentally recorded load P is somewhat less than it would be in a perfectly rigid mill. This effect is more pronounced towards the terminal point I where the loads are maximum. In the case of data for 5/8 in. square bars the corresponding diamond pass (Fig. (2-1)) is located next to the roll neck, and very close to the right bearing mount. The result is to increase the effect of mill spring. The diamond pass for 1/4 in. square bar, is similarly located next to the left bearing mount, and again may result in increased mill spring.

b) Due to slight departure from the case of plane strain deformation, the yield strength in plane strain which should be $2/\sqrt{3}$ times more than the yield strength in uniaxial compression (15.5%more) may not in fact increas so much. Since there is a slight departure from the state of plane strain the actual yield strength should lie between the two states, of course closer to the plane strain state. However this introduces a slight error of over estimating $\bar{k}$ in calculations.

Considering the load parameter, $\frac{P}{\bar{k}h_1}$, both of these effects work in the same direction, that is to under estimate the experimental value of the load parameter. Accounting for these effects the margin of discrepancy would be greatly reduced. The equations (5-8) and (5-11) provide, if not real estimates, slight over-estimates of the load and torque for square-diamond rolling.

## Suggestions for Further Work

The new spread formula (4-10), indicates the general form of the spread equation for square-diamond rolling. It also shows the basic geometrical parameters involved in the process, namely $R/h_1$ and $W/\sqrt{R\delta}$.

For different diamond pass angles, McCrum* has indicated that spread also depends on the pass angle. Considering the general form of the spread formula, the coefficients, $\alpha$, $\beta$ and $\gamma$ can be investigated for any other pass angle by a similar approach.

For average conditions of rolling practice, where formation of scale is inevitable, the values of $\alpha$, $\beta$ and $\gamma$, which might be slightly different should be investigated.

* A.W. McCrum BISRA Report MW/A/14/55

The best method would be to carry out investigations under controlled conditions. Uncontrolled scale has a randomizing effect on the spread measurements. The results should be considered from a statistical view point. A whole series of experiments in the current work became inconclusive, because the scale formation was not effectively controlled. Small sections such as the 1/4" to 5/8" square bars used in this resarch are more sensitive to variations of frictional forces, and the magnitude of the relative errors is greater. Experiments with larger sections, that is 3/4 in. square bars and over, would provide more conclusive data, but would need to be carried out on a larger rolling mill. If the amount of scaling can be controlled it would be advantageous to maintain a corrosive atmosphere, for instance to allow oxygen flow into the heating furnace. Then the two limits of low and high scaling conditions could be compared, and the general effect of scaling more precisely determined.

# APPENDIX

The computor programs for some of the difficult calculations are listed here for easy reference.

I Computer program for elongation calculations

Equation (4.26) for the analytical calculationsof the square bar elongation involves numerical calculation of the integral term

$$As = \frac{2}{3}\left[\left(H_1 - \frac{\sqrt{3}}{\sqrt{3}-1}\,\delta x\right) \cdot S_x + \frac{\sqrt{3}}{\sqrt{3}-1}\int_0^{\delta_x} S_x \, dS_x\right] - \frac{S_x^{\,2}}{3(\sqrt{3}-1)} \qquad (4.26)$$

This was best achieved by the computor precision. The computor program here is given for analytical calculations and calcomp plot of the results. The experimental data in the program is for 1100$^{\circ}$C series.

```
JOB(UMEM045, CM 35000 ,T50,D1)          SOURESRAFIL  IC  FIT
RUN(S,,,,,,5000)
REQUEST(TAPE27,HI,X) IC CALCOMP TAPE    WRITE PERMIT
LGO.
,
      PROGRAM MAIN(INPUT,OUTPUT,TAPE5=INPUT,TAPE6=OUTPUT,TAPE27,TAPE25)
C     THIS IS CALCOMP PROGRAM FOR ELONGATION VS. DRAFT PERCENTAGE
      DIMENSION  X(8) , Y(8)
      DIMENSION YL(112) , YM(182) , YN(242) , YP(322) ,H(4),KK(4)
      DIMENSION XA(112) , XB(182) , XC(242) , XD(322)
      DIMENSION YA(112) , YB(182) , YC(242) , YD(322) , FL(4,322)
      DIMENSION            AA(4,322) ,BB(4,322) ,AS(4,322)
      DIMENSION F(4,322) , AR(322) , AO(4)
      DIMENSION  YTA(112) , YTB(182) , YTC(242) , YTD(322)
      DIMENSION EL1(10) , EL3(10) , EL2(10) , EL4(10)
      DIMENSION HD(10) , HC(10) , HB(10) , HA(10)
      COMMON/CC/ S(4,322)
      DATA(EL1(I) , I=1,8)/ 1.58, 2.77, 4.61, 6.54, 11.31, 19.57,
     A 23.07 , 25.22 /
      DATA(EL2(I) , I=1,8)/ 3.25, 3.75, 8.75, 14.0, 18.85, 24.7,
     B 29.05, 33.5 /
      DATA(EL3(I) , I=1,8)/3.87, 5.14, 9.8, 14.13, 18.9, 26.43,
     C 29.87, 30.63 /
      DATA(EL4(I) , I=1,8)/2.41, 5.04, 10.4, 14.32, 19.53, 25.25,
     D 31.21, 34.86 /
      DATA( H(I) , I= 1,4) / 0.3438 , 0.5198 , 0.6895 , 0.8686 /
      DATA(KK(I), I=1,4)/110,180 , 240 , 320 /
      DATA( AO(I) , I=1,4) /0.0581 , 0.13475 , 0.23755 , 0.37866 /
      DO 16 K = 1,110
      XX = FLOAT(K) /2000.
      YTA(K) =  ( 946.41*(XX/H(1) )**2 )/ (1.-9.4641*(XX/H(1) )**2 )
   16 CONTINUE
      DO 17 K = 1,180
      XX = FLOAT(K) /2000.
      YTB(K) =  ( 946.41*(XX/H(2) )**2 )/ (1.-9.4641*(XX/H(2) )**2 )
   17 CONTINUE
      DO 18 K = 1,240
      XX = FLOAT(K) /2000.
      YTC(K) =  ( 946.41*(XX/H(3) )**2 )/ (1.-9.4641*(XX/H(3) )**2 )
   18 CONTINUE
      DO 19 K = 1,320
      XX = FLOAT(K) /2000.
```

```
      YTD(K) =  ( 946.41*(XX/H(4) )**2 )/ (1.-9.4641*(XX/H(4) )**2 )
      AR(K) = 4.73204*XX**2
   19 CONTINUE
      KA =1
      CALL START
    1 READ(5,10) (X(I) , I = 1,8)
      READ(5,10) (Y(I) , I = 1,8)
      WRITE(6,20) (X(I) , I=1,8)
      WRITE(6,15) (Y(I) , I=1,8)
      GO TO( 21, 22, 23, 24), KA
   21 DO 31 I = 1,8
      HA(I) = 100.*X(I)/H(1)
   31 CONTINUE
      GO TO 2
   22 DO 32 I = 1,8
      HB(I) = 100.*X(I)/H(2)
   32 CONTINUE
      GO TO 2
   23 DO 33 I = 1,8
      HC(I) = 100.*X(I)/H(3)
   33 CONTINUE
      GO TO 2
   24 DO 34 I = 1,8
      HD(I) = 100.*X(I)/H(4)
   34 CONTINUE
    2 KA = KA + 1
      IF ( KA .LE. 4 ) GO TO 1
      KA = 1
      CALL TAB
      DO 40 I = 1,4
      SS= 0.0
      JJ = KK(I)
      DO 40 K = 1, JJ
      XX = FLOAT(K)/1000.
      SS = SS + (0.001)*S(I,K)
      AA(I,K) = ( H(I) - 2.36605*XX)*S(I,K)
      BB(I,K) = ( 1./(2.*(SGRT(3.) -1.)) )*S(I,K)**2
      AS(I,K) =(2./3.)*( AA(I,K) + 2.36605*SS - BB(I,K))
      FL(I,K) =100. *  AS(I,K)/( AO(I) - AR(  K) )
      F(I,K) = (100.)*(AR(K) - AS(I,K) )/( AO(I) -AR(K) + AS(I,K) )
   40 CONTINUE
      DO 70 K = 1, 110
```

```
      XA(K) = FLOAT(K) /(10. *H(1) )
      YA(K) = FL(1,K)
      YL(K) = F(1,K)
   70 CONTINUE
      DO 75 K = 1 , 180
      XB(K) = FLOAT(K) /(10. *H(2) )
      YB(K) = FL(2,K)
      YM(K) = F(2,K)
   75 CONTINUE
      DO 80 K = 1, 240
      YC(K) = FL(3,K)
      XC(K) = FLOAT(K) /(10. *H(3) )
      YN(K) = F(3,K)
   80 CONTINUE
      DO 85 K = 1 ,320
      YD(K) = FL(4,K)
      XD(K) = FLOAT(K) /(10. *H(4) )
      YP(K) = F(4,K)
   85 CONTINUE
      WRITE(6, 95)
      DO 120 K = 1, 110,5
      WRITE(6,90)K, XA(K),YTA(K),YL(K),FL(1,K),F(1,K),AA(1,K),BB(1,K),
     A AS(1,K)
  120 CONTINUE
      WRITE(6,100)
      DO 125 K = 1, 180 ,5
      WRITE(6,90)K, XB(K),YTB(K),YM(K),FL(2,K),F(2,K),AA(2,K),BB(2,K),
     A AS(2,K)
  125 CONTINUE
      WRITE(6,105)
      DO 130 K = 1, 240  ,5
      WRITE(6,90)K, XC(K),YTC(K),YN(K),FL(3,K),F(3,K),AA(3,K),BB(3,K),
     A AS(3,K)
  130 CONTINUE
      WRITE(6,110)
      DO 135 K = 1, 320  ,5
      WRITE(6,90)K, XD(K),YTD(K),YP(K),FL(4,K),F(4,K),AA(4,K),BB(4,K),
     A AS(4,K)
  135 CONTINUE
      CALL PLOT(1. , 1. , -3 )
      CALL SCALE( XD , 5.50 , 320 , 1 )
      CALL SCALE( YTD, 7.0 , 320 , 1 )
```

```
 CALL AXIS(0.,0.,16HDRAFT PERCENTAGE,-16,5.50,0.0,XD(321),XD(322)
 CALL AXIS(0.,0.,22HZERO SPREAD ELONGATION,22,7.0,90. ,YTD(321) ,
A YTD(322) )
 CALL LINE ( XD, YTD ,320 ,1 ,0, 1 )
 CALL MARGIN( 5.5, 7.0)
 YL(111) = YTD(321)
 YM(181) = YTD(321)
 YN(241) = YTD(321)
 YP(321) = YTD(321)
 EL4(9 ) = YTD(321)
 EL3(9 ) = YTD(321)
 EL2(9 ) = YTD(321)
 EL1(9 ) = YTD(321)
 YL(112) = YTD(322)
 YM(182) = YTD(322)
 YN(242) = YTD(322)
 YP(322) = YTD(322)
 EL4(10) = YTD(322)
 EL3(10) = YTD(322)
 EL2(10) = YTD(322)
 EL1(10) = YTD(322)
 HA( 9 ) = XD(321)
 HB( 9 ) = XD(321)
 HC( 9 ) = XD(321)
 HD( 9 ) = XD(321)
 HA(10) = XD(322)
 HB(10) = XD(322)
 HC(10) = XD(322)
 HD(10) = XD(322)
 XC(241) = XD(321)
 XB(181) = XD(321)
 XA(111) = XD(321)
 XC(242) = XD(322)
 XB(182) = XD(322)
 XA(112) = XD(322)
 CALL PLOT( 0.0 , 11. , -3 )
 CALL AXIS(0.,0.,16HDRAFT PERCENTAGE,-16,5.50,0.0,XD(321),XD(322)
 CALL AXIS( 0.0,0.,15HREAL ELONGATION,15,7.0,90.,YP(321),YP(322) )
 CALL LINE( XD , YP , 320 , 1 , 0 , 1 )
 CALL PLOT( 0.0 , 0.0 , -3)
 CALL LINE (HD, EL4 , 8 , 1 , -1 , 0 )
 CALL PLOT( 0.0 , 0.0 , -3)
```

```
      CALL LINE (XC , YN , 240 , 1 , 0 , 1 )
      CALL PLOT( 0.0 , 0.0 , -3)
      CALL LINE (HC, EL3 , 8 , 1 , -1 , 1 )
      CALL PLOT( 0.0 , 0.0 , -3)
      CALL LINE ( XB , YM , 180 , 1 , 0 , 1 )
      CALL PLOT( 0.0 , 0.0 , -3)
      CALL LINE (HB, EL2 , 8 , 1 , -1 , 2 )
      CALL PLOT( 0.0 , 0.0 , -3)
      CALL LINE ( XA , YL , 110 , 1  ,0 , 1 )
      CALL PLOT( 0.0 , 0.0 , -3)
      CALL LINE (HA, EL1 , 8 , 1 , -1 , 3 )
      CALL MARGIN( 5.5, 7.0)
      CALL ENPLOT( 8. )
10    FORMAT( 8F9.4)
15    FORMAT(2X , 34HTHIS IS (D2-D1) , SPREAD IN INCHES   /8(3X,F10.4)/
20    FORMAT(2X,37HTHIS IS (H1-H2) , REDUCTION IN HEIGHT/8(3X,F10.4)//)
90    FORMAT( 2X , I4 , 8(4X , F8.4)   )
95    FORMAT(1H0,3X,1HK,7X,5HXA(K),6X,6HYTA(K),7X,5HYL(K),6X,7HFL(1,K),
     B 5X,6HF(1,K),6X,7HAA(1,K),5X,7HBB(1,K),5X,7HAS(1,K) // )
100   FORMAT(1H0,3X,1HK,7X,5HXB(K),6X,6HYTB(K),7X,5HYM(K),6X,7HFL(2,K),
     B 5X,6HF(2,K),6X,7HAA(2,K),5X,7HBB(2,K),5X,7HAS(2,K) // )
105   FORMAT(1H0,3X,1HK,7X,5HXC(K),6X,6HYTC(K),7X,5HYN(K),6X,7HFL(3,K),
     B 5X,6HF(3,K),6X,7HAA(3,K),5X,7HBB(3,K),5X,7HAS(3,K) // )
110   FORMAT(1H0,3X,1HK,7X,5HXD(K),6X,6HYTD(K),7X,5HYP(K),6X,7HFL(4,K),
     B 5X,6HF(4,K),6X,7HAA(4,K),5X,7HBB(4,K),5X,7HAS(4,K) // )
      STOP
      END
      SUBROUTINE TAB
      COMMON/CC/ S(4,322)
      DIMENSION  D(4) , H(4) , KK(4) , R(4)
      DIMENSION  EX(4,322)
      DATA( KK(I) ,I =1,4 )/110 , 180 , 240 , 320 /
      DATA( H(I) , I = 1,4) /0.3438 ,0.5198 ,0.6895 ,0.8686 /
      DATA(D(I) ,I =1,4)/ 0.3400 ,0.5186 ,0.6898 ,0.8718 /
      DATA(R(I), I=1,4)/ 1.828 ,1.772 ,1.718 ,1.665 /
      DO 5 I = 1,4
      A = .40
      JJ  = KK(I)
      DO 5 K = 1,JJ
      X = FLOAT(K)/1000.
      XX = H(I)/( H(I)-X )
      AS= -((( R(3)/H(3) )*(H(I)/R(I))) ** A  )*(R(I)/H(I) )**.5
```

```
      BS = ( D(I)/SQRT( R(I)*X) )** 1.072
      CS = AS*BS
      EX(I,K) = EXP( CS )
      S(I,K) = D(I)*( XX**EX(I,K)  -1. )
    5 CONTINUE
      WRITE(6,10)
      DO 15 K= 1 ,110 , 5
      WRITE(6,20) K , EX( 1,K) , S(1,K)
   15 CONTINUE
      WRITE(6,10)
      DO 18 K = 1, 180 , 5
      WRITE(6,20) K , EX( 2,K) , S(2,K)
   18 CONTINUE
      WRITE(6,10)
      DO 25 K= 1 ,240 , 5
      WRITE(6,20) K , EX( 3,K) , S(3,K)
   25 CONTINUE
      WRITE(6,10)
      DO 30 K= 1 ,320 , 5
      WRITE(6,20) K , EX( 4,K) , S(4,K)
   30 CONTINUE
   10 FORMAT( 7X, 1HK , 12X, 7HEX(I,K) , 12X, 6HS(I,K)//)
   20 FORMAT( 5X, I4 , 2( 10X , 1PE12.4 ) )
      RETURN
      END
$IBFTC MARGN
      SUBROUTINE   MARGIN(X,Y)
      A=0.05
      B=1.0
      E=1.0
      XM=X+E
      YM=Y+E
      C=0.0
      D=Y+A
      DO 1 I = 1 , 20
      C=C+B
      IF(C.GE.X) GO TO 2
      CALL   PLOT (C,Y,3)
1     CALL   PLOT (C,D,2)
2     C=0.0
      D=X+A
      DO 3 I = 1 , 20
```

```
      C=C+B
      IF(C.GE.Y) GO TO 4
      CALL    PLOT (X,C,3)
3     CALL    PLOT (D,C,2)
4     CALL    PLOT (0.0,0.0,3)
      CALL    PLOT (X   ,0.0,2)
      CALL    PLOT (X   ,Y   ,2)
      CALL    PLOT (0.0,Y   ,2)
      CALL    PLOT (0.0,0.0,2)
      CALL    PLOT (-E,-E,3)
      CALL    PLOT (XM,-E,2)
      CALL    PLOT (XM,YM,2)
      CALL    PLOT (-E,YM,2)
      CALL    PLOT (-E,-E,2)
      CALL    PLOT (0.0,0.0,3)
      RETURN
      END
$IBFTC TAB
$DATA
'
   0.0357   0.0487   0.0578   0.0680   0.0863   0.0996   0.1038   0.108
   0.0011   0.0029   0.0089   0.0159   0.0265   0.0320   0.0414   0.046
   0.0771   0.0864   0.1163   0.1383   0.1531   0.1653   0.1766   0.180
   0.0030   0.0062   0.0207   0.0300   0.0361   C.0435   0.0521   0.058
   0.0989   0.1332   0.1620   0.1852   0.2054   0.2285   0.2376   0.239
   0.0044   0.0121   0.0254   0.0333   0.0381   0.0485   0.0550   0.058
   0.1123   0.1486   0.2030   0.2340   0.2618   0.2658   0.3027   0.314
   0.0050   0.0091   0.0224   0.0331   0.0405   0.0441   0.0522   0.060
'
```

II Computor program for calculations of non-linear differential equation for thermal cooling

The easiest solution for equation (3.2) is obtained by the computor.

$$\frac{dT}{dt} = \frac{4.\varepsilon.\sigma}{l.\rho.c} T^4 + \frac{4.h}{l.\rho.c} T - \left(\frac{4.\varepsilon.\sigma}{l.\rho.c} T_o{}^4 - \frac{4.h}{l.\rho.c} T_o\right) \quad (3.2)$$

By applying the finite difference method, starting from the initial values of furnace temperatures, as given on page ( ), for each series of experiments the square bar temperature is determined at every succeeding second up to five seconds. The total time of the operation from furnace through rolls was determined to be around 3.5 seconds. The temperature listed at the bottom of the program, for each second of time lapse, indicates the actual temperature of the rolling for each bar size.

COMPUTOR PROGRAM FOR CALCULATION OF NON-LINEAR DIFFERENTIAL EQUATION OF THERMAL COOLING

```
JOB(UMEM045,X)
RUN(S)
LGO.
'
      PROGRAM FIT  (INPUT,OUTPUT,TAPE5=INPUT,TAPE6=OUTPUT)
C     SOLUTION OF NON LINEAR DIFFERENTIAL EQUATION
C     EMISIVITY = 0.82 AT 1100C , DENSITY =7.8 GM/ CU.CM.
C     SPECIFIC HEAT 0.153 CAL/GM. C  BOLTZMAN COEF. 1.355*(10. **-12)
      DIMENSION  U(140,4) , A(4) , X(4) , Z(140,4)
      DIMENSION  XX(140,4) , Y(140,4)   ,P(4)
      READ(5,30) (X(I)    , I= 1,4)
      READ(5,30) ( P(I) , I = 1,4)
      KA = 1
   50 CONTINUE
      DO 5 I= 1 , 4
      GO TO (1,2,3,4) KA
    1 CONTINUE
      IF(I .EQ. 1) U(1,I) = 1263.
      IF(I .EQ. 2) U(1,I) = 1243.
      IF(I .EQ. 3) U(1,I) = 1228.
      IF(I .EQ. 4) U(1,I) = 1223.
      GO TO 40
    2 CONTINUE
      IF(I .EQ. 1) U(1,I) = 1378.
      IF(I .EQ. 2) U(1,I) = 1355.
      IF(I .EQ. 3) U(1,I) = 1338.
      IF(I .EQ. 4) U(1,I) = 1331.
      GO TO 40
    3 CONTINUE
      IF(I .EQ. 1) U(1,I) = 1493.
      IF(I .EQ. 2) U(1,I) = 1469.
      IF(I .EQ. 3) U(1,I) = 1448.
      IF(I .EQ. 4) U(1,I) = 1439.
      GO TO 40
    4 CONTINUE
      IF(I .EQ. 1) U(1,I) = 1623.
      IF(I .EQ. 2) U(1,I) = 1593.
      IF(I .EQ. 3) U(1,I) = 1568.
      IF(I .EQ. 4) U(1,I) = 1548.
   40 A(I) = 4. * (1.355*0.82)/( 7.8*0.153 * X(I) )
```

```
      Z(1,I) = U(1,I) - 273.
    5 CONTINUE
      H = 0.05
      V=0.0
      DO 10 I = 1,4
      DO 10 J = 1, 121
      K= J+1
      XX(J,I) = H*A(I)*(((U(J,I)/1000.)**4)-((298./1000.)**4))
      Y(J,I) = H*((4.* P(I) )/(7.8 *0.153 *X(I) ))*(U(J,I)-298.)
      V =U(J,I) -H*A(I) *(((U(J,I)/1000.)**4)-((298./1000. )**4))-Y(J,I)
      U(K,I) = V
      Z(K,I) = U(K,I) - 273.
   10 CONTINUE
      WRITE( 6,25)
      DO 15 K= 1, 120, 20
      J= (K-1)/20
      WRITE(6,20) J , ( Z(K,I) , I=1,4)
   15 CONTINUE
      KA = KA + 1
      IF(KA .LE. 4 ) GO TO 50
      WRITE(6,30) (X(I) , I= 1,4 )
      WRITE(6,30) (P(I) , I= 1,4 )
   20 FORMAT( 6X , I3 , 11X , 4( F7.2 , 12X ) )
   25 FORMAT( 1H1 ////// 21X , 38HCOOLING OF THE SQUARE BARS IN THE AIR
     A ///5X, 7HTIME IN , 4X, 4( 15HTEMP.    OF   THE , 4X)/
     B  5X , 7HSECONDS , 4X, 15H1/4  SQUARE BAR , 4X , 15H3/8  SQUARE BA
     CR , 4X , 15H1/2  SQUARE BAR , 4X , 15H5/8  SQUARE BAR //)
   30 FORMAT(4F10.4)
      STOP
      END

   0.6250     0.9375     1.2500     1.5625
   0.0013     0.0016     0.0022     0.0028
```

COOLING OF THE SQUARE BARS IN THE AIR

| TIME IN SECONDS | TEMP. OF THE 1/4 SQUARE BAR | TEMP. OF THE 3/8 SQUARE BAR | TEMP. OF THE 1/2 SQUARE BAR | TEMP. OF THE 5/8 SQUARE BAR |
|---|---|---|---|---|
| 0 | 990.00 | 970.00 | 955.00 | 950.00 |
| 1 | 968.71 | 955.39 | 942.92 | 939.25 |
| 2 | 948.52 | 941.29 | 931.17 | 928.74 |
| 3 | 929.32 | 927.67 | 919.73 | 918.47 |
| 4 | 911.02 | 914.49 | 908.58 | 908.43 |
| 5 | 893.57 | 901.72 | 897.72 | 898.60 |
| | | | | |
| 0 | 1105.00 | 1082. | 1065.00 | 1058.00 |
| 1 | 1076.95 | 1063.00 | 1049.59 | 1044.52 |
| 2 | 1050.69 | 1044.81 | 1034.69 | 1031.40 |
| 3 | 1026.02 | 1027.38 | 1020.27 | 1018.64 |
| 4 | 1002.77 | 1010.64 | 1006.29 | 1006.21 |
| 5 | 980.80 | 994.55 | 994.55 | 994.11 |
| | | | | |
| 0 | 1220.00 | 1196.00 | 1175.00 | 1166.00 |
| 1 | 1183.59 | 1171.48 | 1155.53 | 1149.22 |
| 2 | 1150.01 | 1148.25 | 1136.84 | 1132.99 |
| 3 | 1118.90 | 1126.18 | 1118.96 | 1117.28 |
| 4 | 1089.93 | 1105.18 | 1101.56 | 1102.06 |
| 5 | 1062.85 | 1085.15 | 1084.89 | 1087.31 |
| | | | | |
| 0 | 1350.00 | 1320.00 | 1295.00 | 1275.00 |
| 1 | 1301.93 | 1288.10 | 1270.13 | 1254.23 |
| 2 | 1258.46 | 1258.24 | 1246.47 | 1234.28 |
| 3 | 1218.86 | 1230.21 | 1223.92 | 1215.08 |
| 4 | 1182.54 | 1203.81 | 1202.38 | 1196.59 |
| 5 | 1149.05 | 1178.87 | 1181.77 | 1178.76 |

# REFERENCES


1. Jernkontorets Annaler, III (1927), pp 39 - 97 Ekelund.

2. Ekelund S. 1953 Steel Vol. 93, August p. 8.

3. "Roll Pass Design" 1960, The United Steel Companies Ltd.

4. A. Helmi and J.M. Alexander "Journal of the Iron and Steel Institute" Vol. 206, Nov. 1968.

5. Wusatowski, Z. 1955, Iron and Steel, Vol. 28, pp. 49 - 89, "Hot Rolling, A Study of Draught, Spread and Elongation".

6. Wusatowski, Z. 1958 Arch Hutnictwa, Vol 3, No. 3.

7. A.W. McCrum "Progress Report on Experimental Investigations of Spread, Load and Torque in Hot Flat Rolling", BISRA report, MW/A/10/56.

8. Hill, R. Private Communication to A.W. McCrum, 1955

9. Sparling, L.G. Proc. IME, 1961, 175, pp. 604.

10. Tselikov, 1967 "Stress and Strain in Metal Rolling".

11. R.B. Sims and H. Wright, Journal of Iron and Steel Institute, 1963, Vol. 201.

12. A.E. Lendl, Iron and Steel, Sept. 1948 and Dec. 1948.

13. Tarnovski I. Ya, Pozdeyev A.A., Lyashkov V.B. "Deformation of Metals During Rolling" Pergamon Press 1965.

14. R.C. Brewer and J,M. Alexander, J. Mech. Phys. Solids, 1960, Vol 8, pp. 76 - 78.

15. G. Wallquist "The Influence of Different Factors in Plastic Deformation, Especially in Hot Rolling". Jernkontorets, Annaler, Vol. 153, 1969, P.5-32.

16. P. Polukhin, N. Fedosou, A. Korolyov, "Rolling Mill Practice". Peace Publishers, Moscow.

17. R.B. Sims, J.A. Place and A.D. Morley "Load Meters for Industrial Mill" Engineering, Vol. 173, Jan. and Feb. 1952.

18. R.B. Sims and A.D. Morley, "Torque Meter for Industrial Applications", Engineering, Vol. 174, July 1952.

19. P. W. Whitton, and H. Ford, 1955 "Surface Friction and Lubrication in Cold Strip Rolling", Proc. Inst. Mech. Engrs., 169, 123.

20. C.R. Skelton (1965) "The Effect of Stock Temperature, Rolling Speed and Stock Surface Scale Condition on Spread in the Rolling of Square Bars" BISRA Report MW/INT/7/65.

21. Siebel, 1924, Berichte des Walzwerksauss - Chusses, Verein Deutscher Eisenhuttenleute, No. 37, Also Stahl and Eisen, 1925, Vol. 45, p. 1563.

22. Karman, Von, T. 1925 Zeitschrift Fur Angewandte und Matematik, Vol. 5, p. 139.

23. H. Ford, Proc. Inst. of Mech. Eng. 1948, 159, 115 - 143.

24. Sobolevsky, N.A. 1935, Blast Furnace and Steel Plant, Vol. 23, pp. 685, 763. 1936, Vol. 24 pp. 149, 237, 313, 413.

25. Orowan, E. "The Calculation of Roll Pressure in Hot and Cold Flat Rolling". Pro. Inst. Mech. Eng. 1943, 150, 140.

26. Nadai, A. "Plasticity" 1931, McGraw Hill.

27. Bland, D.R. and H. Ford, 1948. Proc. IME, Vol 159, p. 145 "The Calculation of Roll Force and Torque in Cold Strip Rolling with Tension".

28. R.B. Sims, Proc. IME, 1954, 168, pp. 191 - 200.

29. Stewart R, 1954, Proc. IME, 168, pp. 201 - 208.

30. P.M. Cook and A.W. McRum "The Calculation of Load and Torque in Hot Flat Rolling" B.I.S.R.A., London, March, 1958.

31. R.B. Sims and H. Wright "Roll Force and Torque in Hot Rolling Mills" J. of Iron and Steel Inst. March 1963.

32. W. Prager, 1953, Trans. Royal Institute of Technology, Stockholm, Sweden, No. 65. "A Geometrical Discussion of the Slip Line Field in Plane Plastic Flow".

33. J.M. Alexander, 1955, Proc. IME, 169, (50) "A Slip Line Field for the Hot Rolling Process".

34. J.M. Alexander and H. Ford, Progress in Applied Mechanics, Prager Anniversary Volume, 1963. "On the Limit Analysis of Hot Rolling".

A.W. McCrum

35. H. Ford and J.M. Alexander, J. of Inst. of Metals, 1963 - 1964, Vol. 92, 397. "Simplified Hot Rolling Calculations".

36. B. Avitzur, "Maximum Reduction in Cold Strip Rolling". Proc. IME, Vol. 174, No. 32, 1960 pp. 865 - 884.

37. B. Avitzur, J. of Engineering for Industry, Feb. 1963, "Power Analysis of Cold Strip Rolling".

38. R. Hill, "The Mathematical Theory of Plasticity", 1950.

39. M. Ya. Brovman, and S.M. Genzelev, B.I.S.R.A., Translation from Kuznechno - Shtampovochnoe Proizvodstuo, 1960.

40. E. Orowan and K. Pascoe, First Report of the Rolling Mill Research Sub-Committee (Special Rep. No. 34) p. 124, 1964, London (Iron Steel Institute).

41. El-Kalay and L.G.M. Sparling "Factors Affecting Friction and Their Effect upon Load, Torque and Spread in Hot Flat Rolling". J. of Iron and Steel Inst. Feb. 1968.

42. Cook, P.M. Proceedings of Conference on Properties of Materials of High Rate of Strain, IME, 1957.

43. J.M. Alexander, Communications on R.B. Sims's papr, 1954, Proc. IME, 1954, 168, p. 209.

44. P. W. Whitton, H. Ford, Proc. IME, 1955, 169. pp. 123 - 133.

45. C.R. Skelton, BISRA Report 1965 MW/INT/7/65.

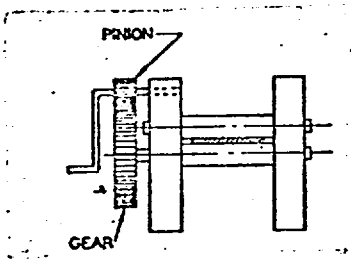


FIG 1-1 LEONARDO DE VINCI'S DESIGN 1495

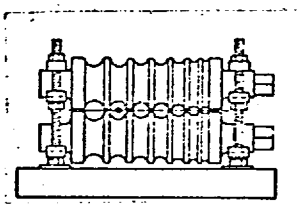

FIG1-2 JOHN PAYNE'S DESIGN 1728

| DRAWING NUMBER |
|---|
| 1 |

| LIMITS ON DIMENSIONS | | |
|---|---|---|
| DEC. | ± .010" | |
| FRACT. | ± | 1"/32 |
| DEC. MM | ± | 0·25 MM |
| UNIT MM | ± | 1 MM |
| UNLESS SPECIFIED | | |

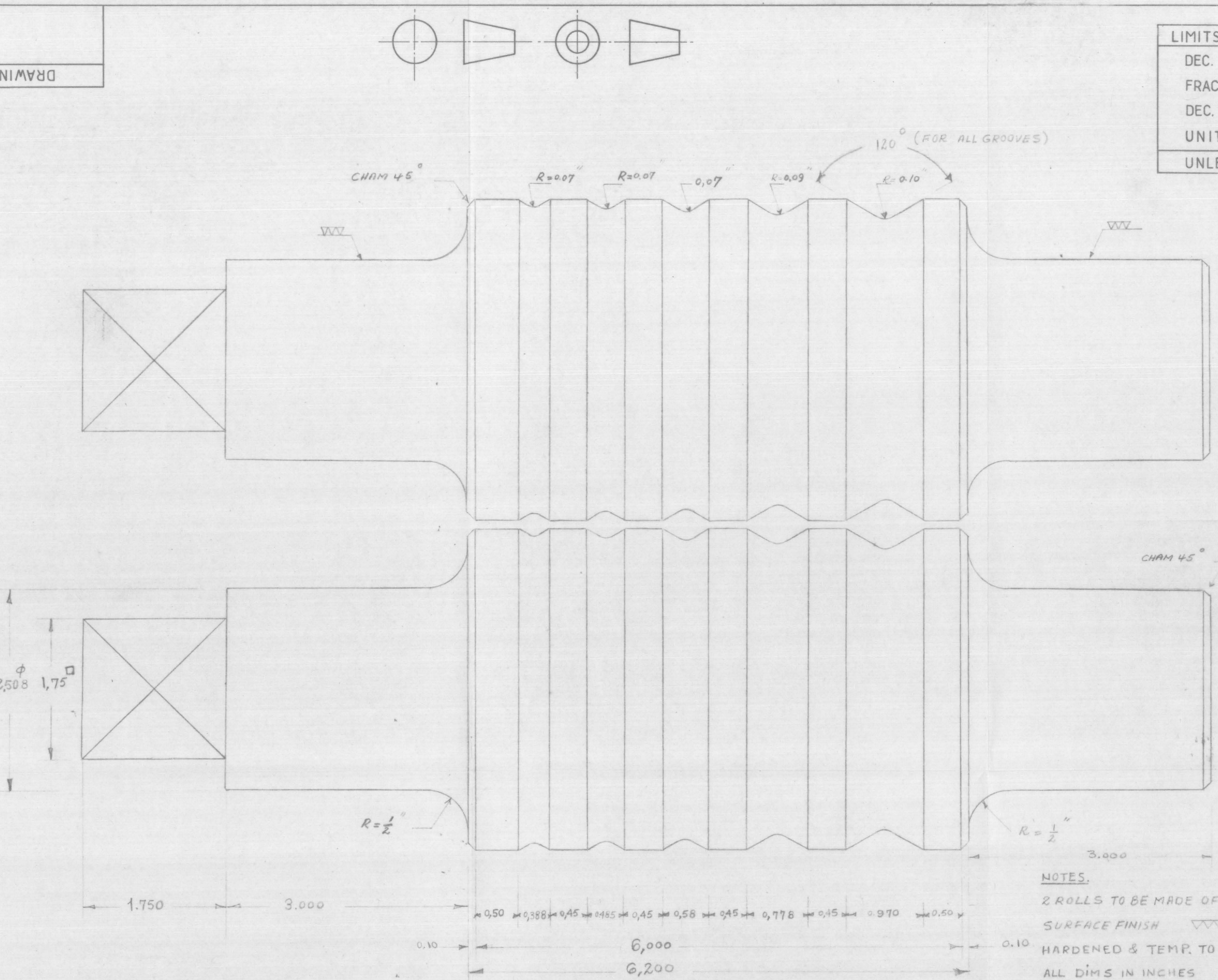


FIG 2-1

NOTES.

2 ROLLS TO BE MADE OF ST EN25

SURFACE FINISH ▽▽▽ AS INDICATED.

HARDENED & TEMP. TO "X" CONDITION

ALL DIMS IN INCHES

ROLLS SHOULD BE MADE IDENTICAL

| PART Nº | Nº OFF | DESCRIPTION | MATERIAL | REMARKS |
|---|---|---|---|---|
| — | — | DIAMOND GROOVED ROLLS | EN25 | |

| Mechanical Engineering Dept. Imperial College London S.W.7 | | | | | | |
|---|---|---|---|---|---|---|
| DRAWN | SOURESRAFIL | SCALE | TITLE | DIAMOND GROOVED ROLLS | CLASS | DRAWING NUMBER |
| APPROVED | — | 1:1 | | | P.G. RES. | 1 |
| TRACED | — | DATE | AMMDTS. | | GROUP | NAME |
| CHECKED | — | Feb. 20, 68 | | | APP. MECH. | DIAMOND GROOVED ROLLS |

NOTE:
LIMIT ON DIMENSIONS IS ±0.001"

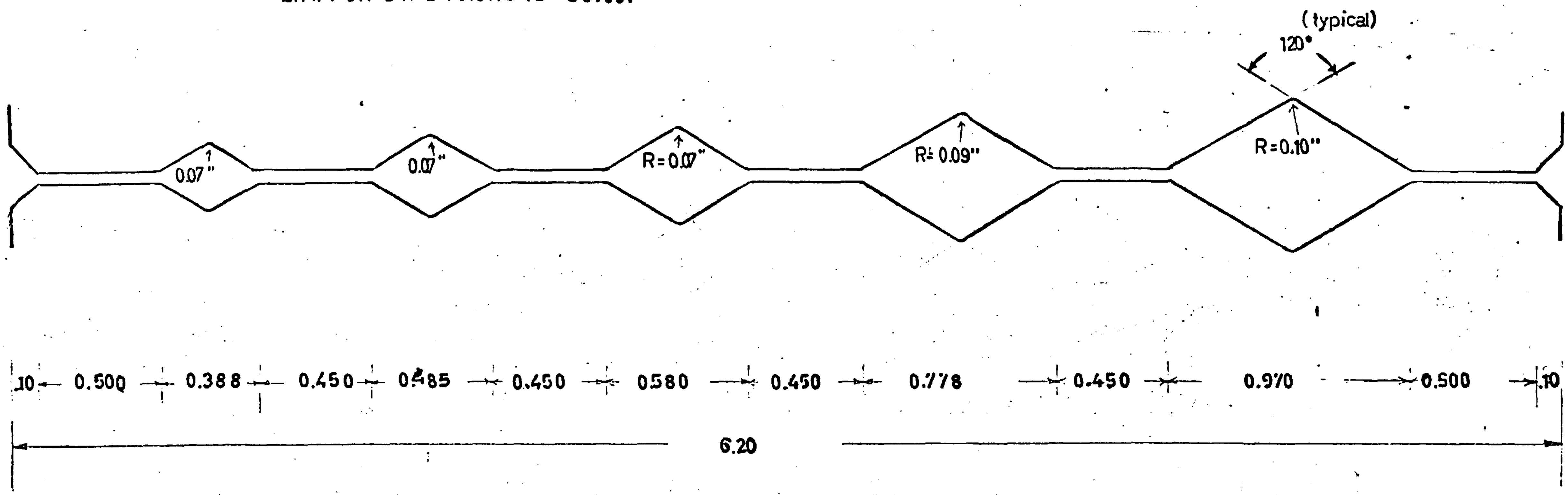


FIG 2-2 ROLL PASS DIMENSIONS

DRAWING NUMBER

| LIMITS ON DIMENSIONS | |
|---|---|
| DEC. | ± ·010" |
| FRACT. | ± 1/32" |
| DEC. MM | ± 0·25 MM |
| UNIT MM | ± 1 MM |
| UNLESS SPECIFIED | |

129

SHT 1 OF 2

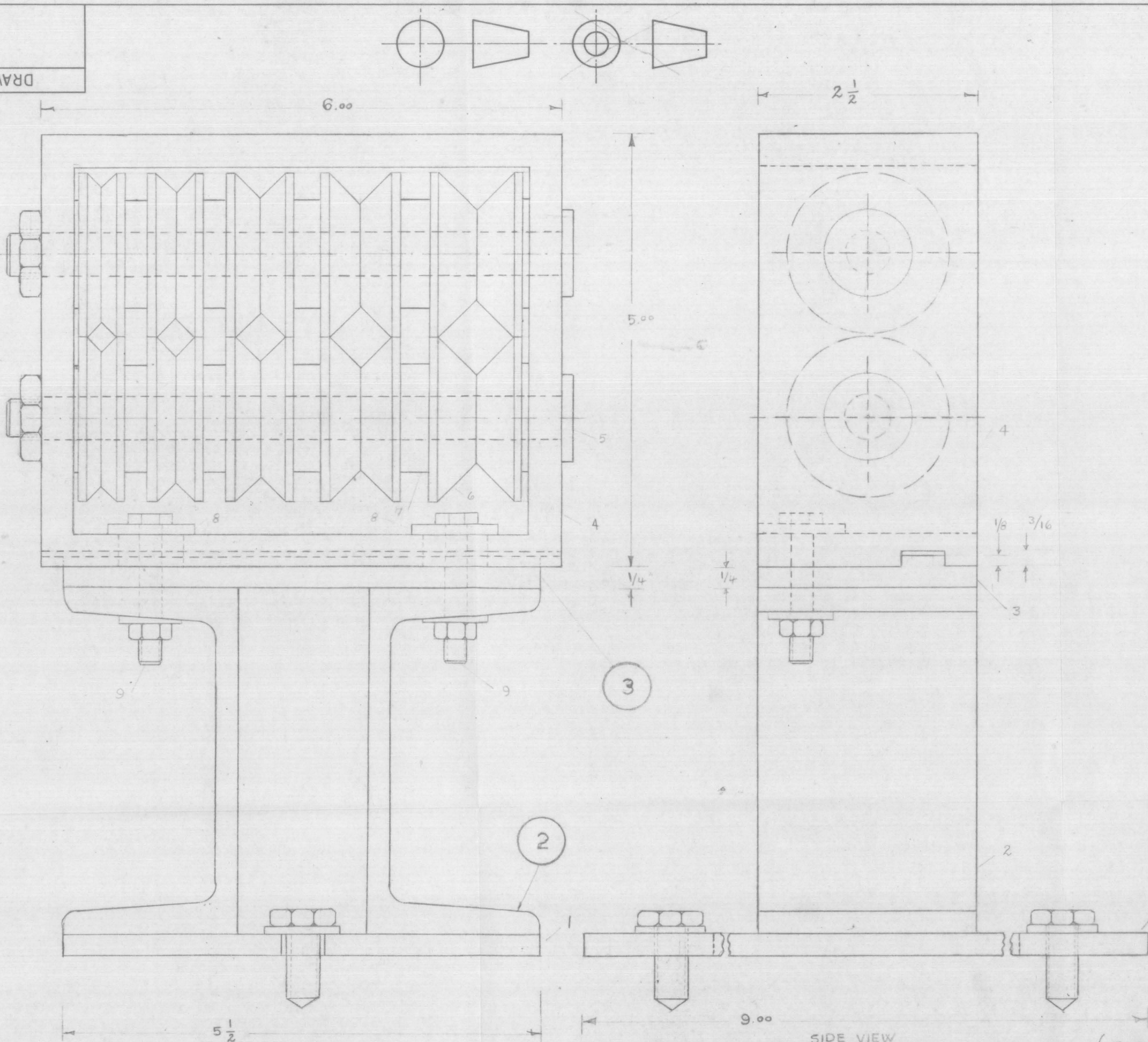


(SEE SHT 2 FOR MATERIAL)

FIG 2-3

| PART Nº | Nº OFF | DESCRIPTION | MATERIAL | REMARKS |
|---|---|---|---|---|

| | | | | | | |
|---|---|---|---|---|---|---|
| Mechanical Engineering Dept. Imperial College London S.W.7 | DRAWN | SOURESRAFIL | SCALE | TITLE | ROLLING MILL GUIDE | CLASS: RESEARCH — DRAWING NUMBER: 2 |
| | APPROVED | | 1 | | | |
| | TRACED | | DATE | AMMDTS. | | GROUP: APP. MECH — NAME: ROLLING MILL GUIDE |
| | CHECKED | | MAR 14, 68 | | | |

DRAWING NUMBER

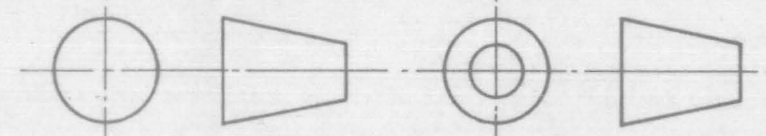

| LIMITS ON DIMENSIONS | |
|---|---|
| DEC. | ± ·010" |
| FRACT. | ± 1/32" |
| DEC. MM | ± 0·25 MM |
| UNIT MM | ± 1 MM |
| UNLESS SPECIFIED | |

130

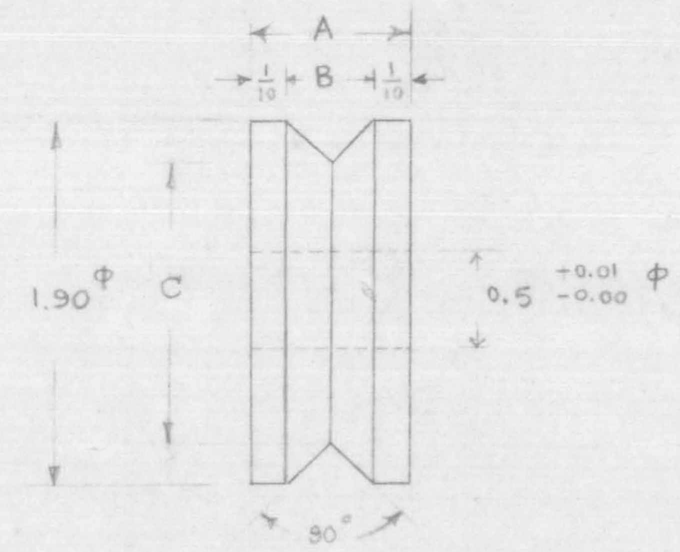


| | A | B | C | REQUIRED |
|---|---|---|---|---|
| I | 0.553 | 0.353 | 1.547 | 2 |
| II | 0.642 | 0.442 | 1.458 | 2 |
| III | 0.730 | 0.530 | 1.370 | 2 |
| IV | 0.907 | 0.707 | 1.193 | 2 |
| V | 1.083 | 0.883 | 1.017 | 2 |

SPOOL DIMENSIONS (A, B AND C)

6 SPOOL

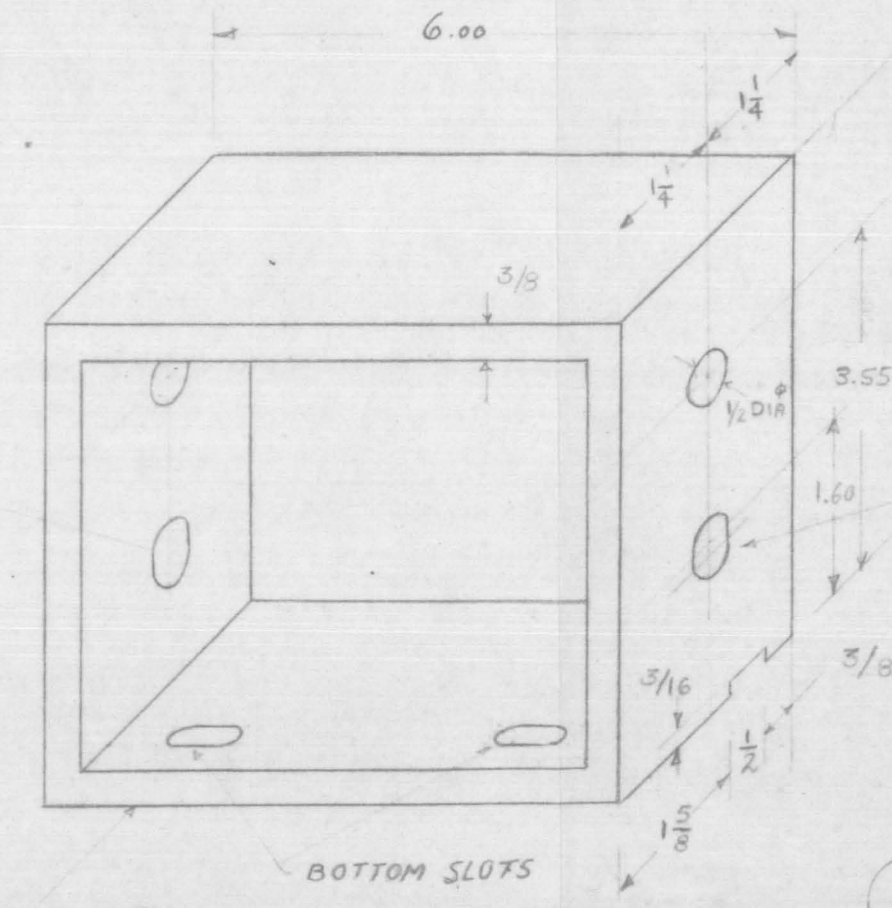


4 FRAME (SCALE 1/2)

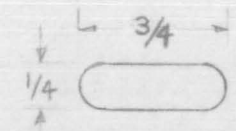


BOTTOM SLOTS OF THE FRAME (4)

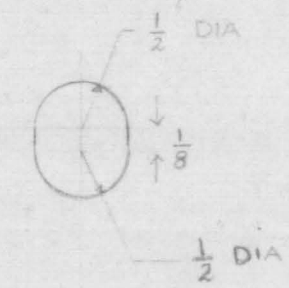


SIDE SLOTS OF THE FRAME (4)

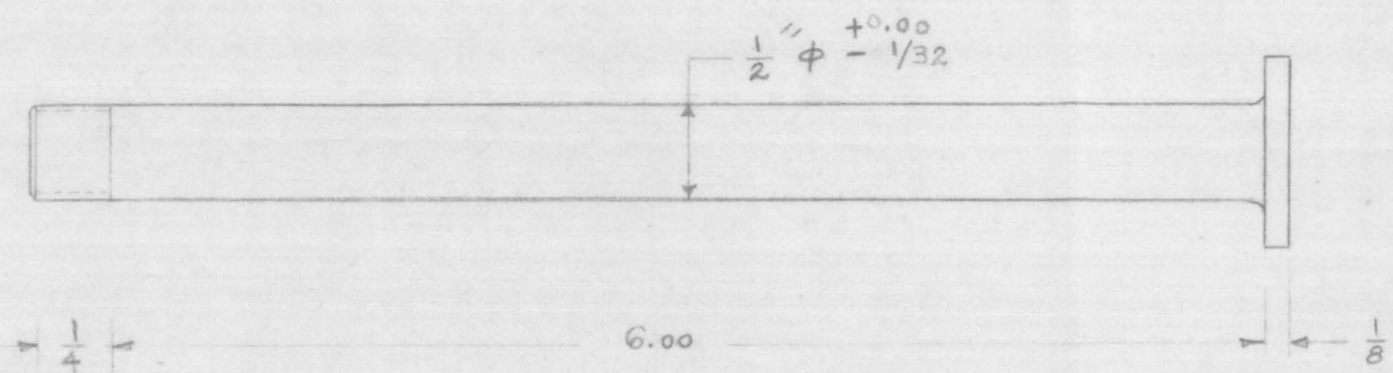


5 PIN

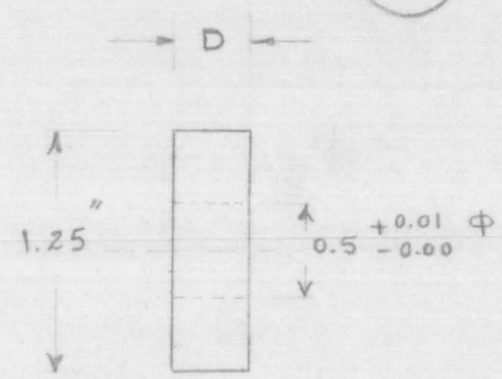


7 SEPARATING WASHERS

| NO. | D |
|---|---|
| I | 0.329 |
| II | 0.310 |
| III | 0.296 |
| IV | 0.289 |
| V | 0.045 |
| VI | 0.045 |

SEPARATING WASHER DIMENSION "D" (TO BE MADE OF MS)

SHT 2 OF 2

FIG 2-3

| PART № | № OFF | DESCRIPTION | MATERIAL | REMARKS |
|---|---|---|---|---|
| 9 | 2 | 1/4" BOLT AND WING NUT | — | |
| 8 | 4 | WASHER 1" DIA | STL | |
| 7 | 6 | SEPARATING WASHERS | STL ROD | |
| 6 | 10 | SPOOL (2" DIA ROD) | STL ROD | MACHINED |
| 5 | 2 | PIN | STL ROD | MACHINED TO THE SIZE |
| 4 | 1 | FRAME $2\frac{1}{2}$ x 3/8" STRIP | MS | |
| 3 | 1 | TOP PLATE $2\frac{1}{2} \times 5\frac{1}{2} \times 3/8$" | MS | |
| 2 | 2 | CHANNEL SECT. 4x2" | | |
| 1 | 1 | BASE PLATE $9 \times 5\frac{1}{2} \times 1/4$ | MS | |

| Mechanical Engineering Dept. Imperial College London S.W.7 | DRAWN | SOURESRAFIL | SCALE | TITLE | ROLLING MILL GUIDE | CLASS | DRAWING NUMBER |
|---|---|---|---|---|---|---|---|
| | APPROVED | — | 1 | | | RESEARCH | 2 |
| | TRACED | | DATE | AMMDTS. | | GROUP | NAME |
| | CHECKED | — | MAR.14.68 | | | APP. MECH. | ROLLING MILL GUIDE |

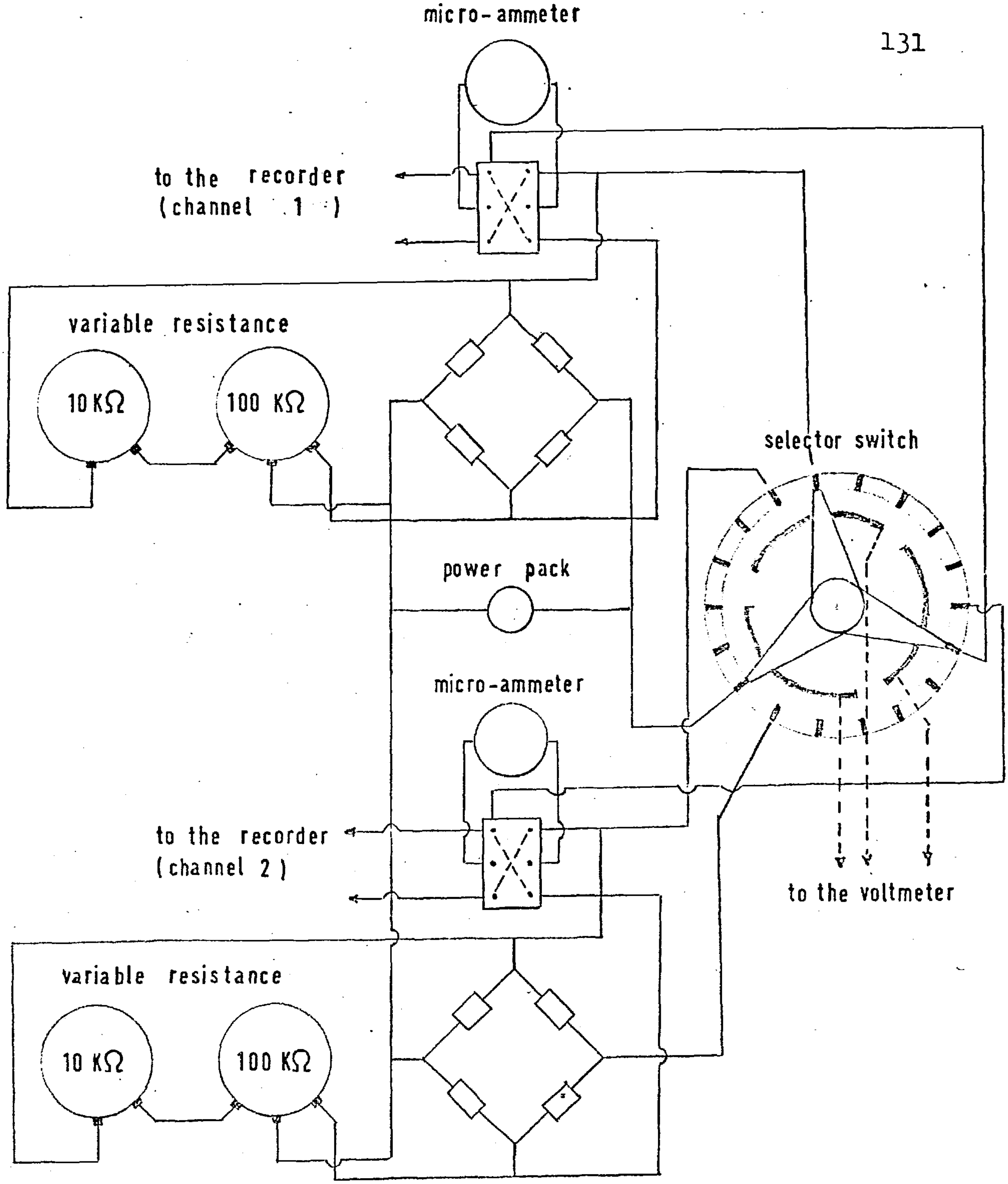


EIG(2-4) LOAD CELL CIRCUIT
TOP: R.H. LOAD CELL
BELOW L.H. LOAD CELL

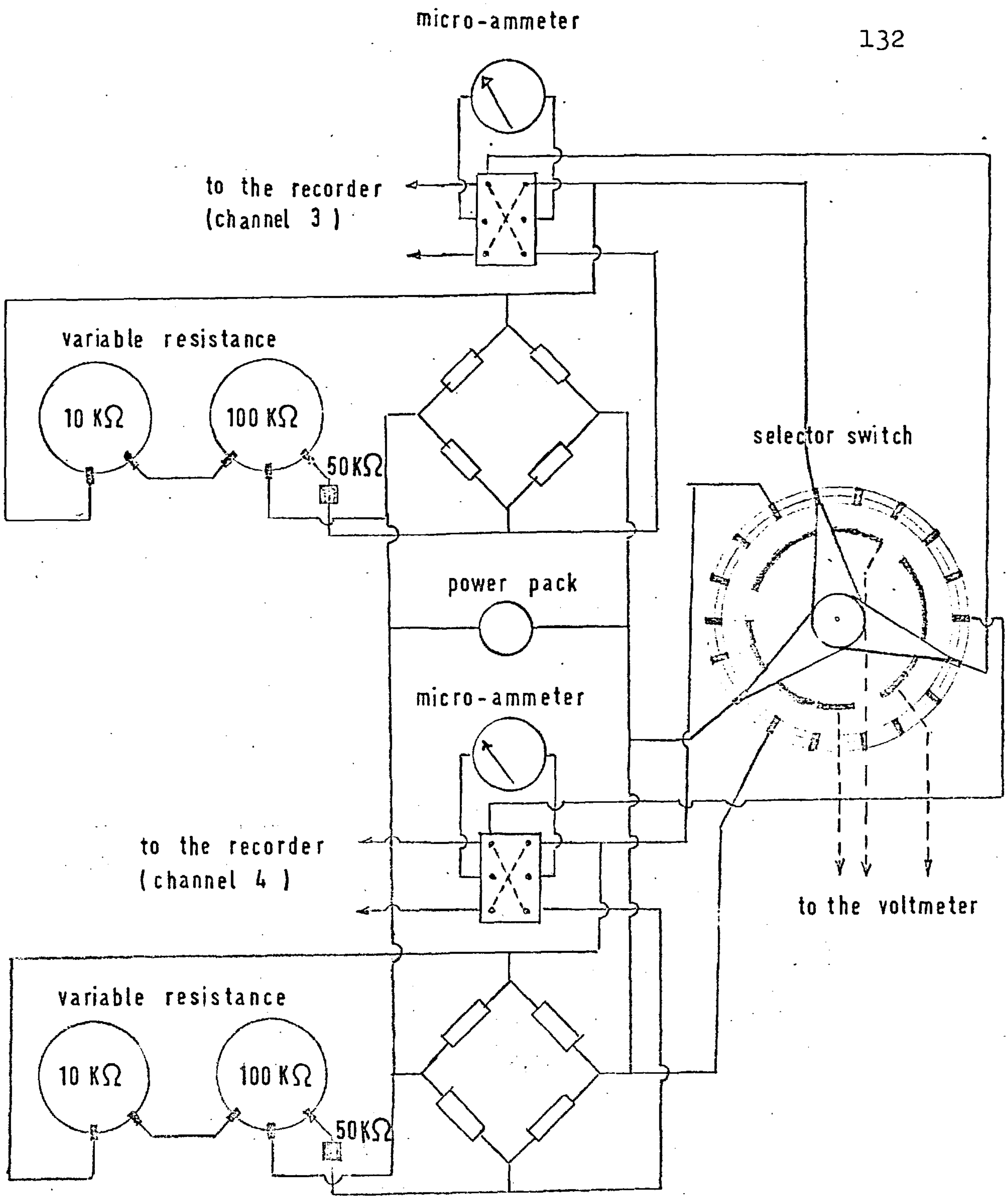


FIG(2-5) TORQUE CELL CIRCUIT
TOP UPPER SPINDLE
BELOW LOWER SPINDLE

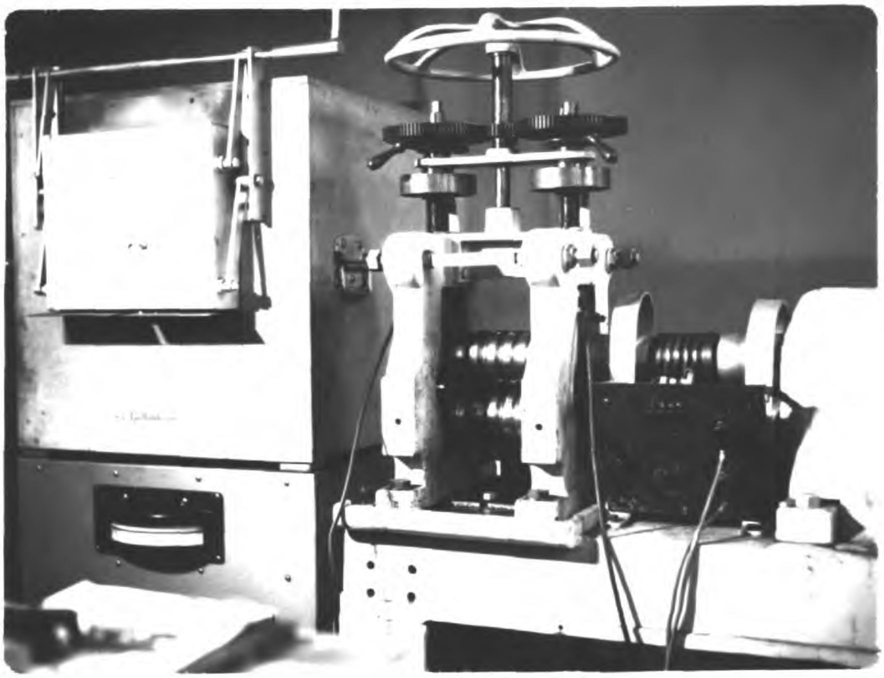

(a)

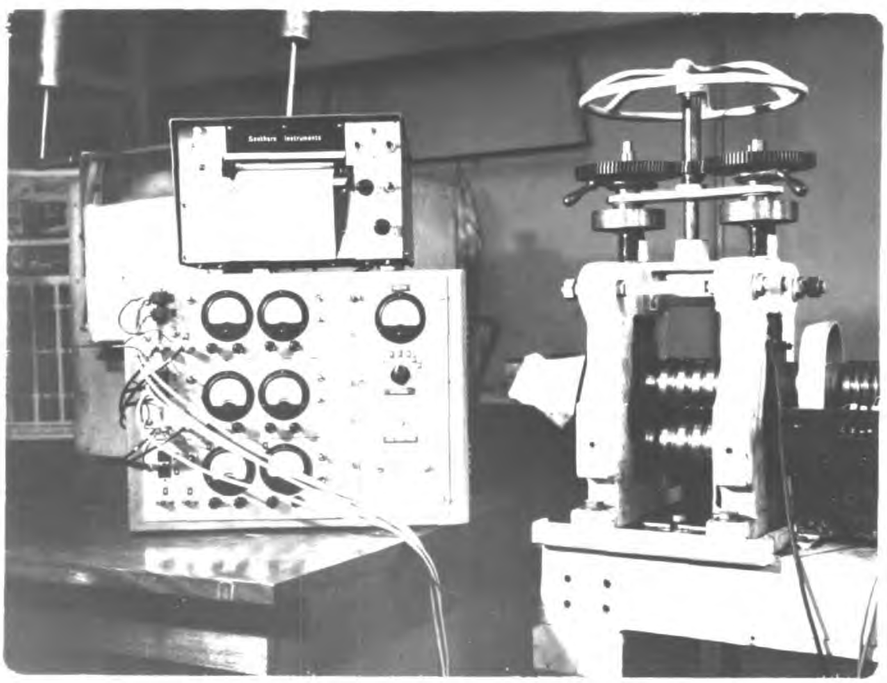


(b)

FIG (2-6) a - ROLLING MILL & FURNACE

b - ROLLING MILL, RECORDER & CONTROL PANEL

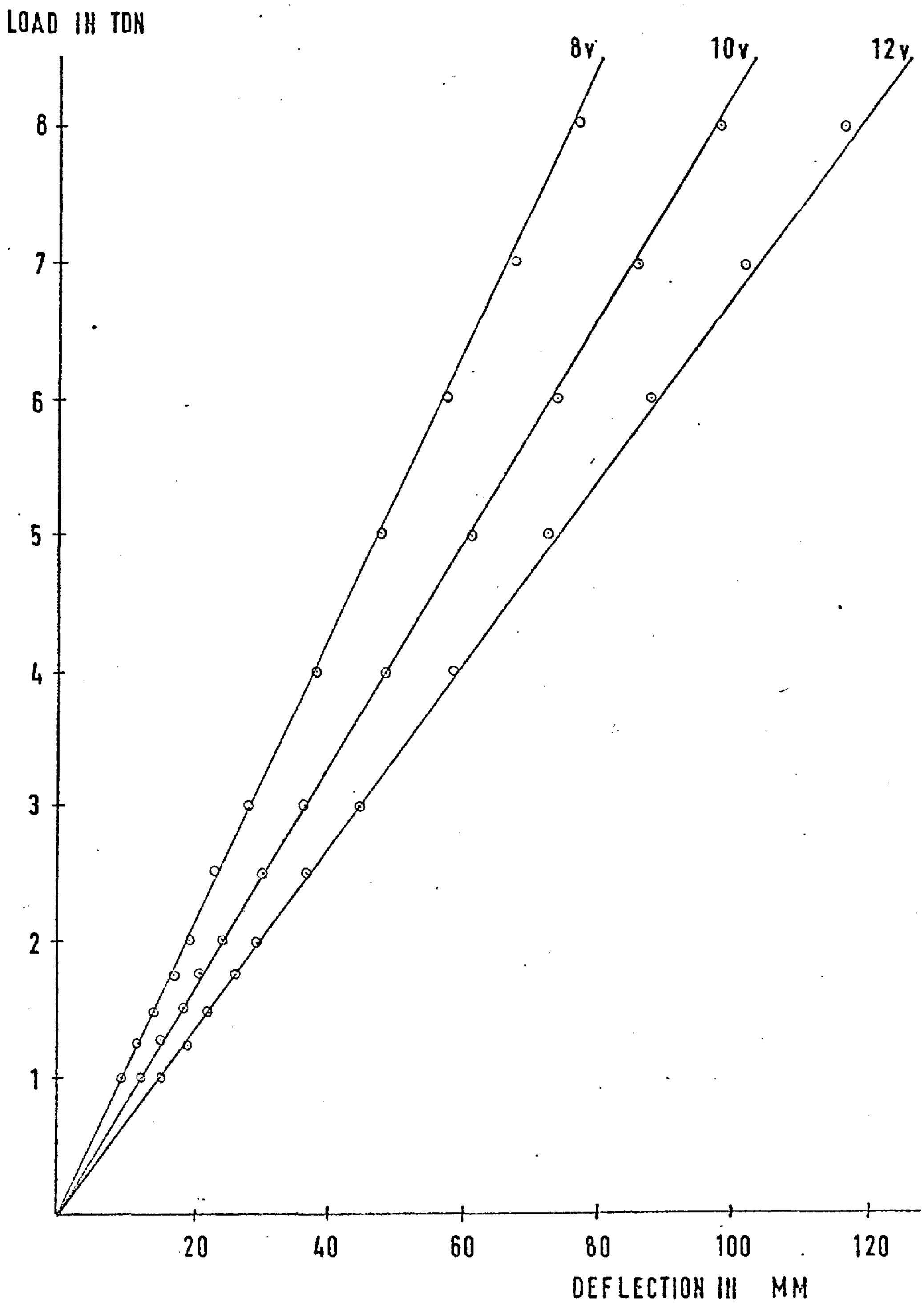


FIG (3-1) CALIBRATION CURVE
LOAD CELL 1

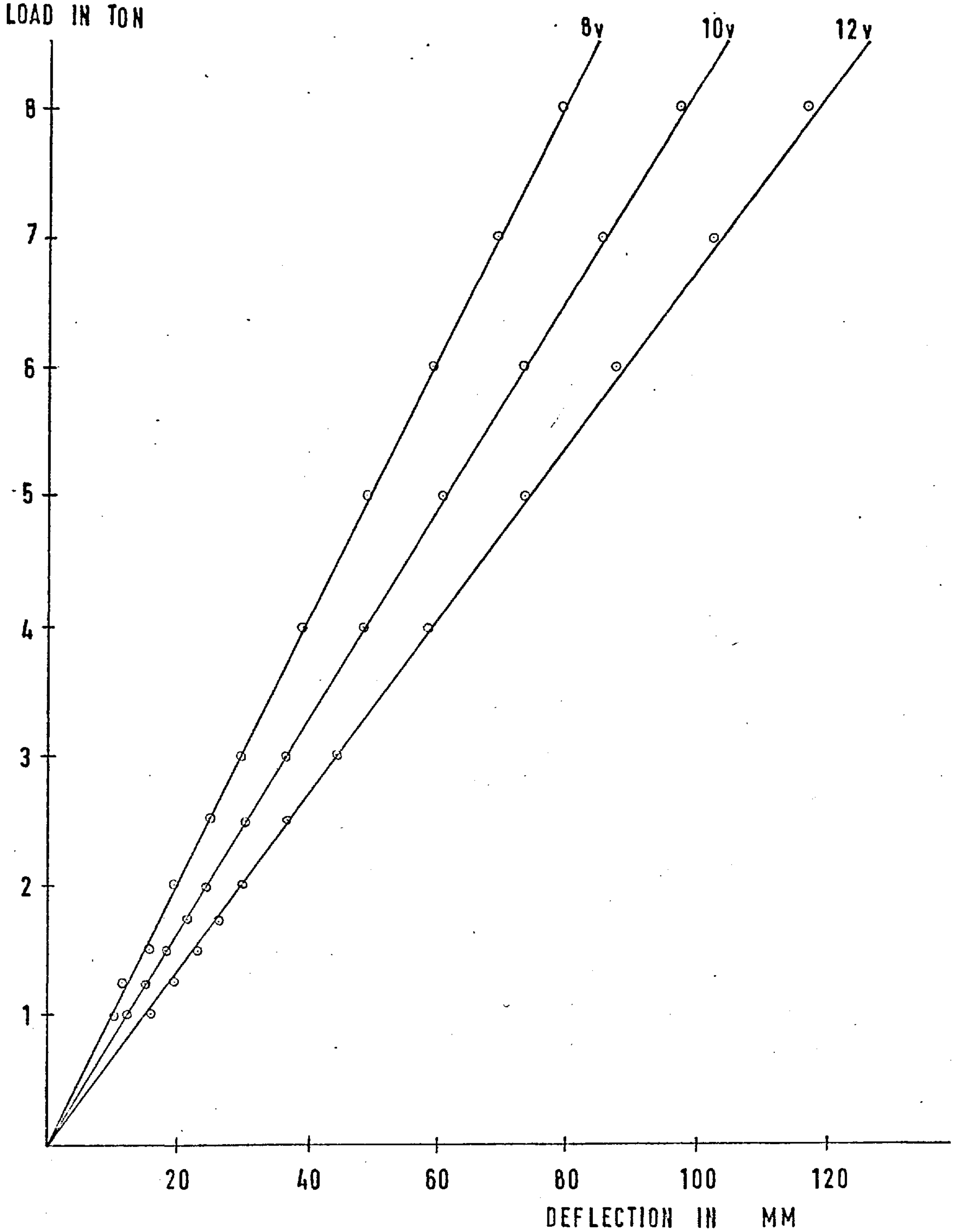


FIG(3-2) CALIBRATION CURVE

LOAD CELL 2

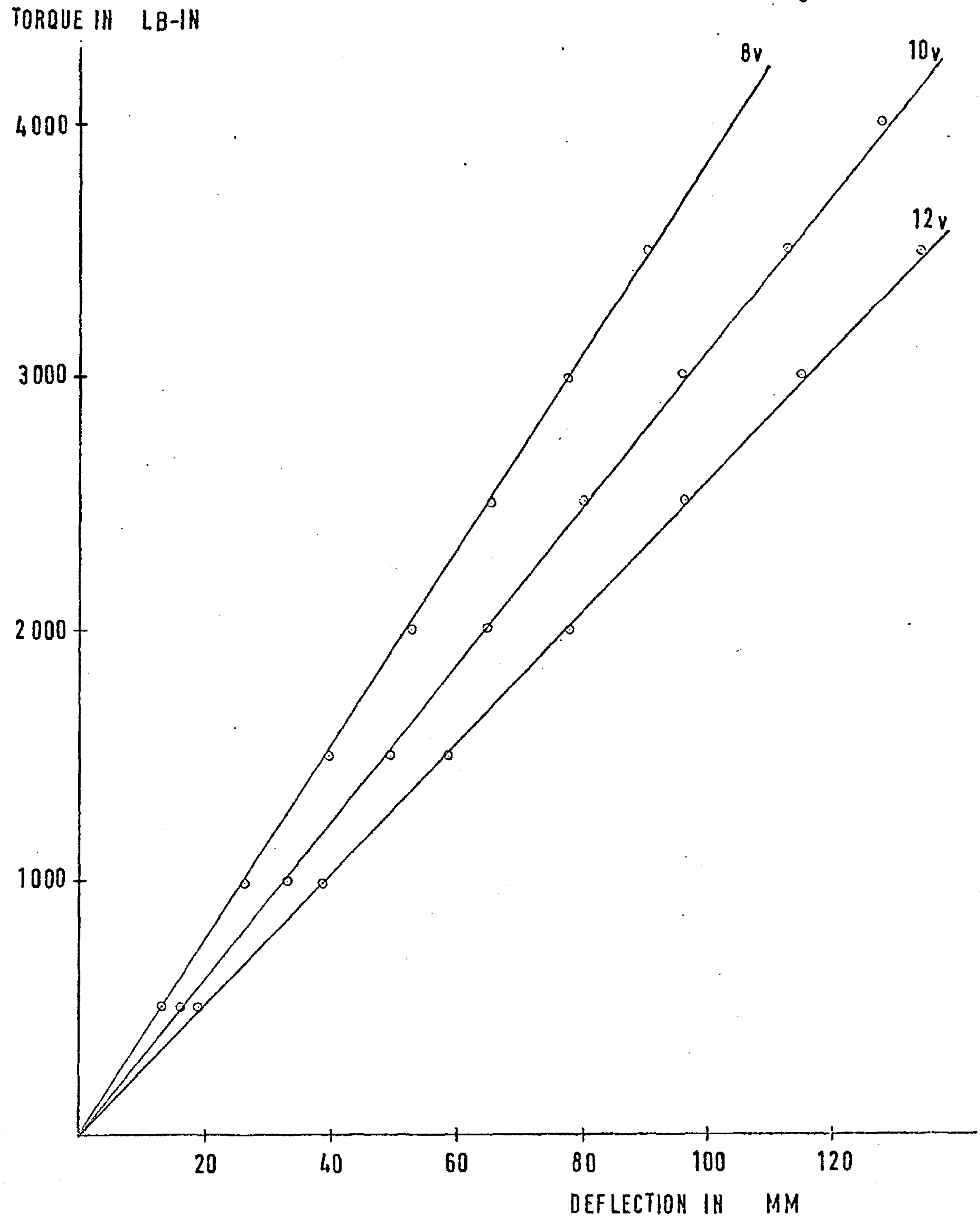


FIG(3-3) CALIBRATION CURVE
UPPER SPINDLE

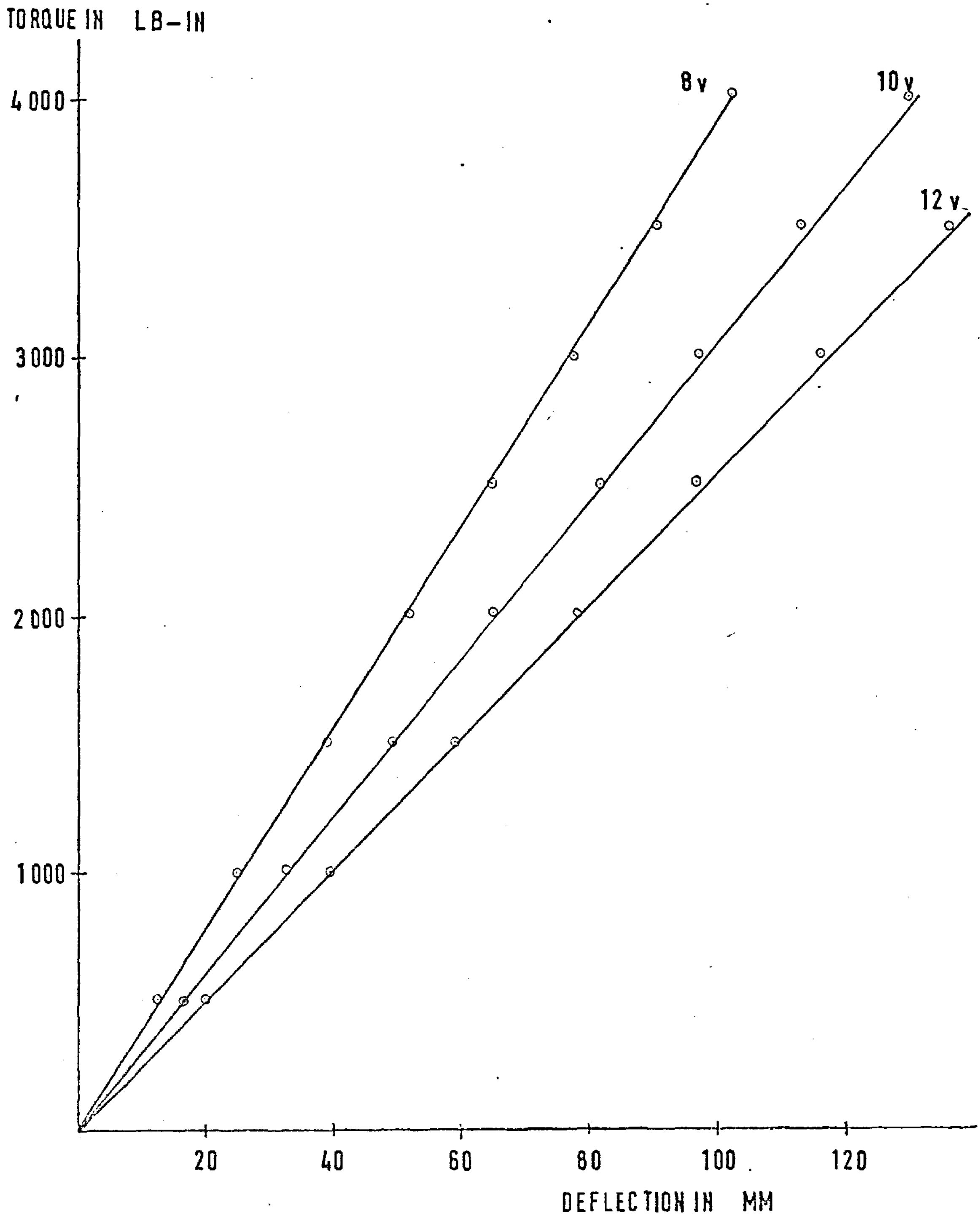


FIG(3-4) CALIBRATION CURVE
LOWER SPINDLE

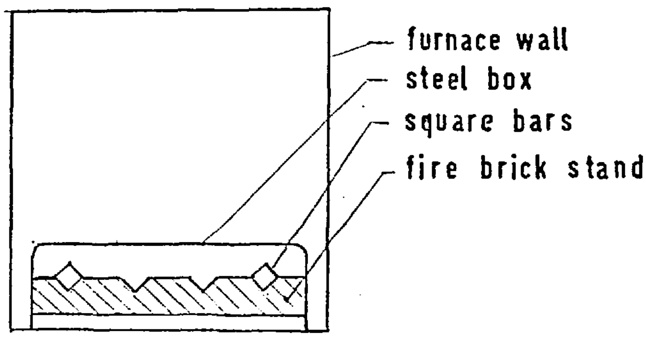


FIG(3-5) STEEL BOX IN THE FURNACE

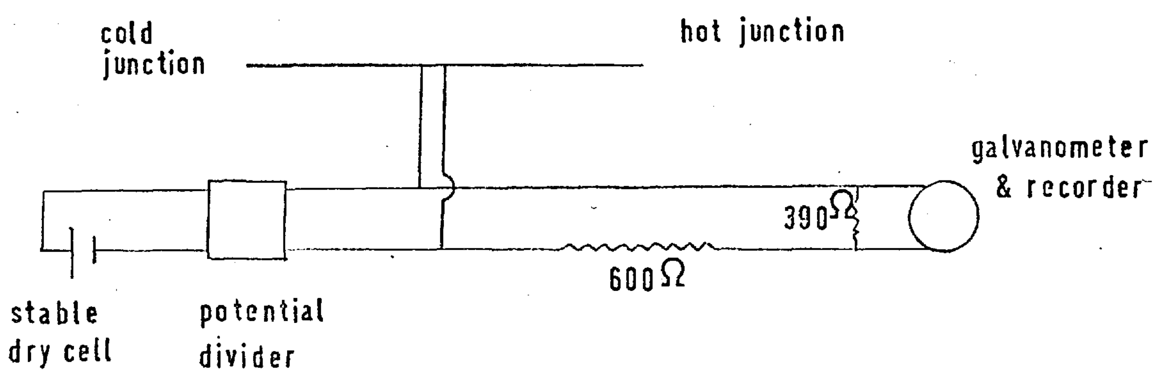


FIG(3-6) COLLING CURVE CIRCUIT

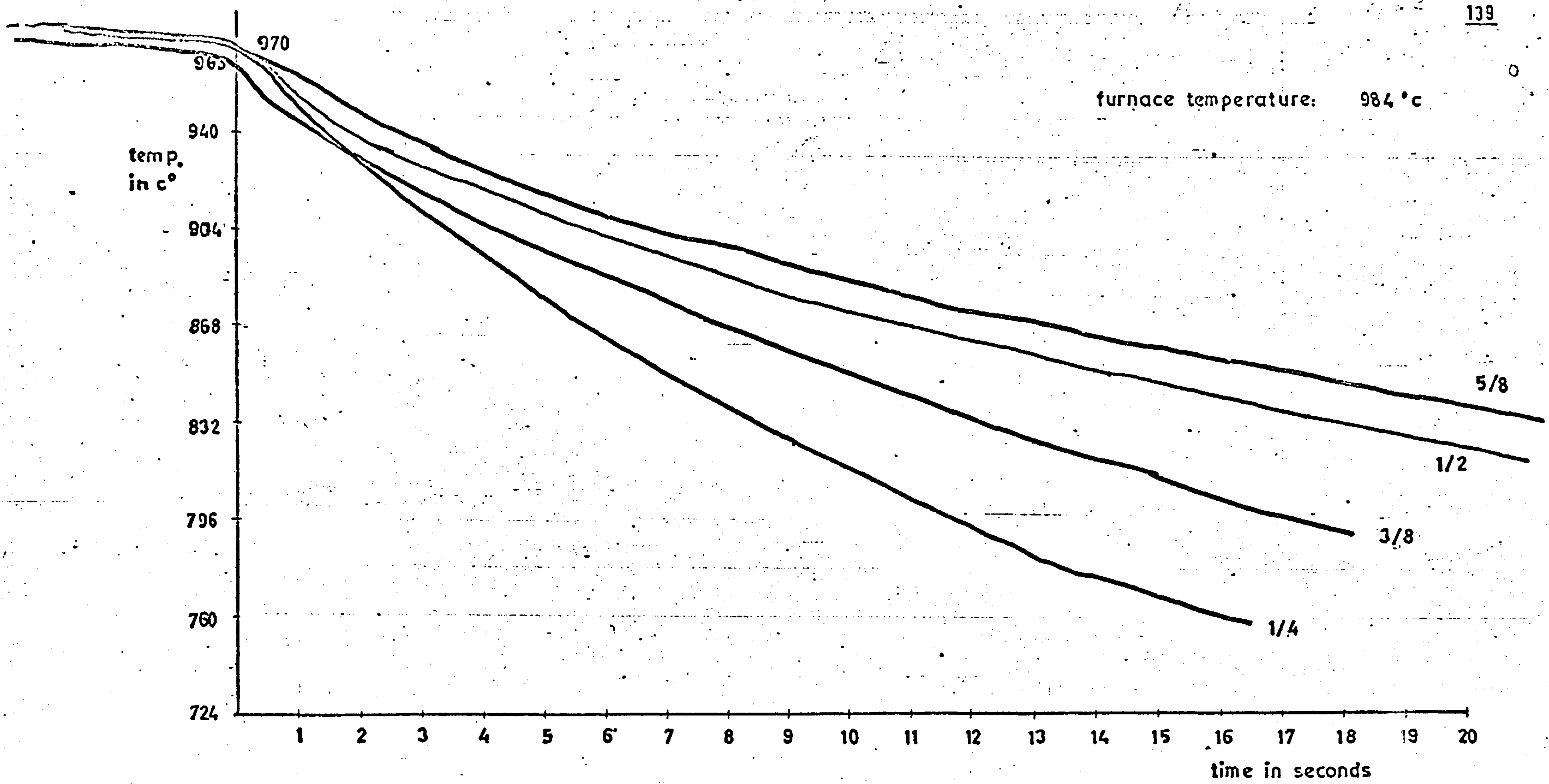


FIG(3-7) COOLING CURVES OF 1/4 3/8 1/2 and 5/8 BARS FROM 984°c

scale 1 mm = 1.8 °c
1 inch = 2 seconds.

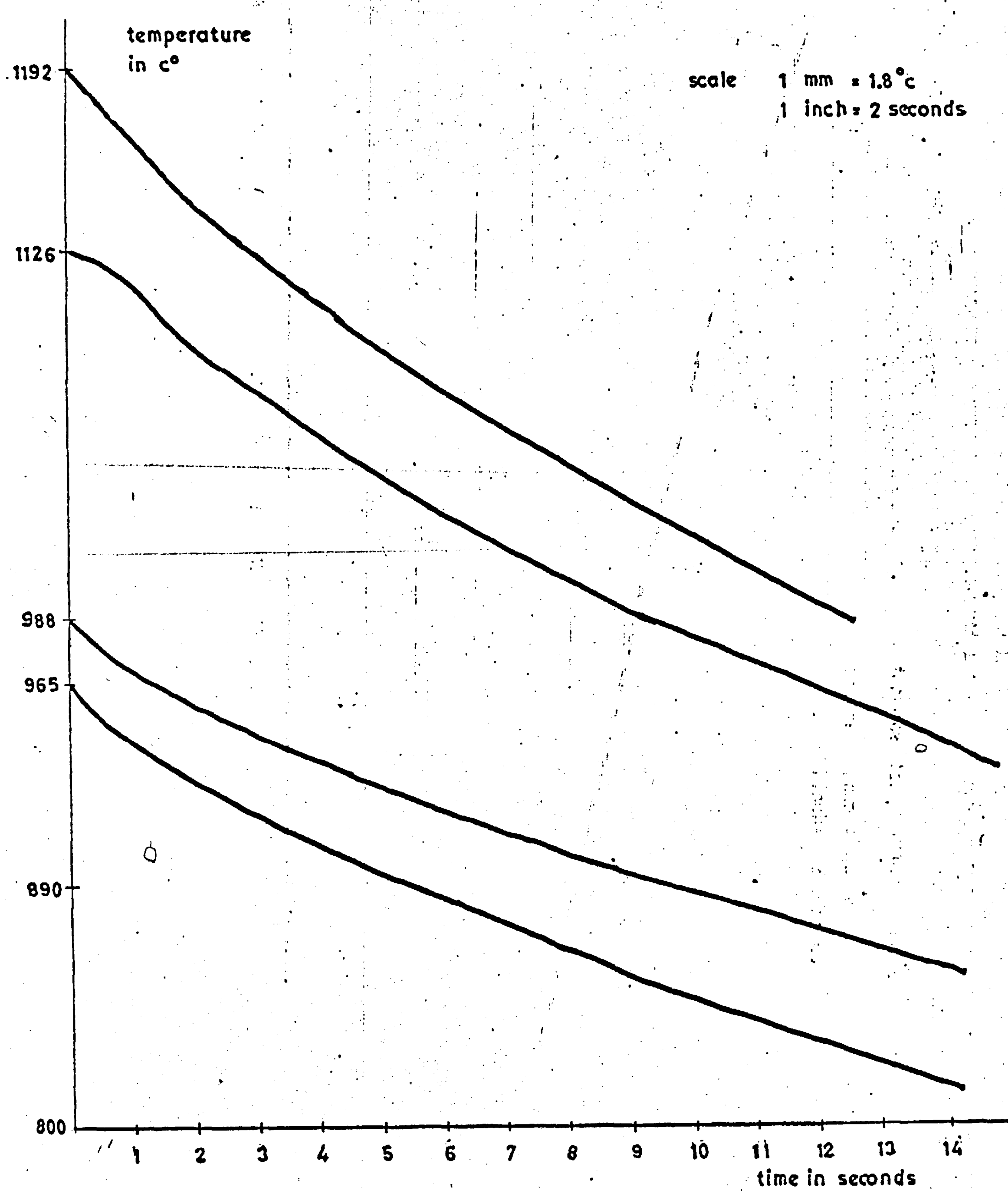


FIG (3-8) COOLING CURVES
OF 3/8 BARS

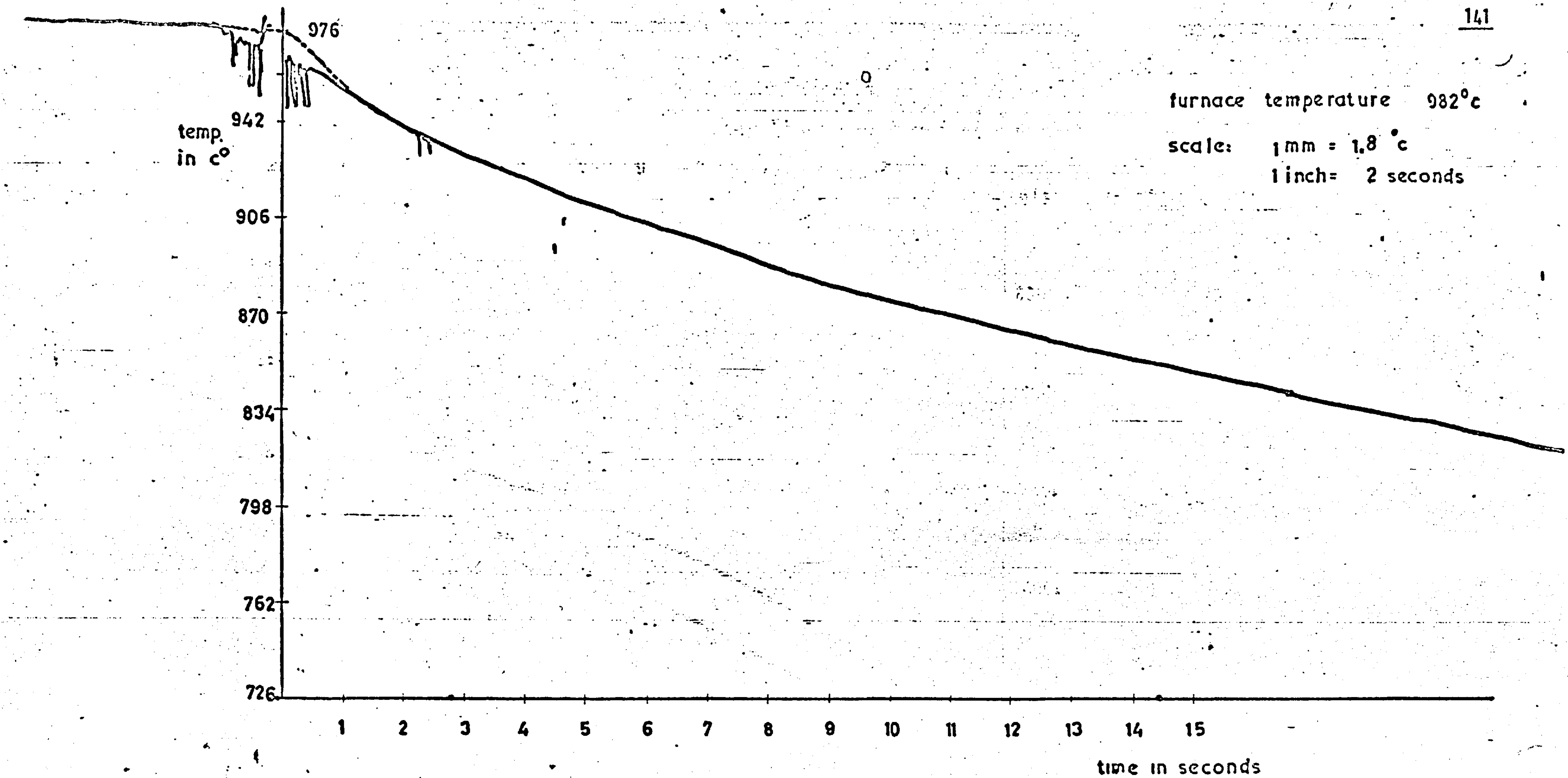


FIG(3-9) COOLING CURVE OF
1/2 BAR

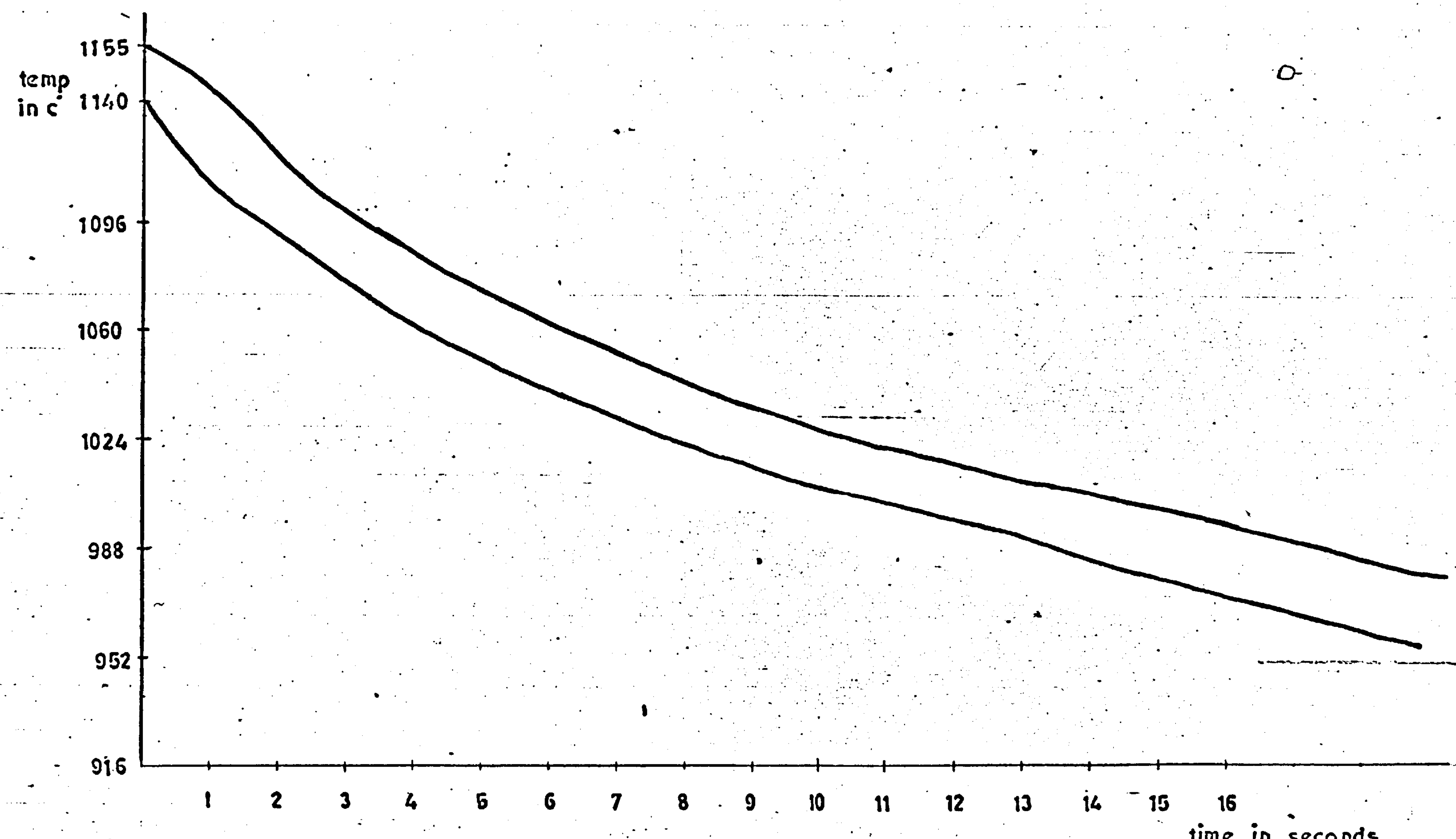


FIG(3-10) COOLING CURVE OF
5/8 BAR

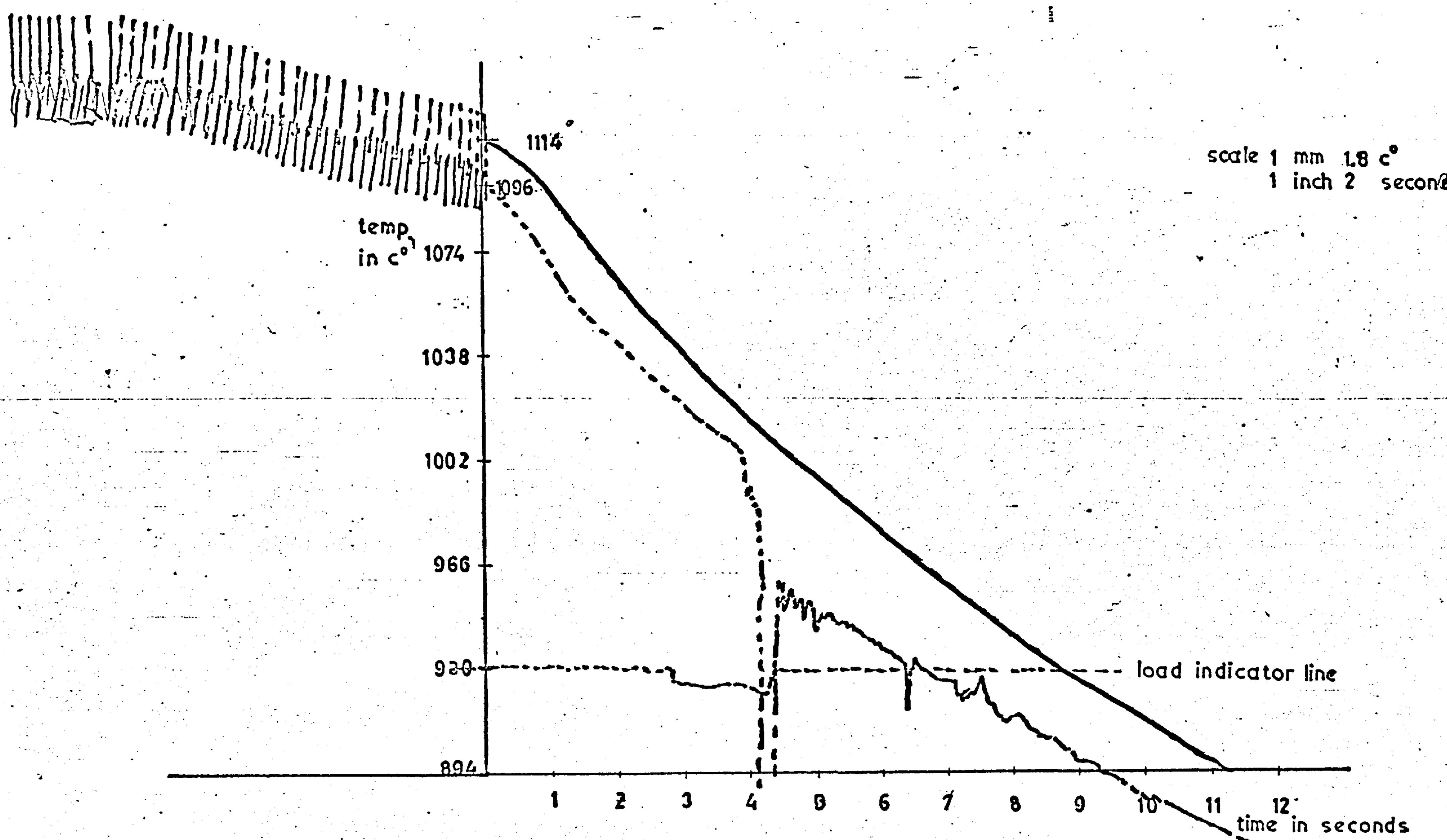


FIG (3-11) COOLING CURVE OF 1/4 BAR

—— AIR COOLED

····· AIR COOLED AND ROLLED

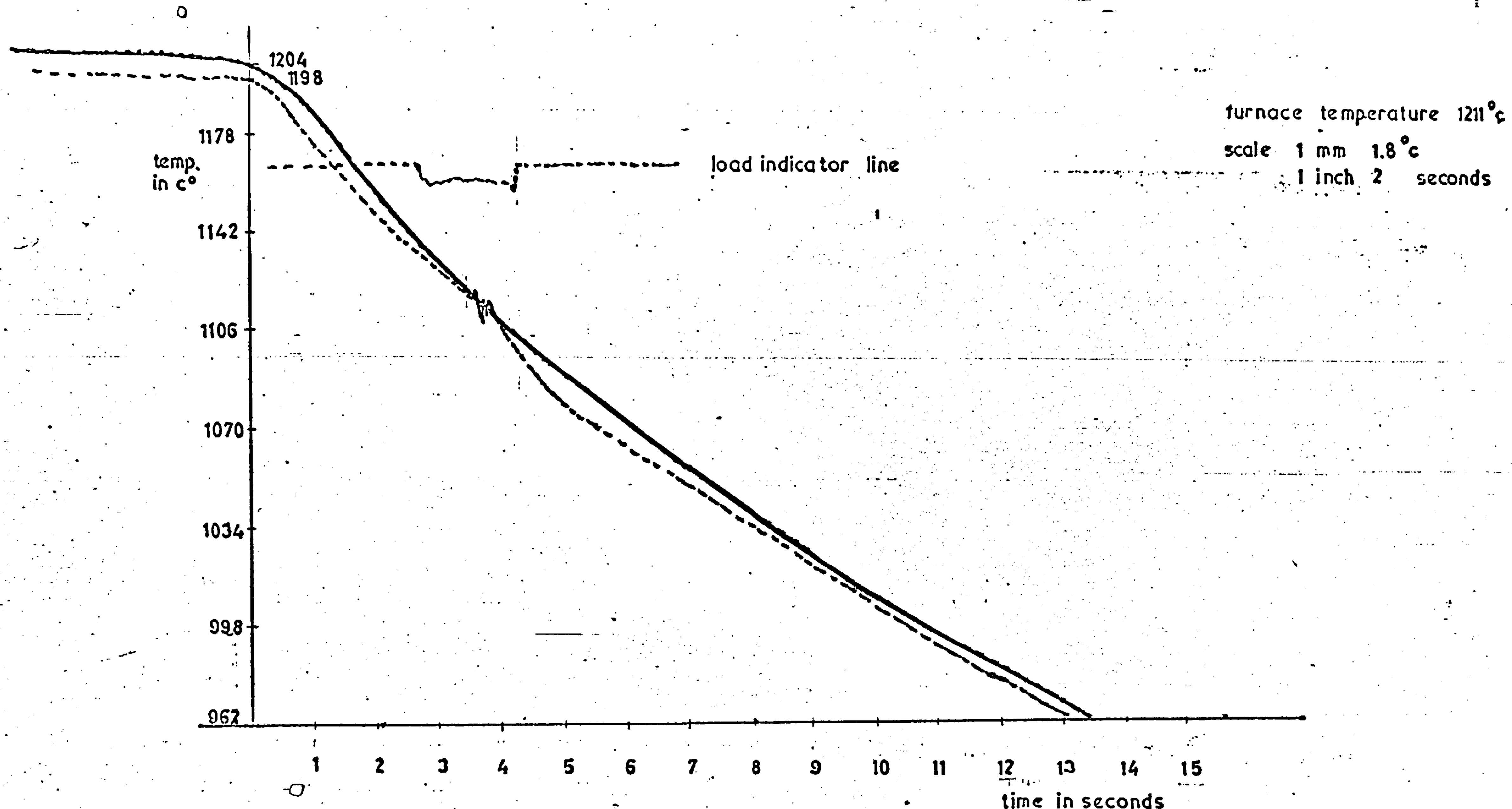


FIG(3-12) COOLING CURVES OF 1/4 BAR

AIR COOLED

AIR COOLED AND ROLLED

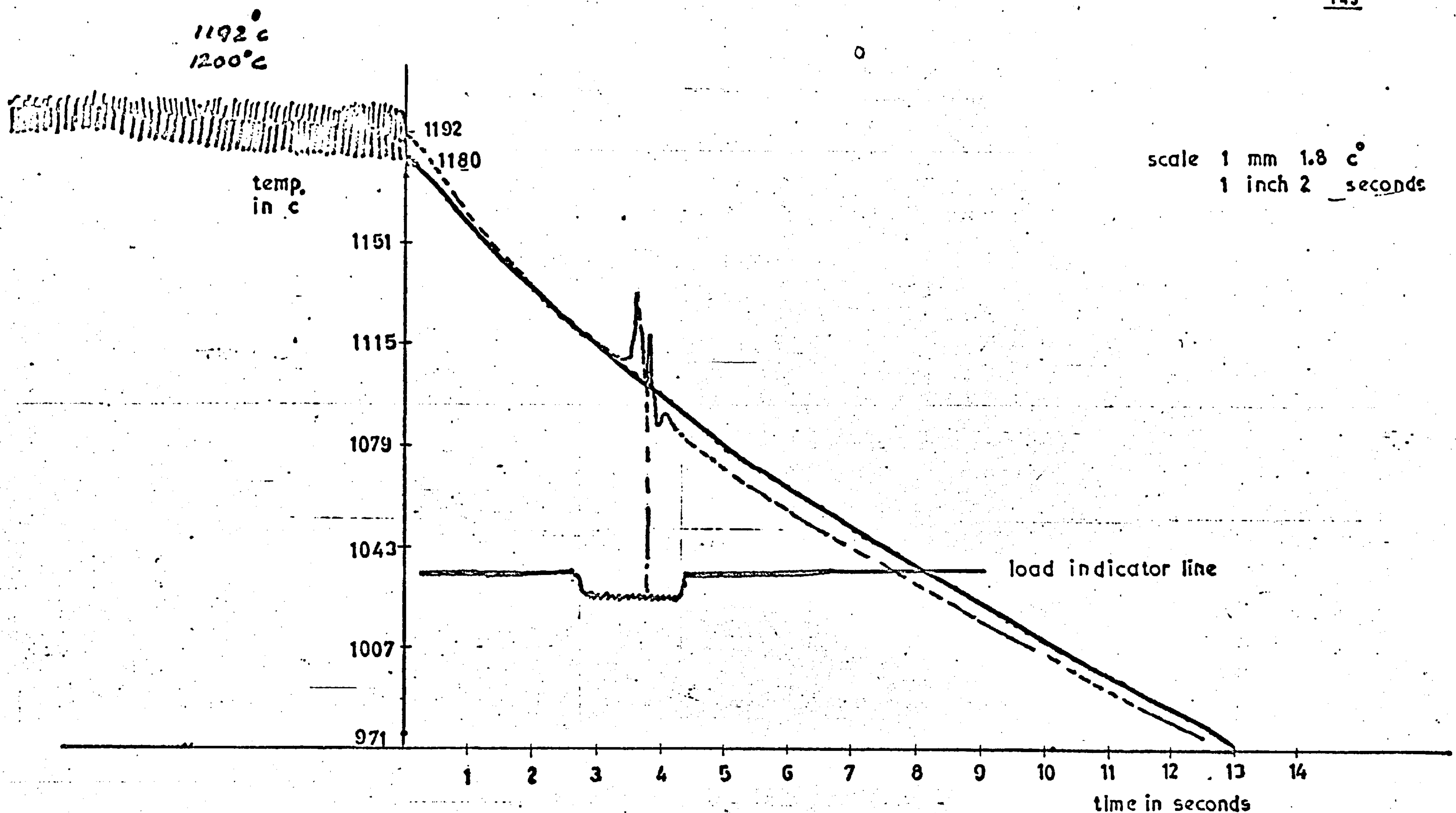


FIG(3-13) COOL CURVE OF 3/8 BAR
AIR COOLED
AIR COOLED AND ROLLED

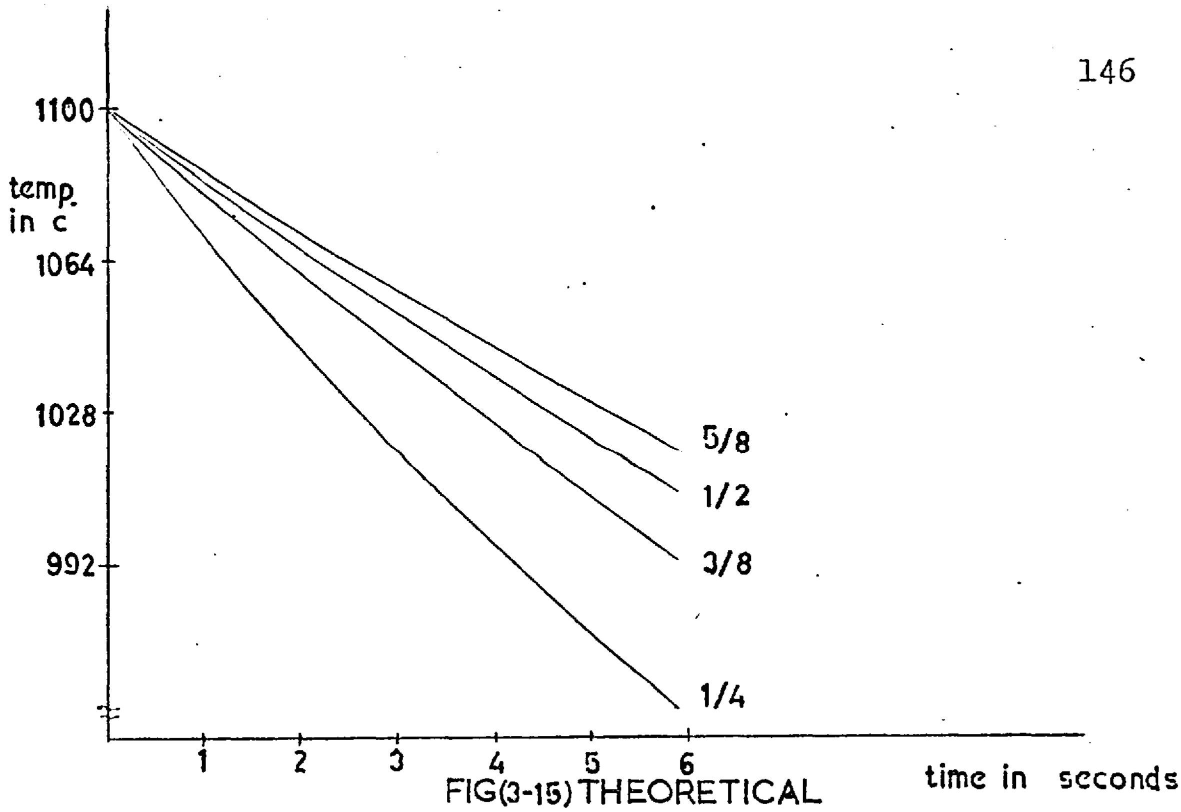


FIG(3-15) THEORETICAL COOLING CURVES

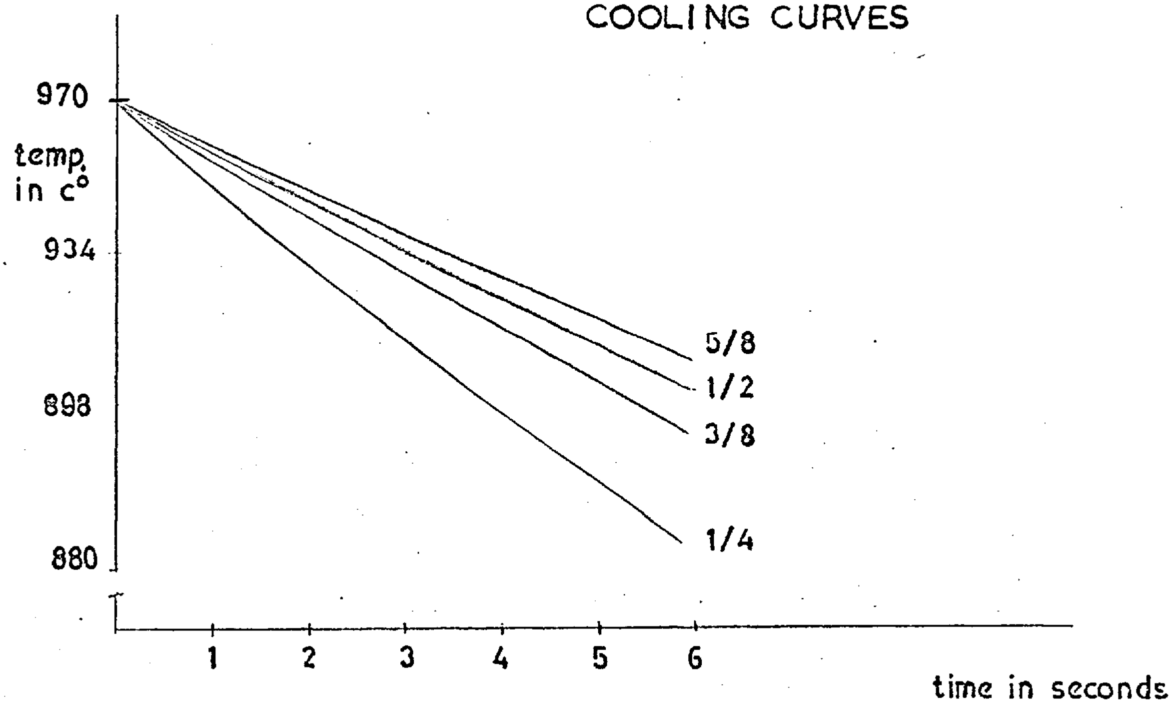


FIG(3-14)THEORETICAL COOLING CURVES

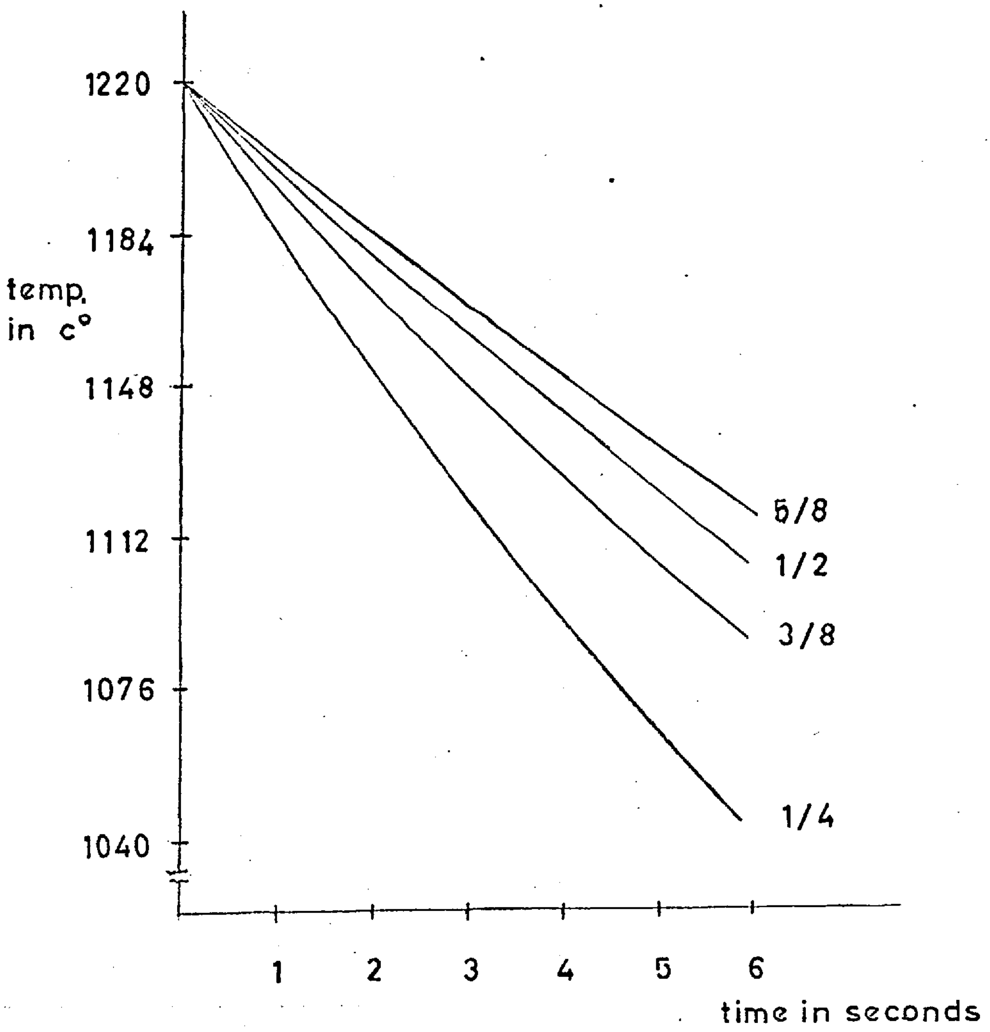


FIG(3-16) THEORETICAL COOLING CURVES

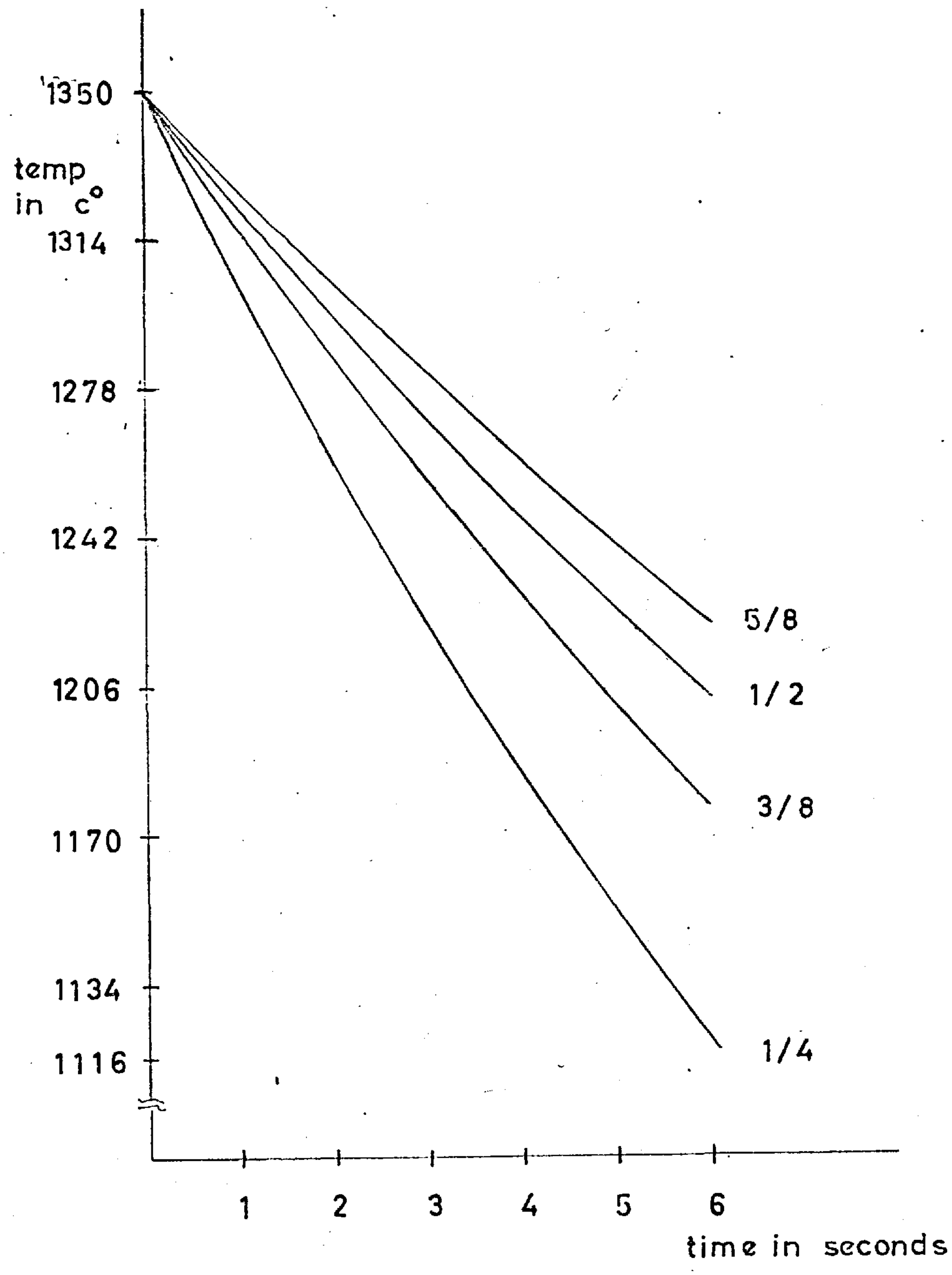


FIG(3-17) THEORETICAL COOLING CURVES

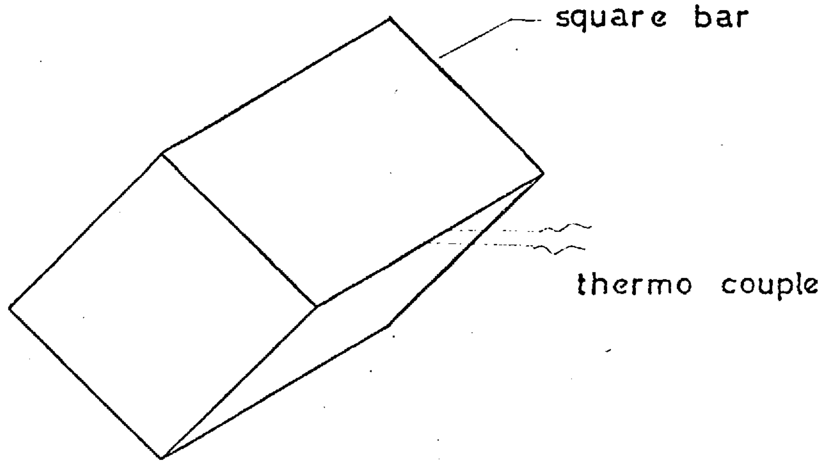


FIG(3-18) THERMO COUPLE CONNECTION

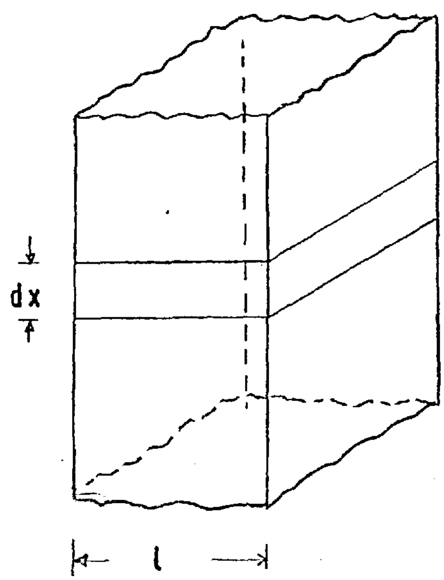


FIG(3-19) AN ELEMENT OF THE
SQUARE BAR

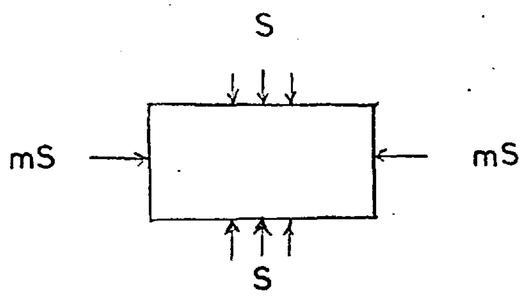


FIG(4-1)

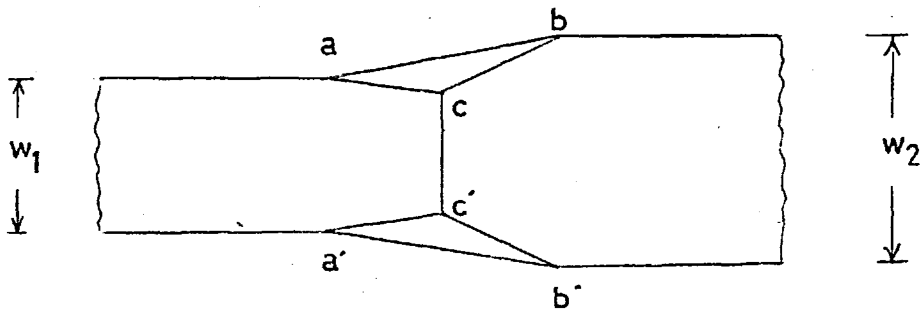


FIG(4-2) abc ARE a'b'c' THE EDGE ZONES WHICH CONTRIBUTE TO SPREADING

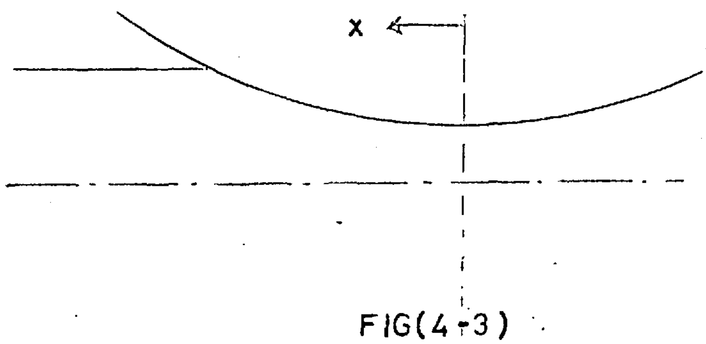


FIG(4-3)

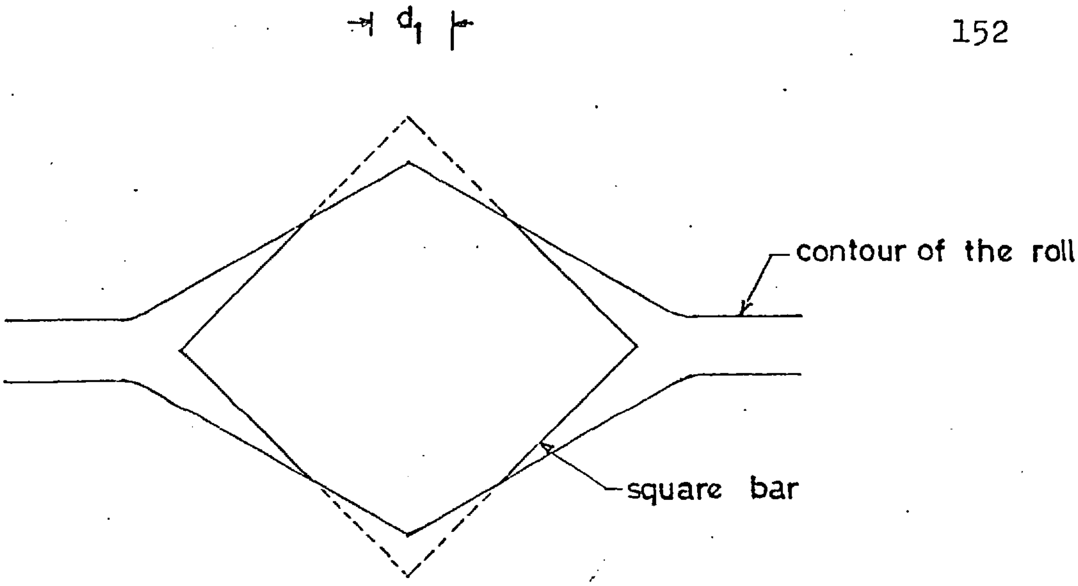


front view of the diamond pass
and square bar

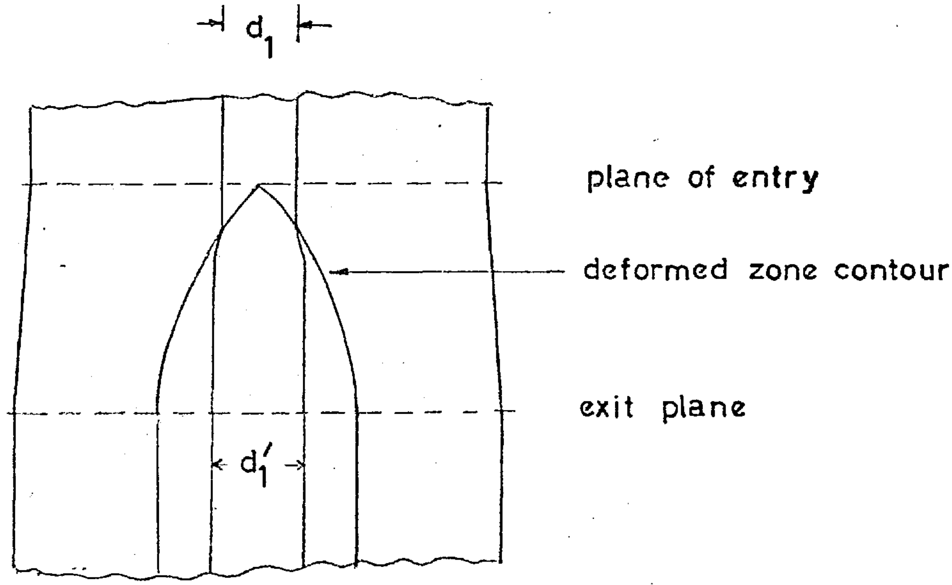


top view of the deformed square bar

FIG (4 - 4 )

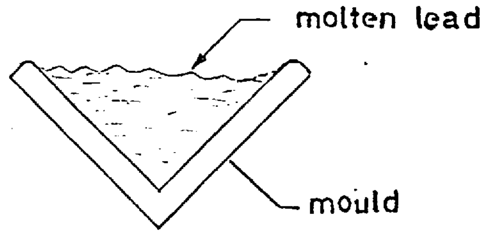


FIG (4-5)

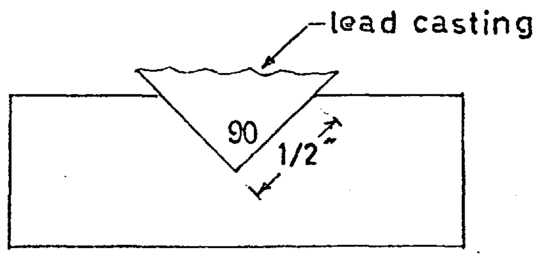


FIG(4-6) JIG PLATE WITH V GROOVE

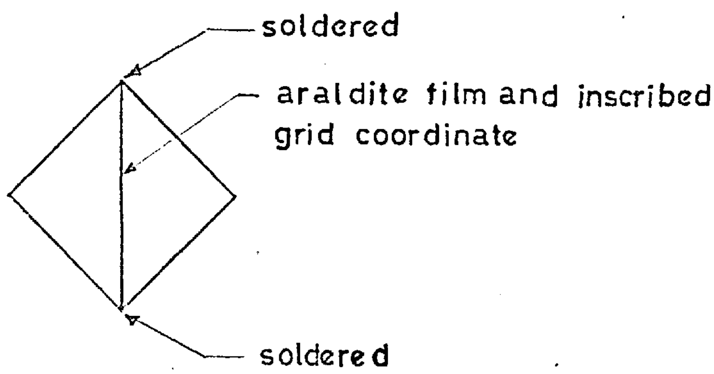


FIG(4-7) TYPICAL LEAD BAR SPECIMEN

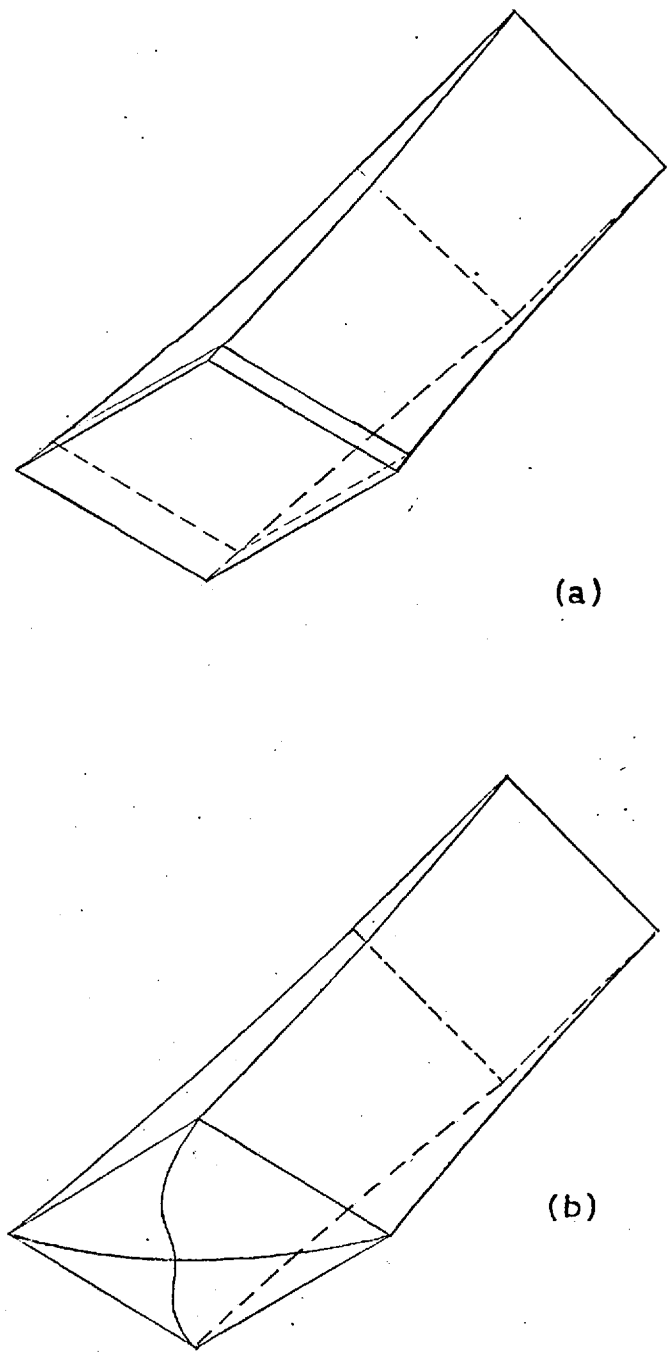


FIG(4-8) a - HOMOGENEOUS DEFORMATION

b - NON HOMOGENEOUS DEFORMATION

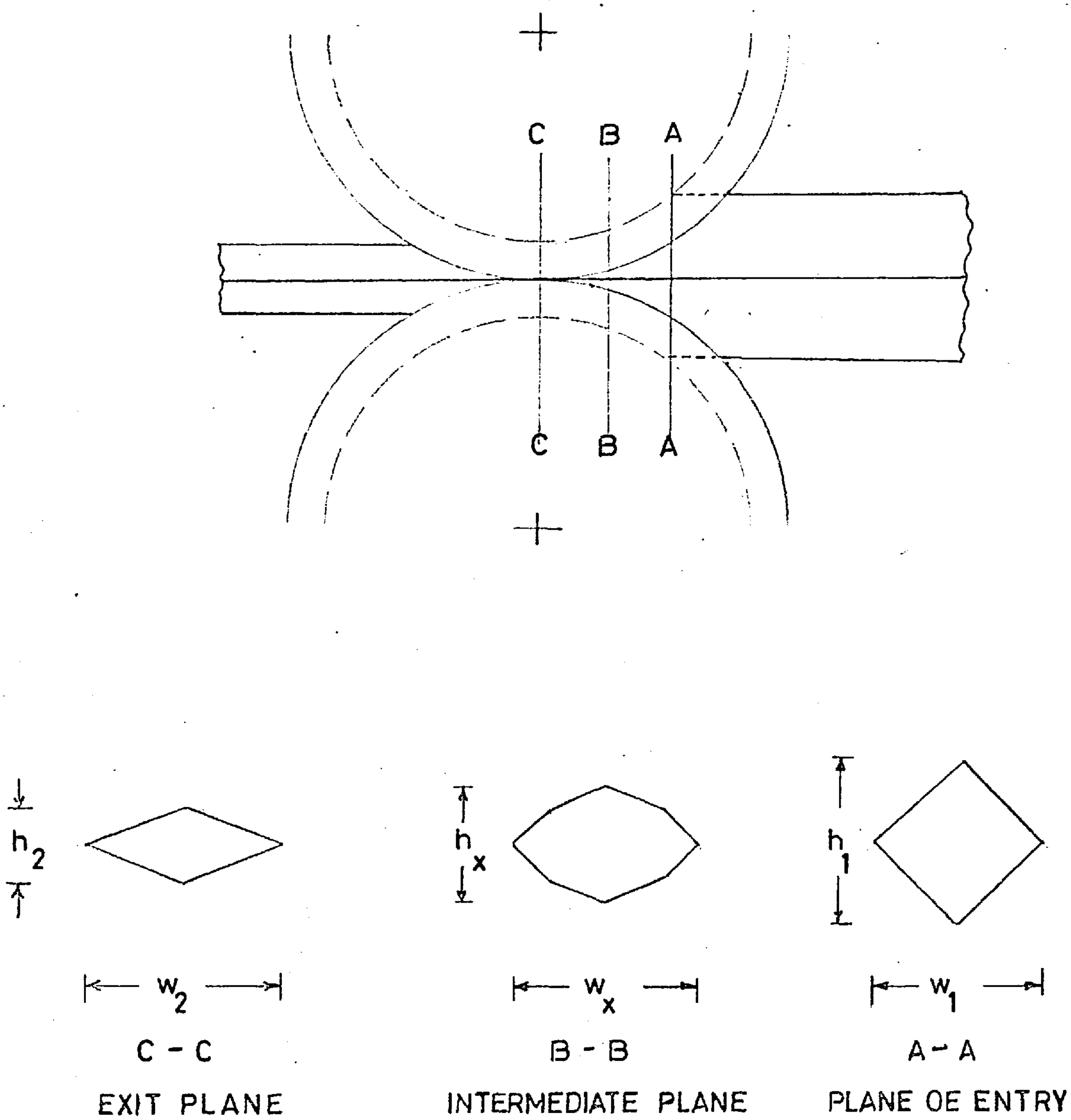


FIG(4-9) GEOMETRICAL CHANGE OF SECTION.

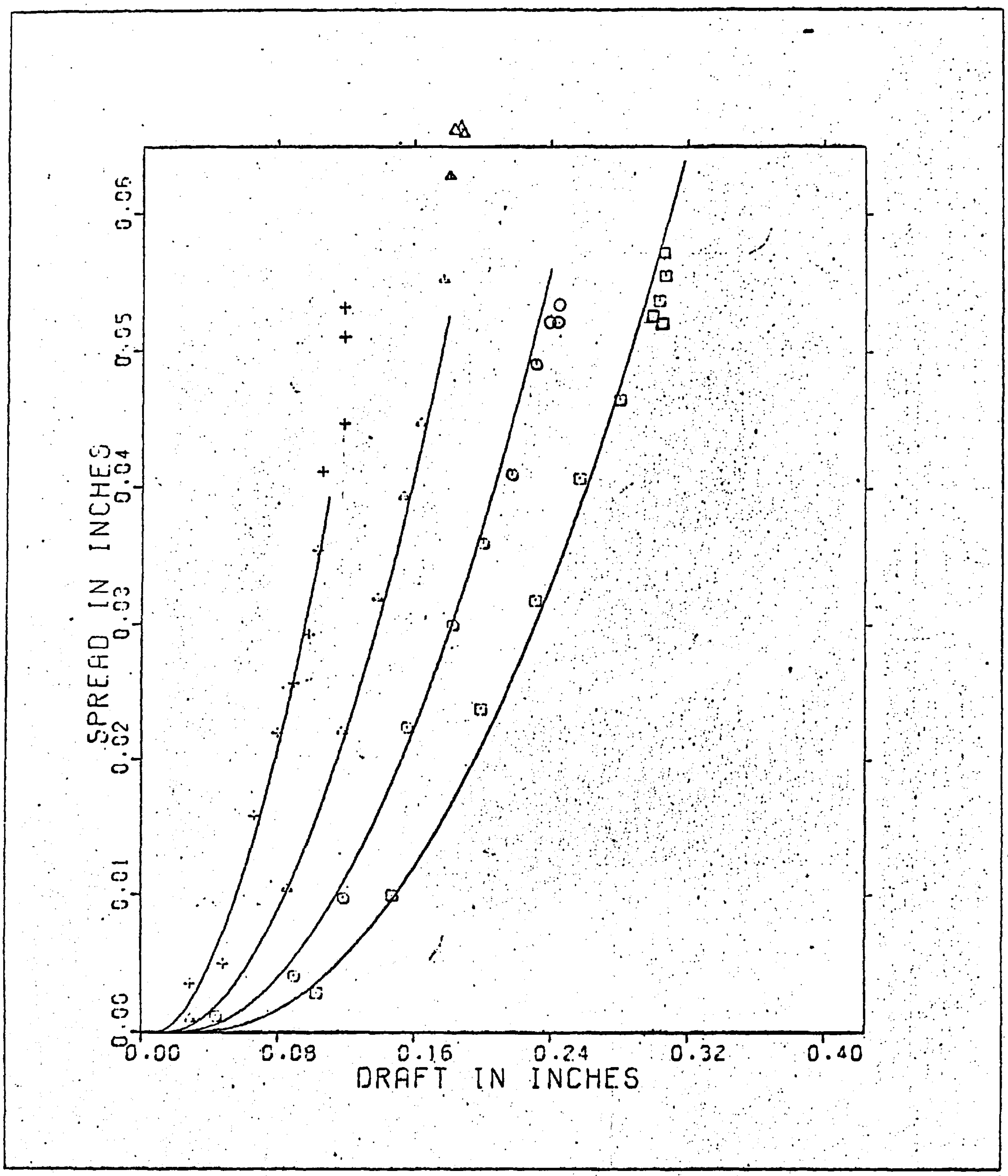


FIG(4-10) DRAFT SPREAD THEORETICAL CURVES
AND EXPERIMENTAL DATA FOR 900 °C.

1/4 —— +  3/8 —— △

1/2 —— o  5/8 —— □

(SQUARE BAR SIZE AND SYMBOLS)

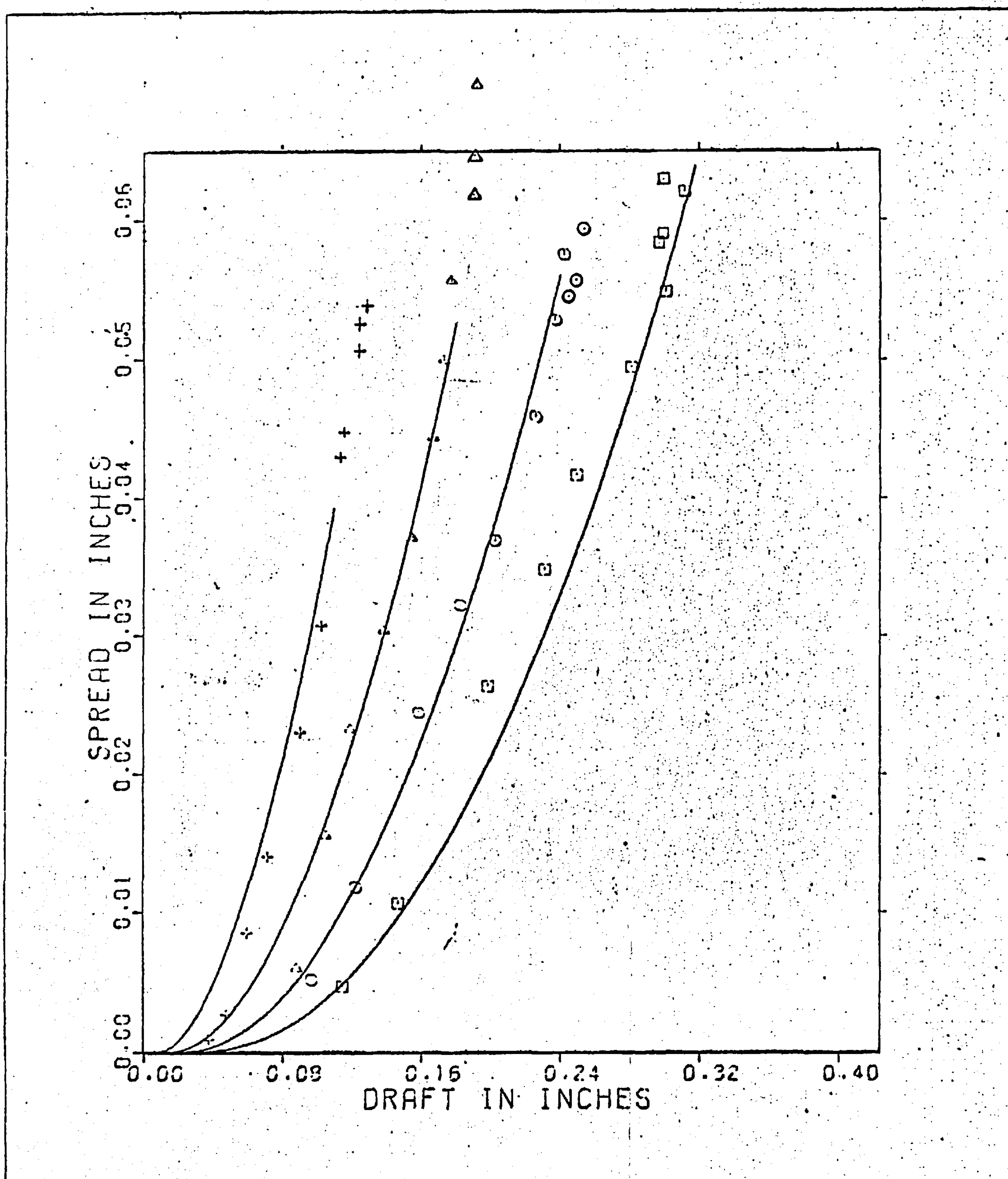


FIG(4-11) DRAFT SPREAD THEORETICAL CURVES
AND EXPERIMENTAL DATA FOR 1000 °C.

1/4 —— +    3/8 —— △

1/2 —— o    5/8 —— □

(SQUARE BAR SIZE AND SYMBOLS)

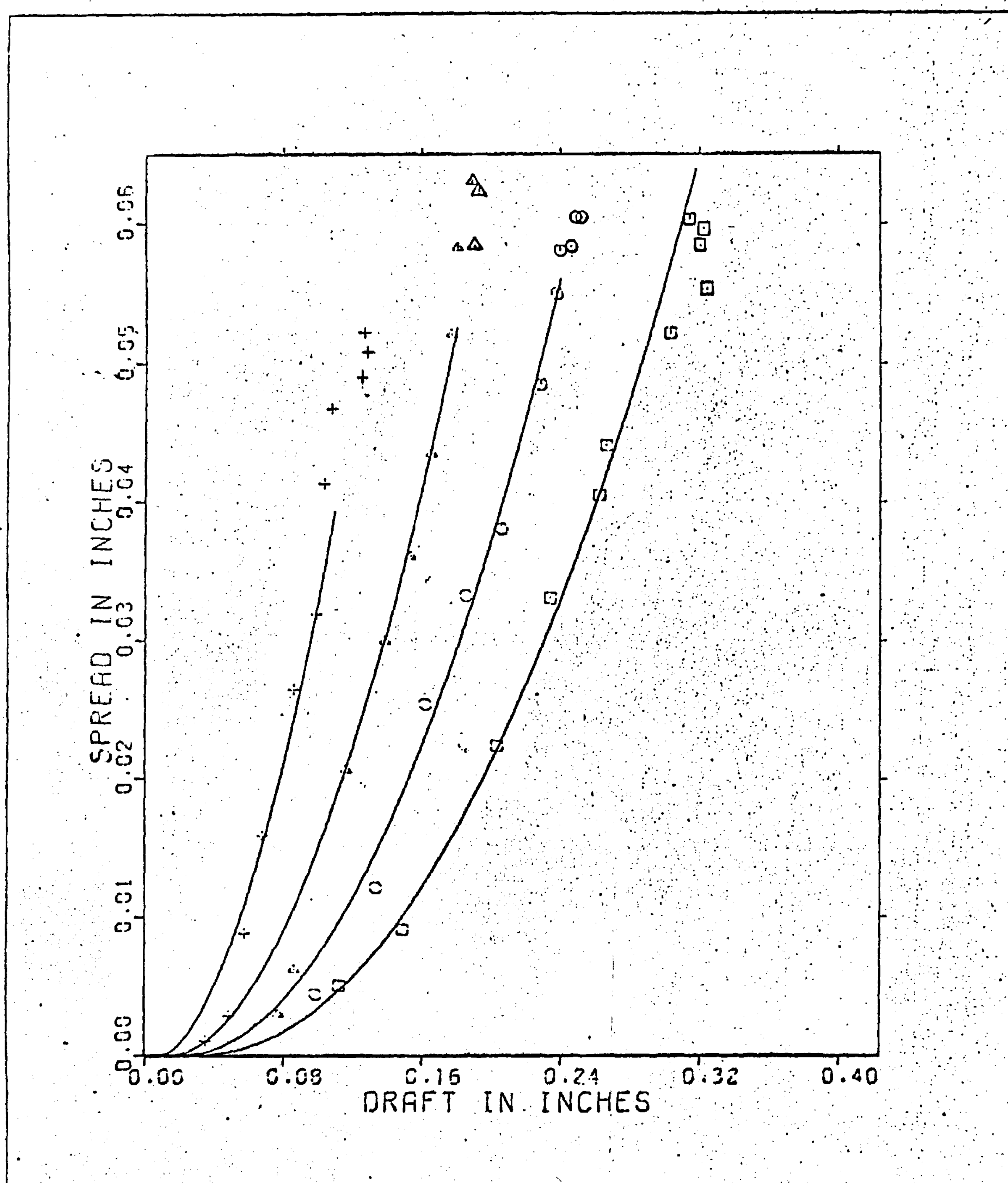


FIG(4-12) DRAFT_SPREAD THEORETICAL CURVES
AND EXPERIMENTAL DATA FOR 1100 °C.

1/4 —— +     3/8 —— △

1/2 —— o     5/8 —— □

(SQUARE BAR SIZE AND SYMBOLS)

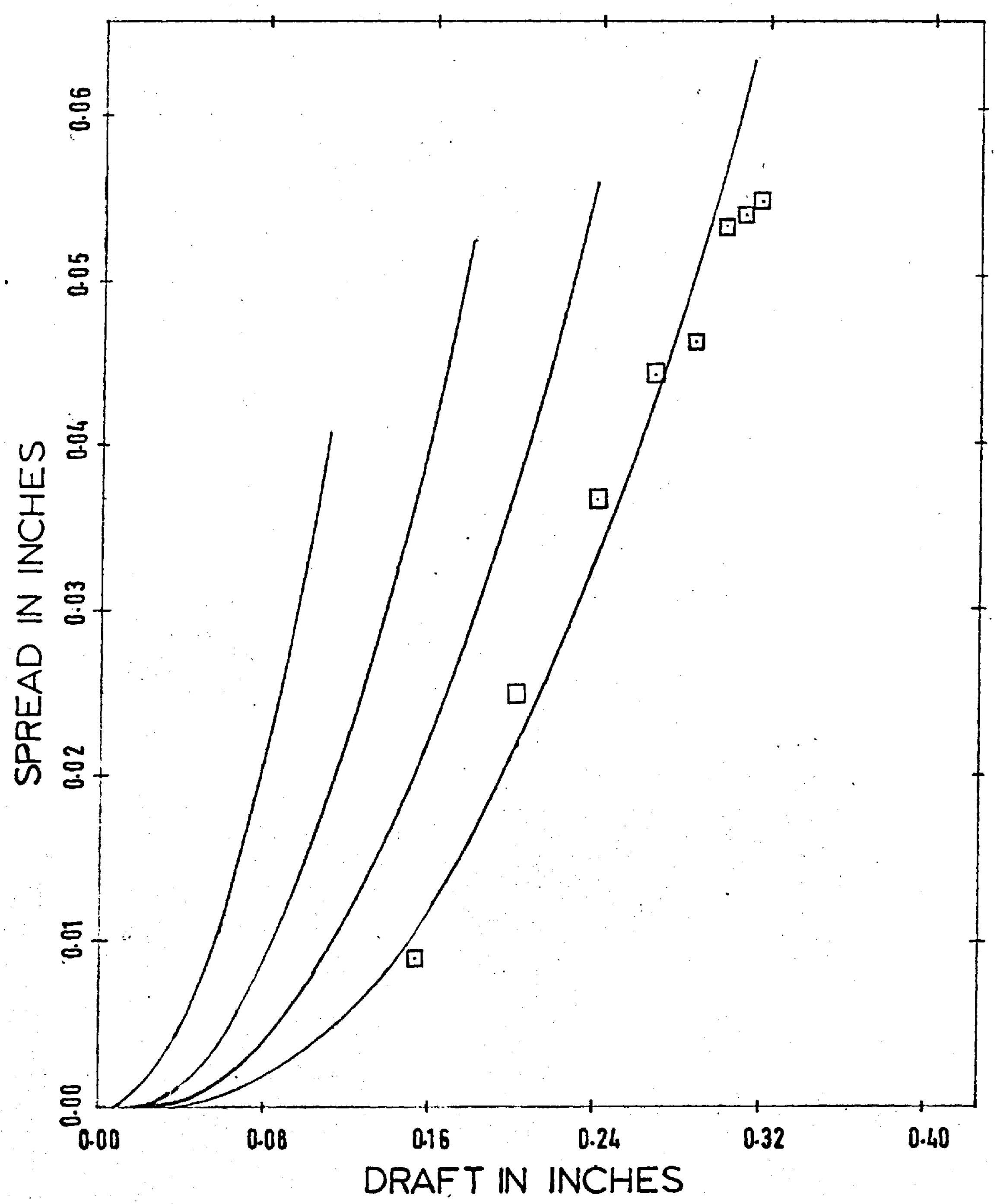


FIG(4-13) DRAFT SPREAD THEORETICAL CURVES
AND EXPERIMENTAL DATA FOR 1200 °C.
(the only obtainable experimental data was
for 5/8 square bar)

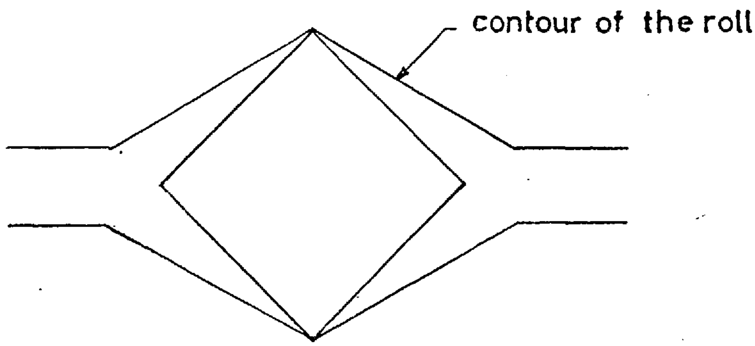


FIG (4-14) FULLY OPEN POSITION OF THE ROLLS.

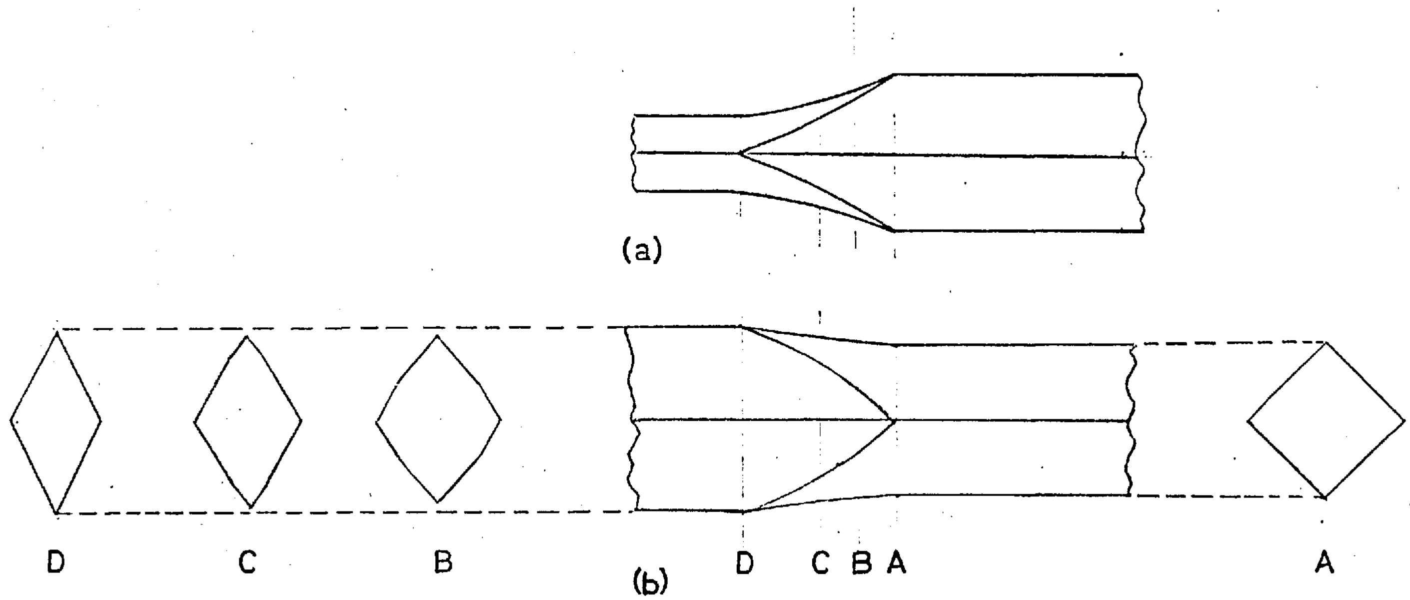


FIG (4-15) PROGRESSIVE CHANGE IN GEOMETRY OF SQUARE BAR IN DIAMOND PASS.

(a) SIDE VIEW (b) TOP VIEW

A BAR CROSS SECTION AT THE PLANE OF ENTRY

B &C BAR CROSS SECTION AT AN INTERMEDIATE PLANE

D BAR CROSS SECTION AT THE EXIT PLANE

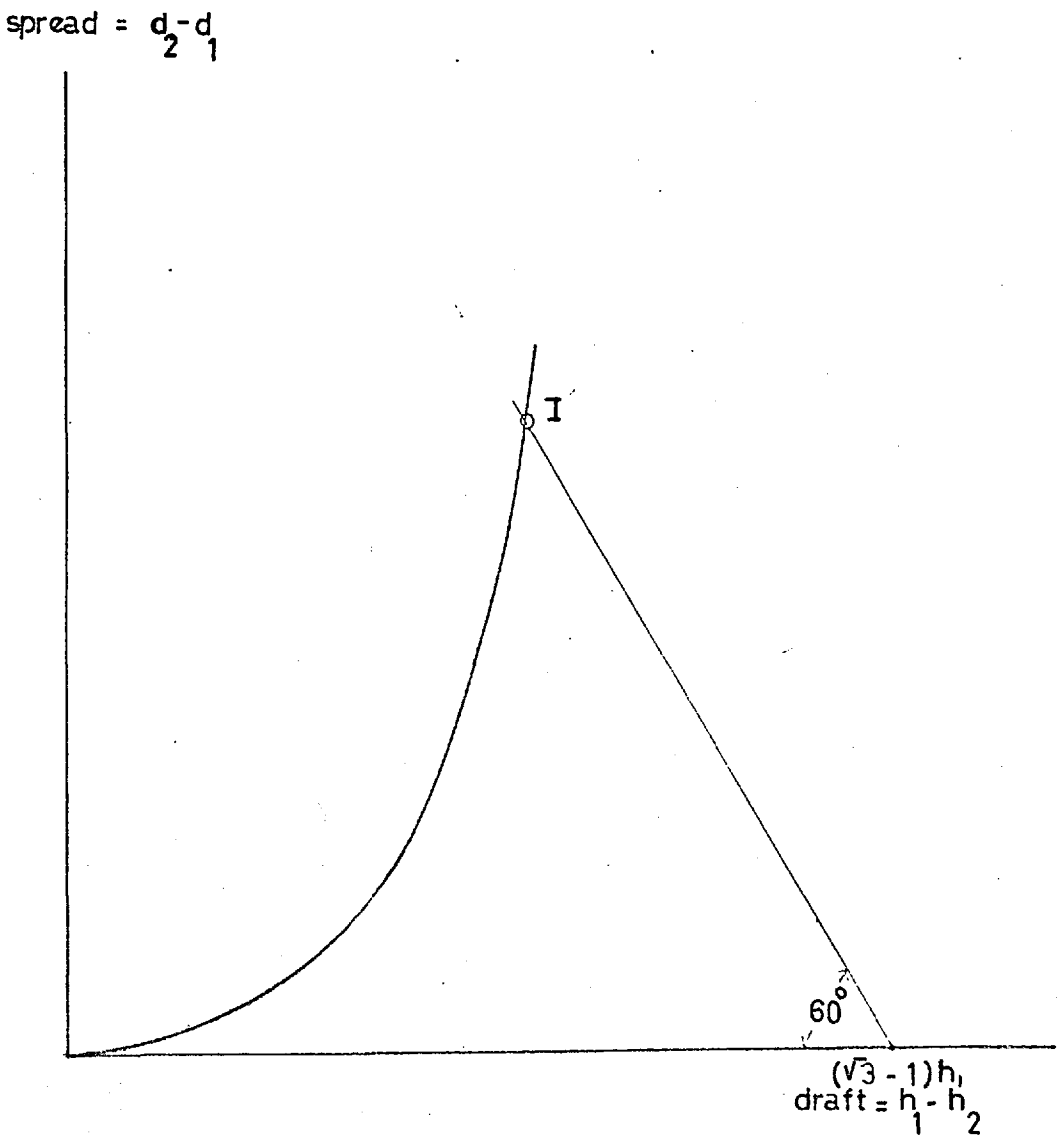


FIG(4-16) GENERAL FORM OF THE NEW SPREAD-DRAFT FORMULA (ALONG THE ARC OF CONTACT). I REPRESENTS THE POINT WHERE THE BAR CROSS SECTION ATTAINS DIAMOND GEOMETRY.

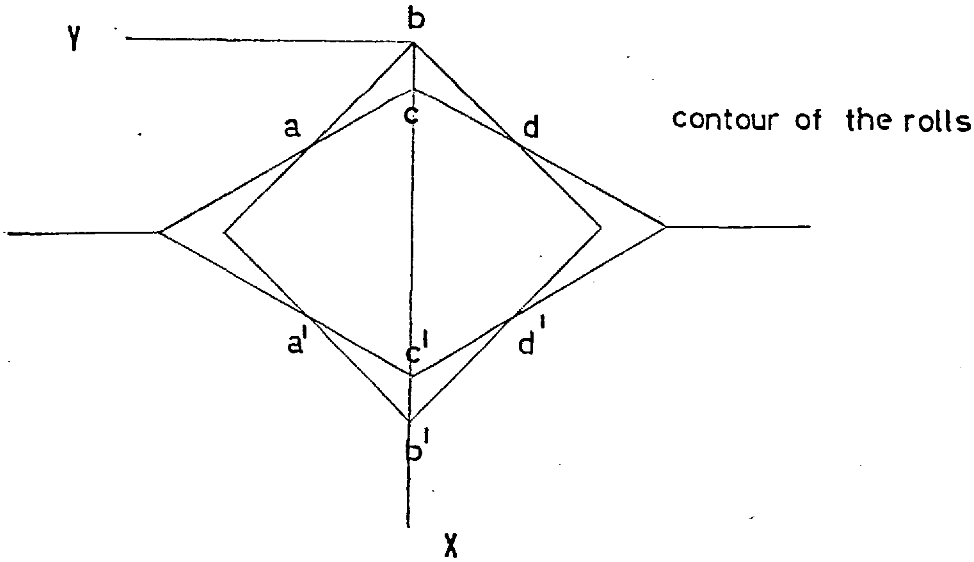


FIG (4-17) RELATIVE CONFIGURATION OF SQUARE BAR AND DIAMOND PASS.
abcd AND a'b'c'd' ARE THE EXCESS AREA DISPLACED FORWARD AND SIDEWAYS

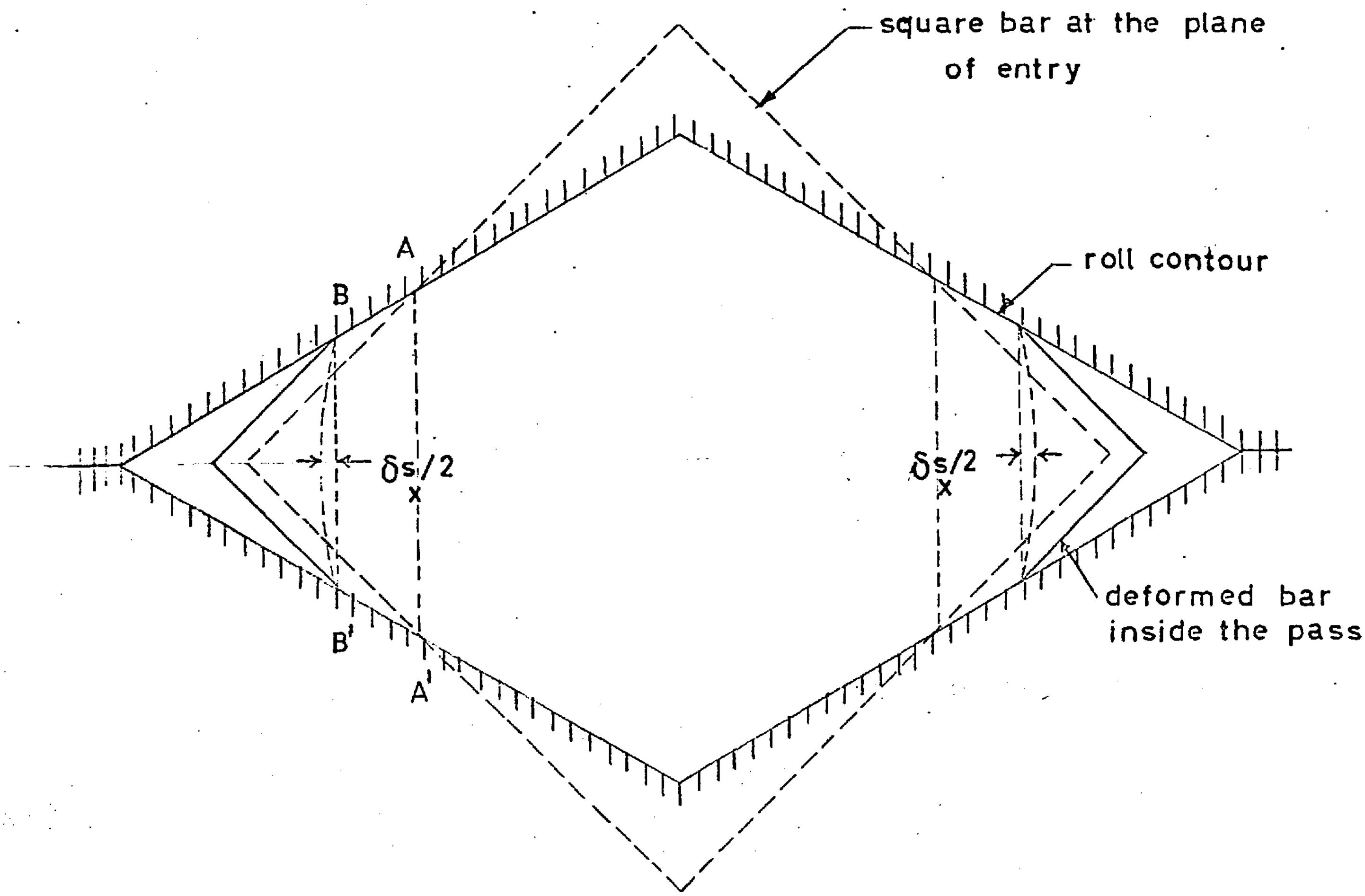


FIG(4-18) DEFORMED SQUARE BAR INSIDE THE PASS
AT DISTANCE X FROM THE PLANE OF ENTRY

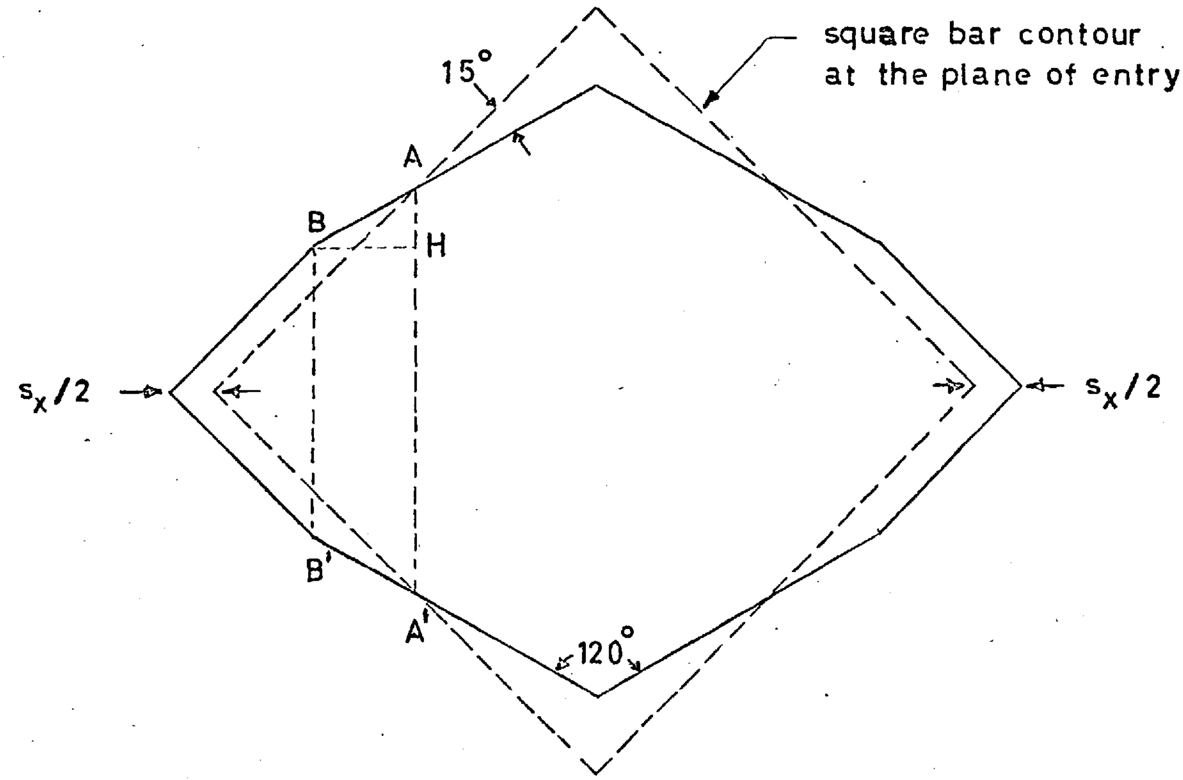


FIG (4-19) DEFORMED CROSS SECTION
AT DISTANCE X FROM THE
PLANE OF ENTRY.

$AB = A'B' = l$

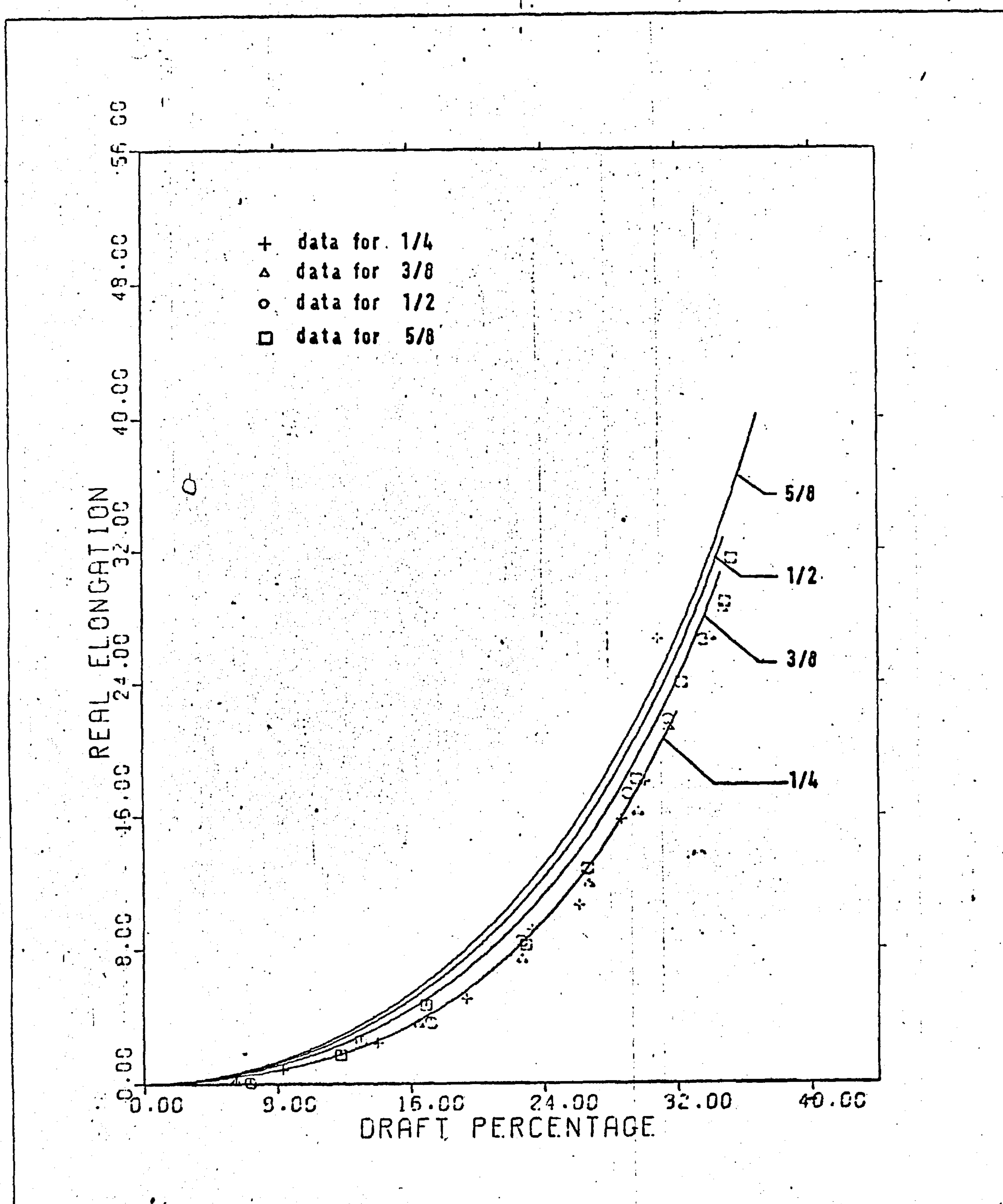


FIG(4-20) ELONGATION DRAFT PERCENTAGE
SOLID LINES: THEORETICAL FOR 1/4
TO 5/8 SQUARE BARS.

TEMPERATURE: 900 °C

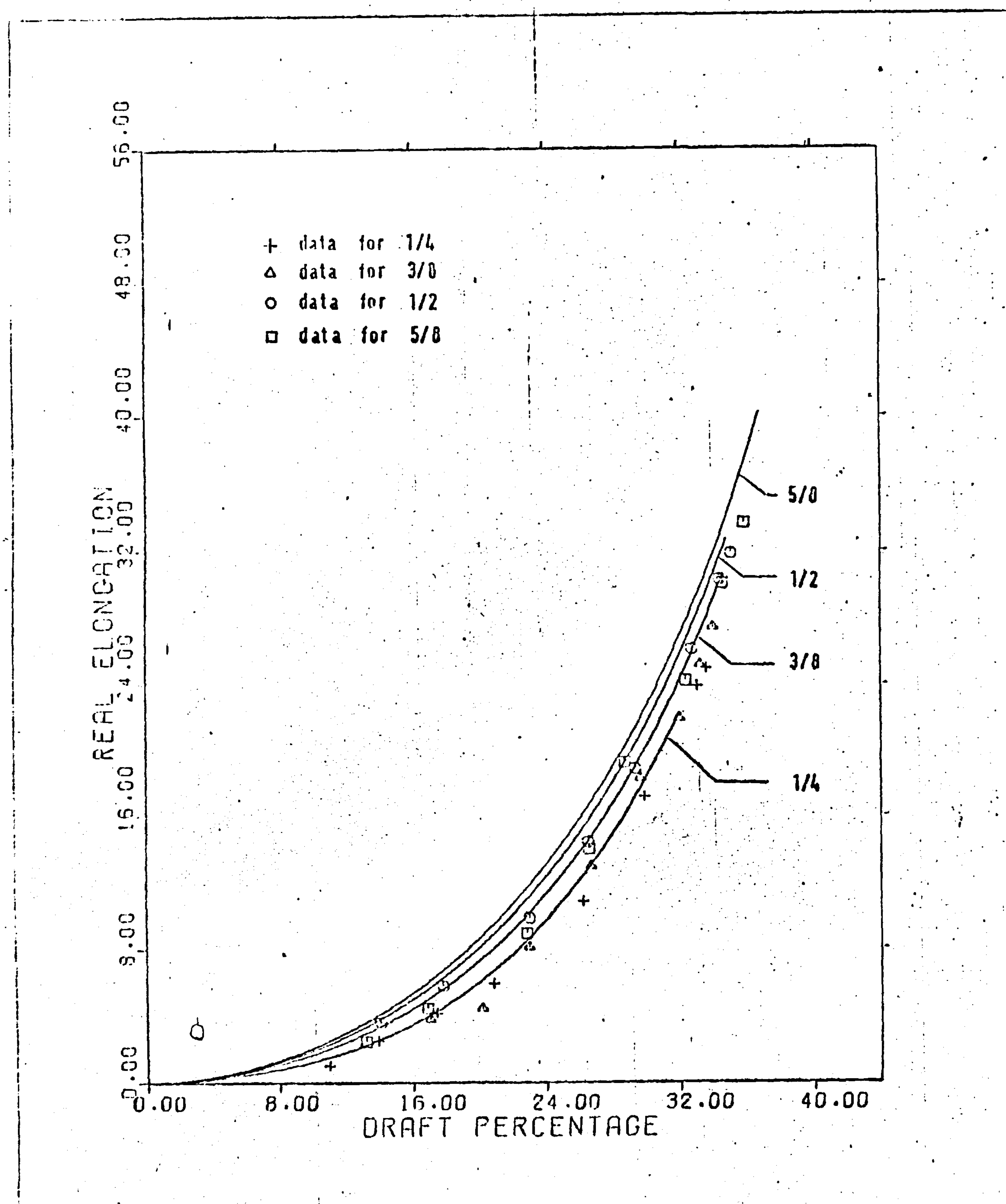


FIG(4-21) ELONGATION DRAFT PERCENTAGE
SOLIDE LINES: THEORETICAL FOR 1/4
TO 5/8 SQUARE BARS.

TEMPERATURE: 1000 °C

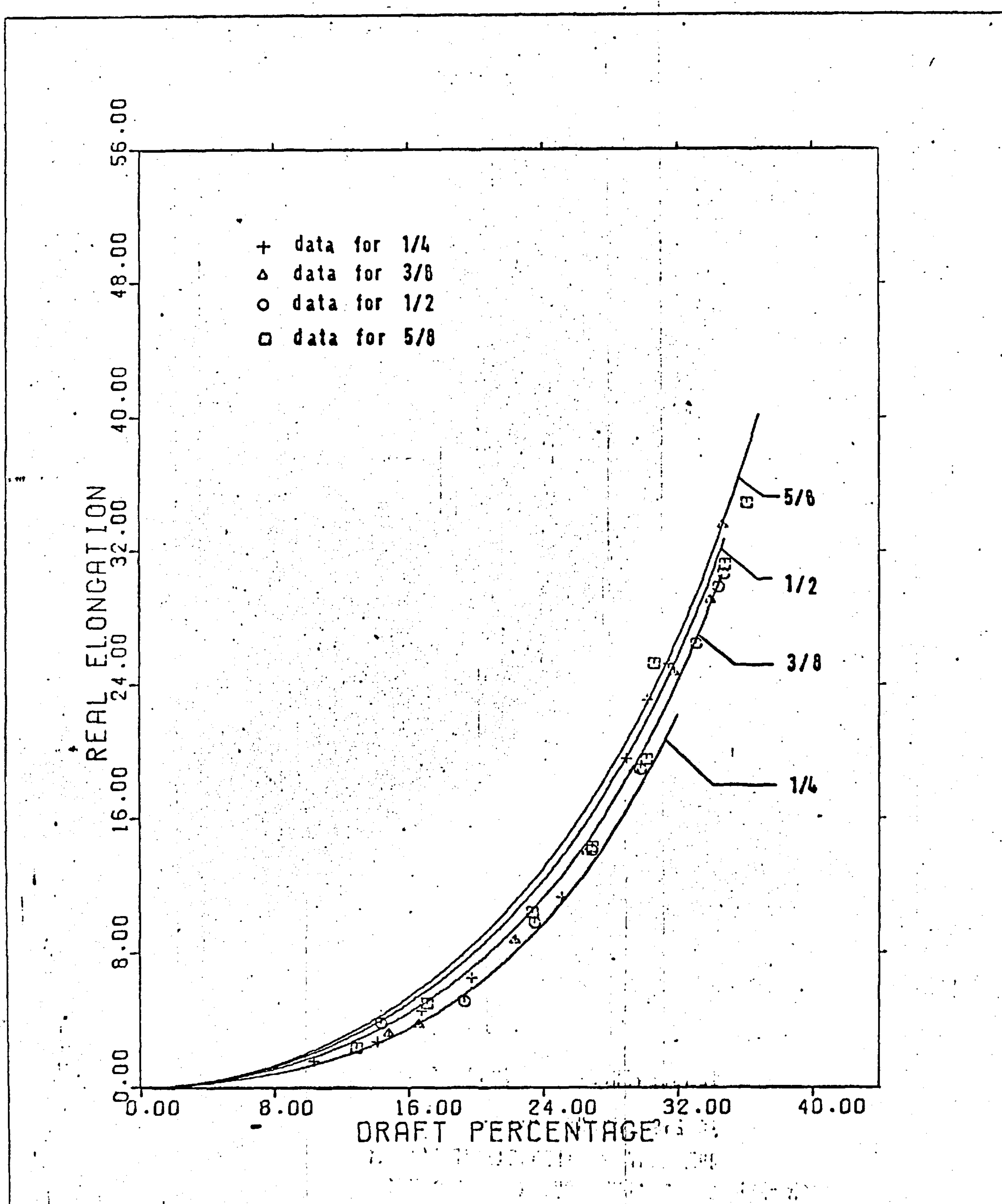


FIG(4-22) ELONGATION–DRAFT PERCENTAGE
SOLID LINES: THEORETICAL FOR
1/4 TO 5/8 SQUARE BARS.

TEMPERATURE: 1100 °C

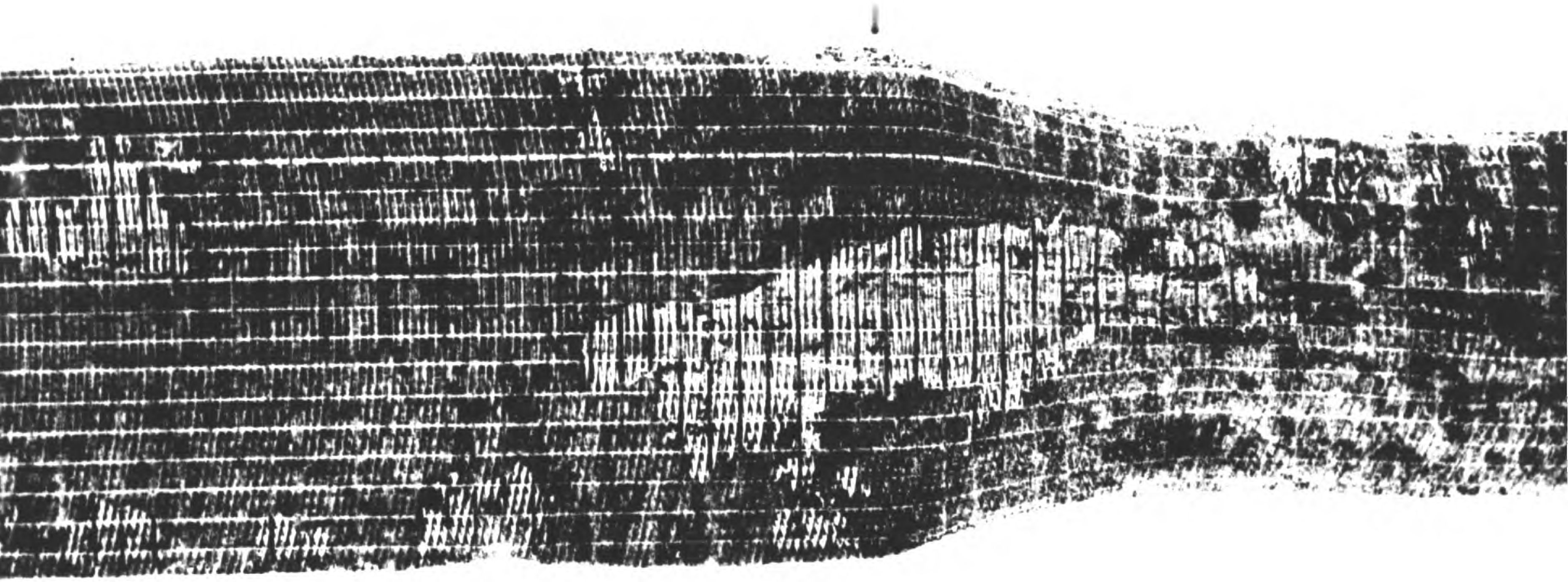

FIG(4-23) DISTORTED GRID COORDINATE ON DIAGONAL PLANE OF THE 1/2 LEAD SQUARE BAR

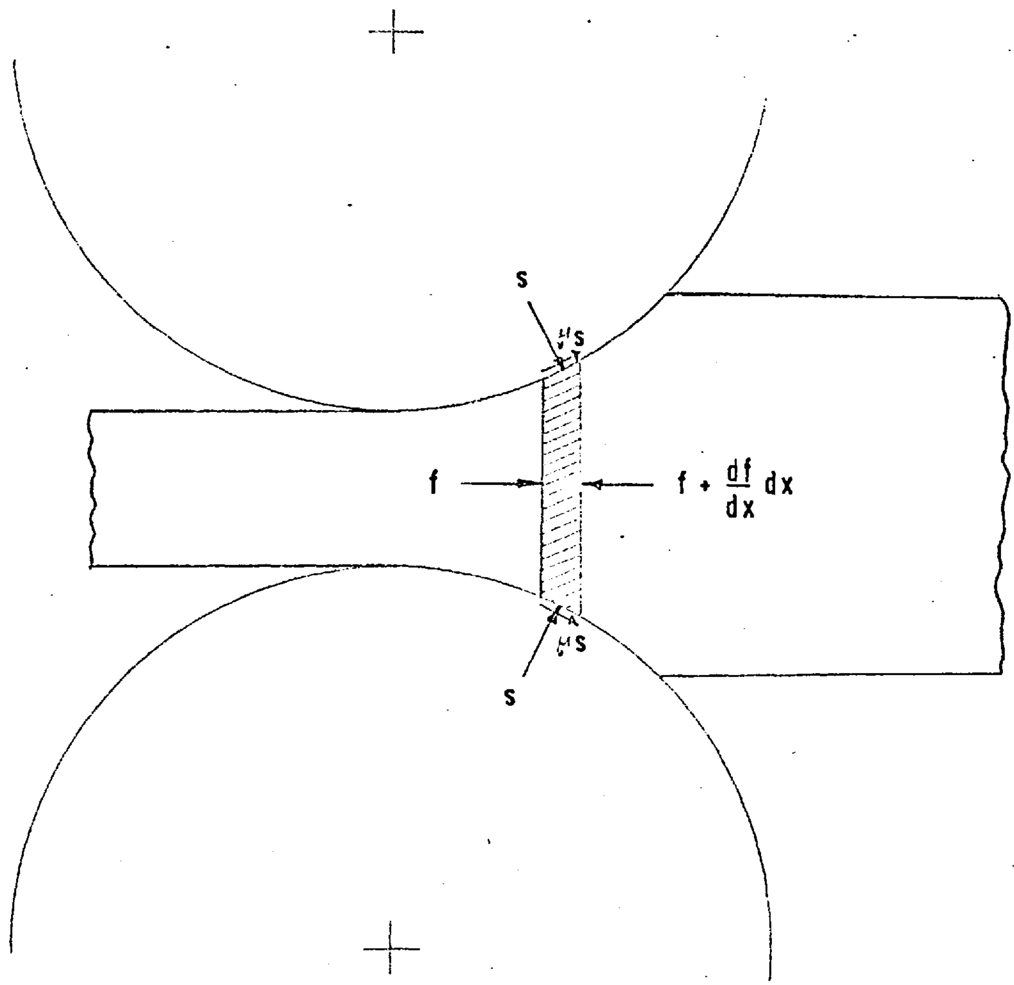


FIG (5-1) FORCES ACTING ON A SEGMENT OF MATERIAL IN FLAT ROLLING

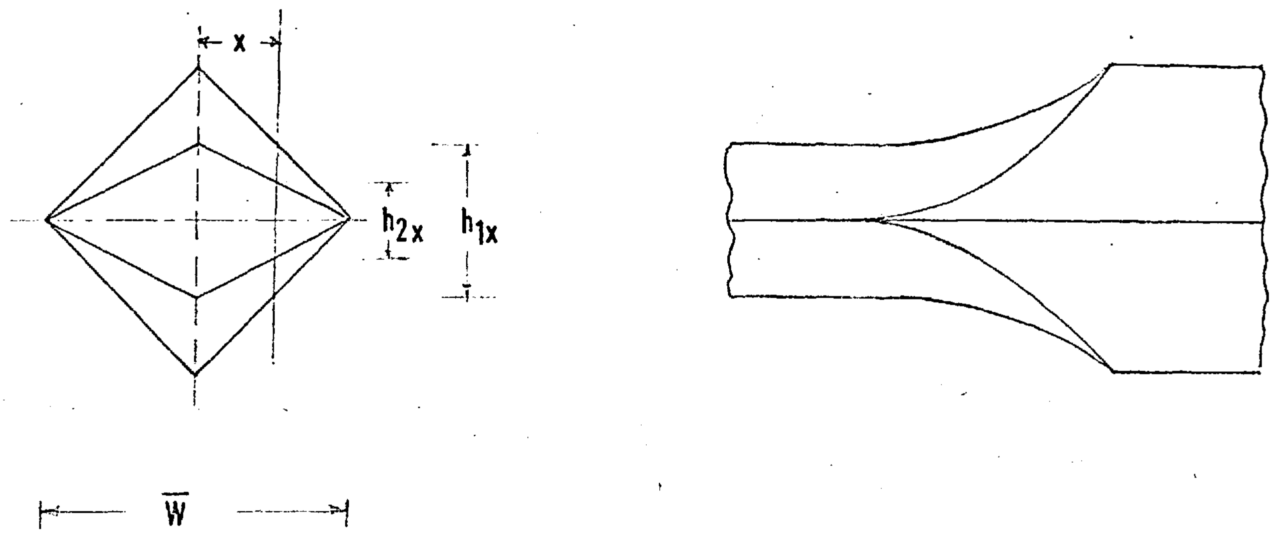


FIG(5-2) SECTION X AT THE DISTANCE
x FROM DIAGONAL

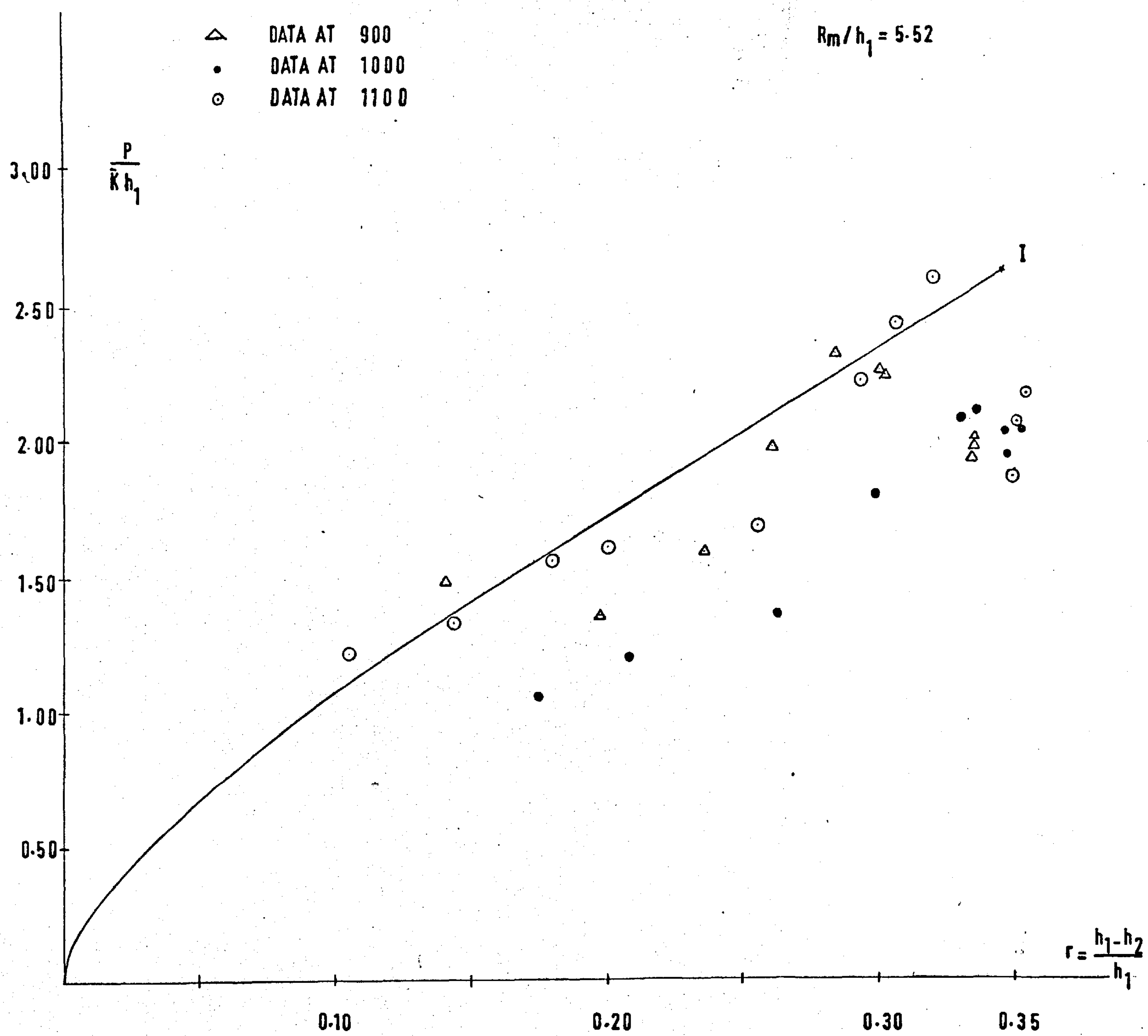


FIG(5-3) 1/4 SQUARE BAR
I CORRESPONDS TO OPTIMAL REDUCTION
FOR COMPLETE FILLING OF THE DIAMOND PASS

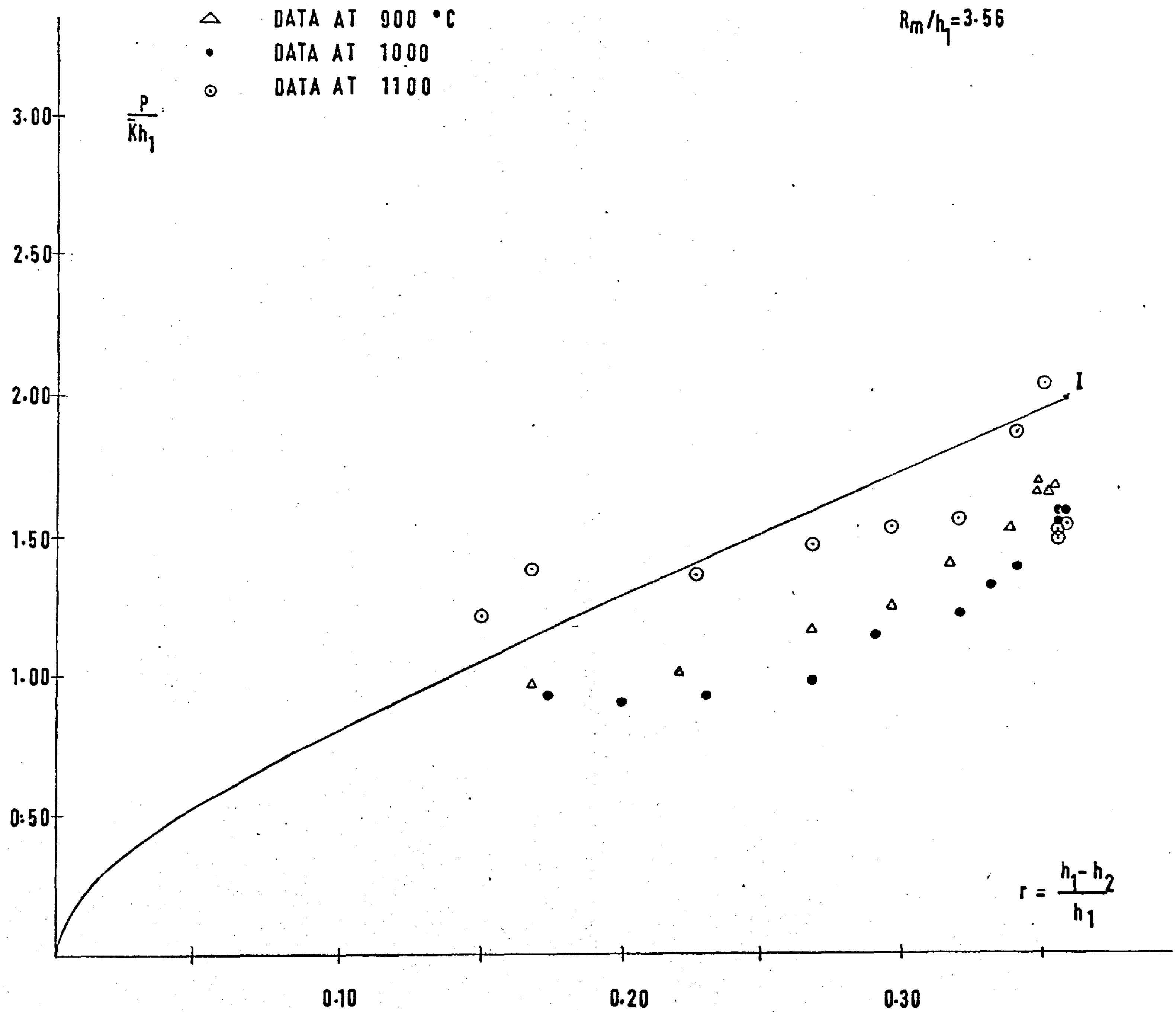


FIG(5-4) 3/8 SQUARE BAR

I CORRESPONDS TO OPTIMAL REDUCTION FOR COMPLETE FILLING OF THE DIAMOND PASS

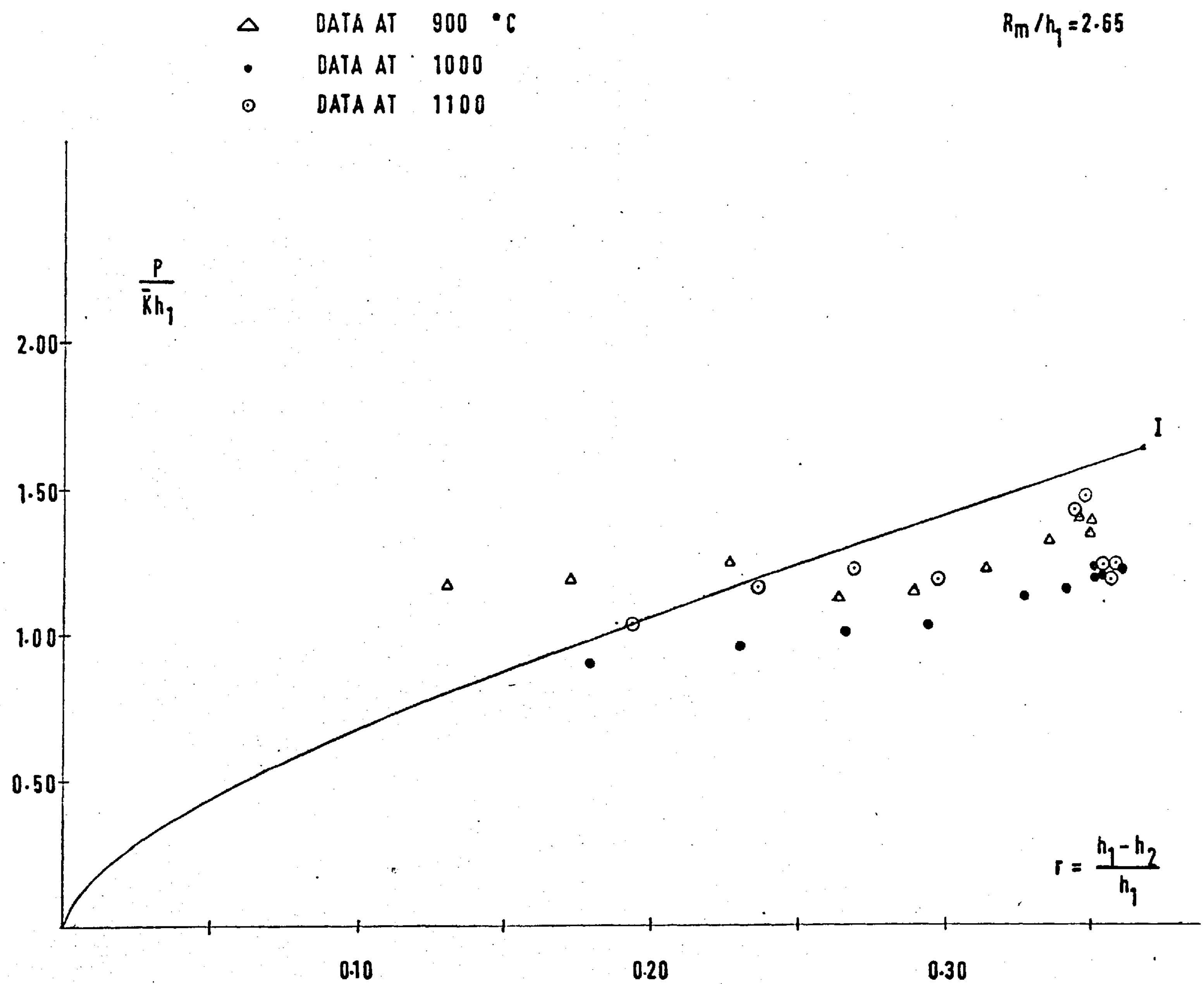


FIG(5-5) 1/2 SQUARE BAR
I CORRESPONDS TO OPTIMAL REDUCTION FOR
COMPLETE FILLING OF THE DIAMOND PASS

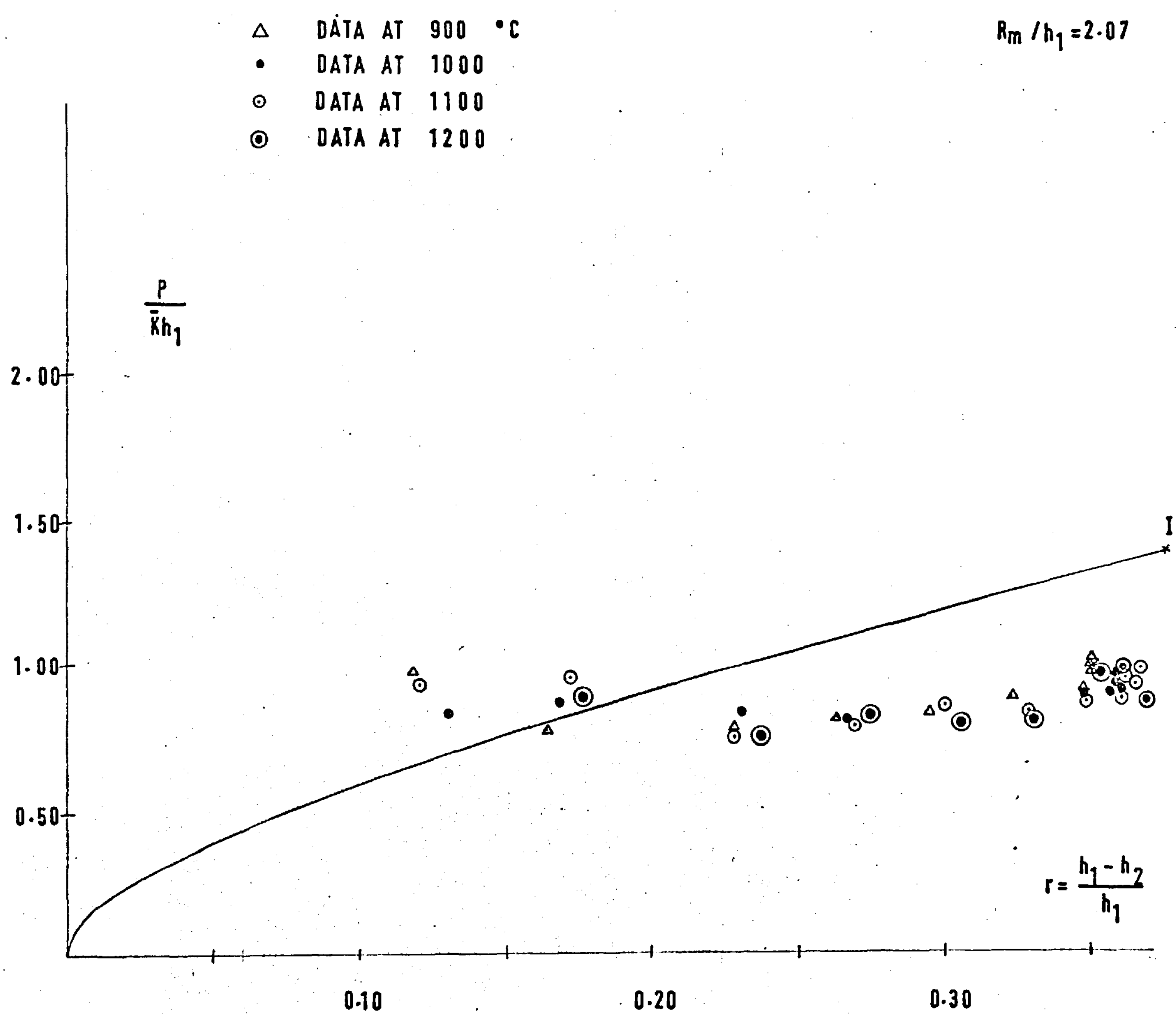


FIG (5-6) 5/8 SQUARE BAR
I CORRESPONDS TO OPTIMAL REDUCTION FOR
COMPLETE FILLING OF THE DIAMOND PASS

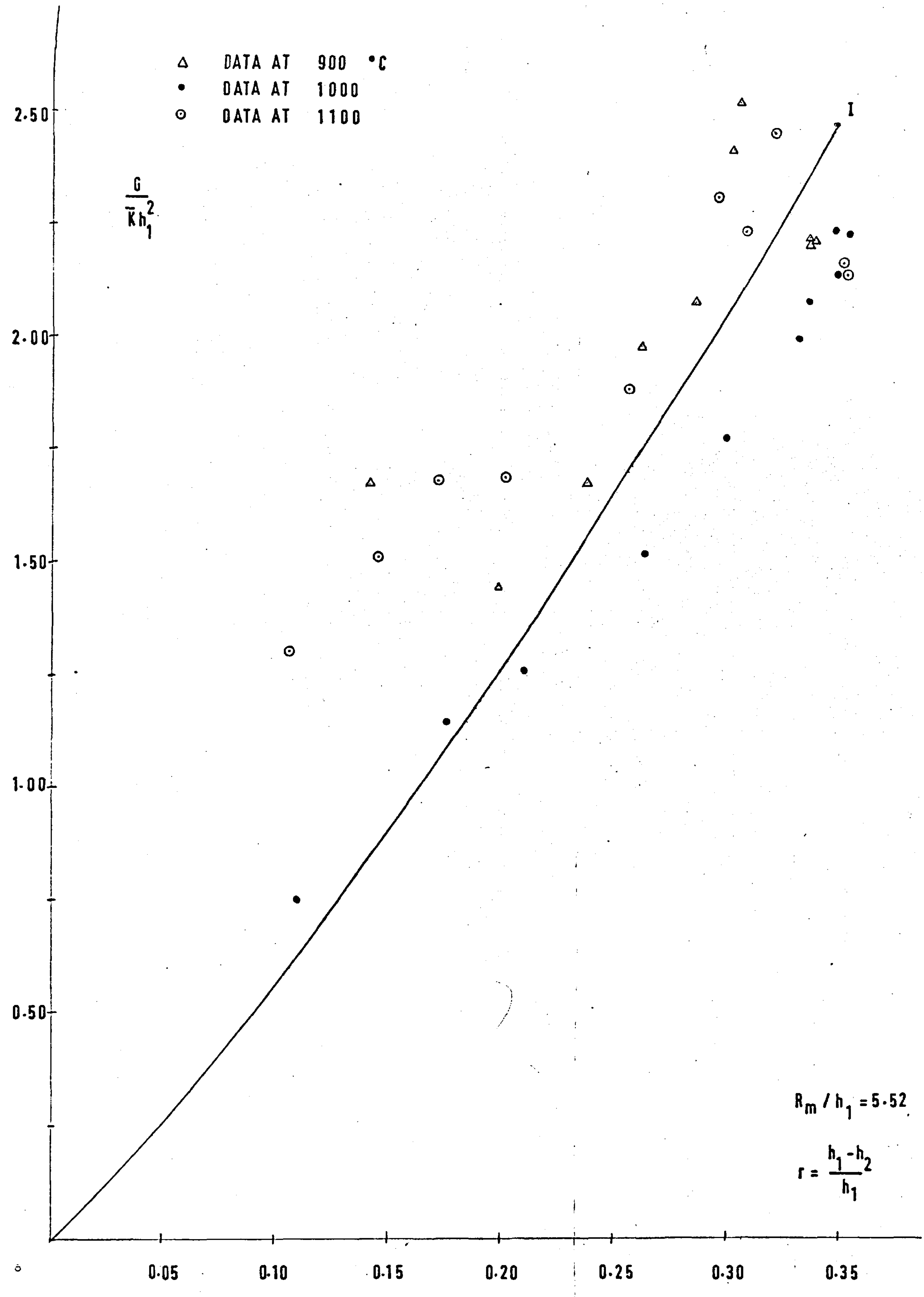


FIG(5-7) 1/4 SQUARE BAR

I CORRESPONDS TO OPTIMAL REDUCTION FOR COMPLETE FILLING OF THE DIAMOND PASS

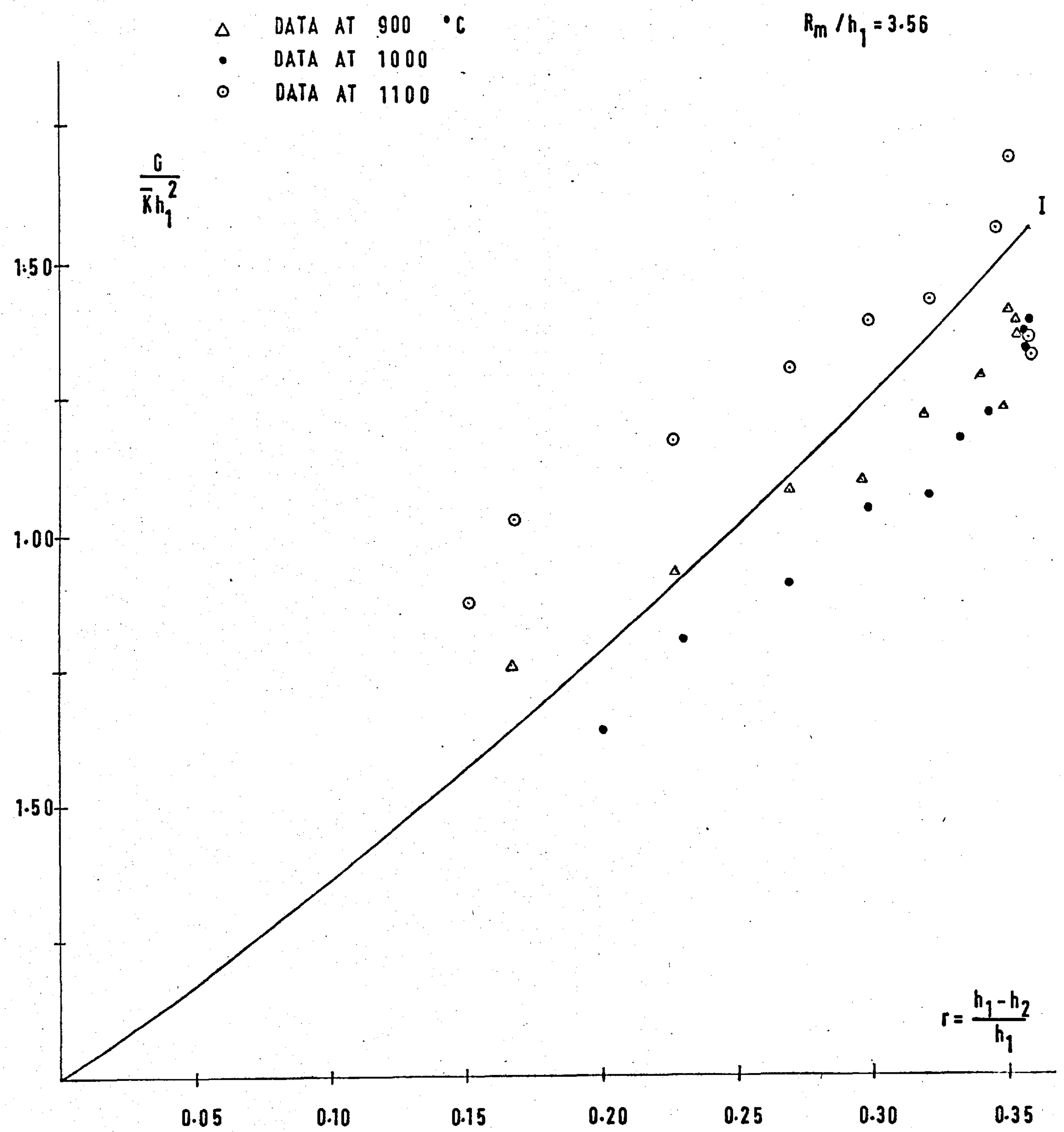


FIG(5-8) 3/8 SQUARE BAR
I CORRESPONDS TO OPTIMAL REDUCTION FOR
COMPLETE FILLING OF THE DIAMOND PASS

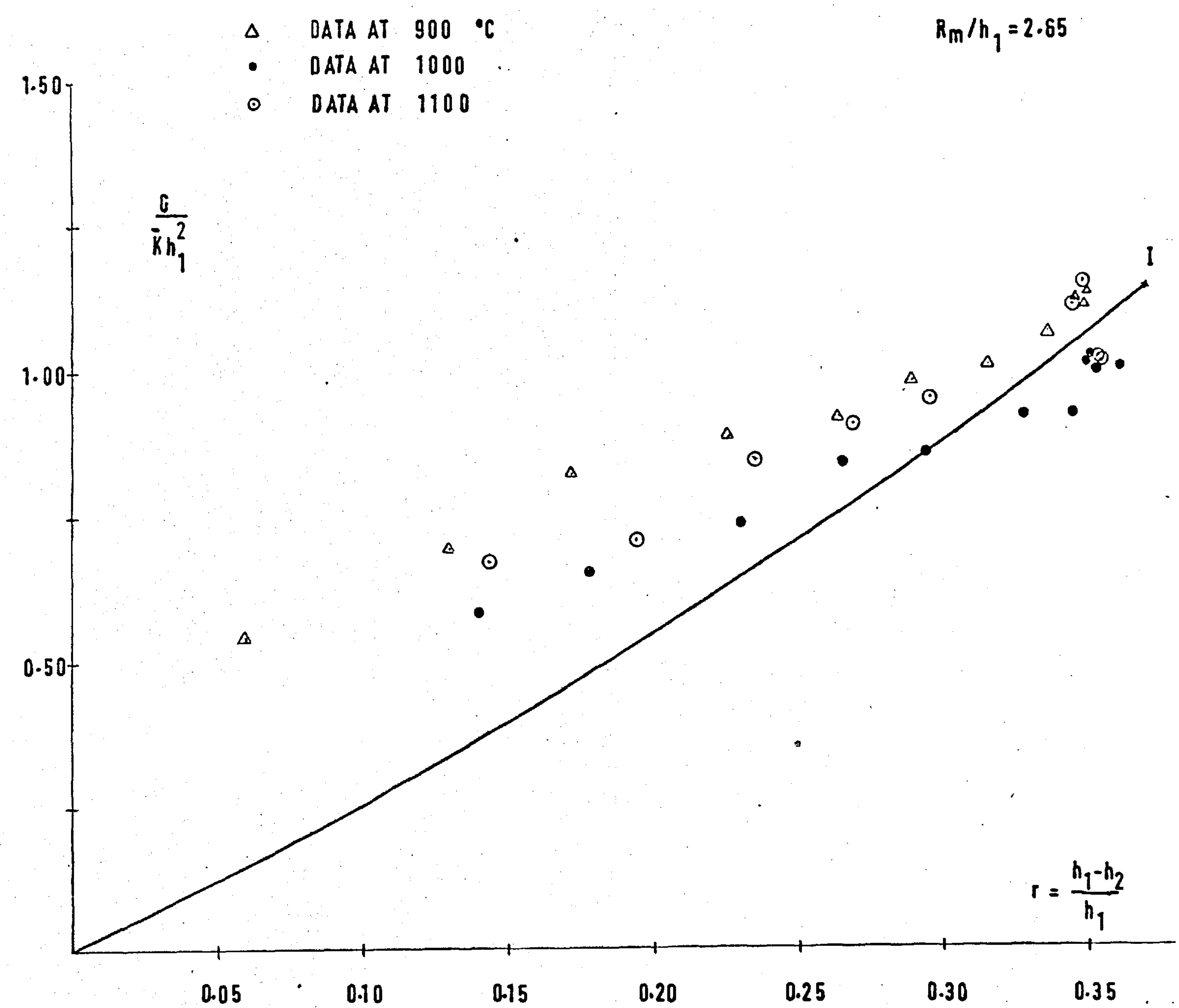


FIG(5-9) 1/2 SQUARE BAR

I CORRESPONDS TO OPTIMAL REDUCTION FOR COMPLETE EILLING OF THE DIAMOND PASS

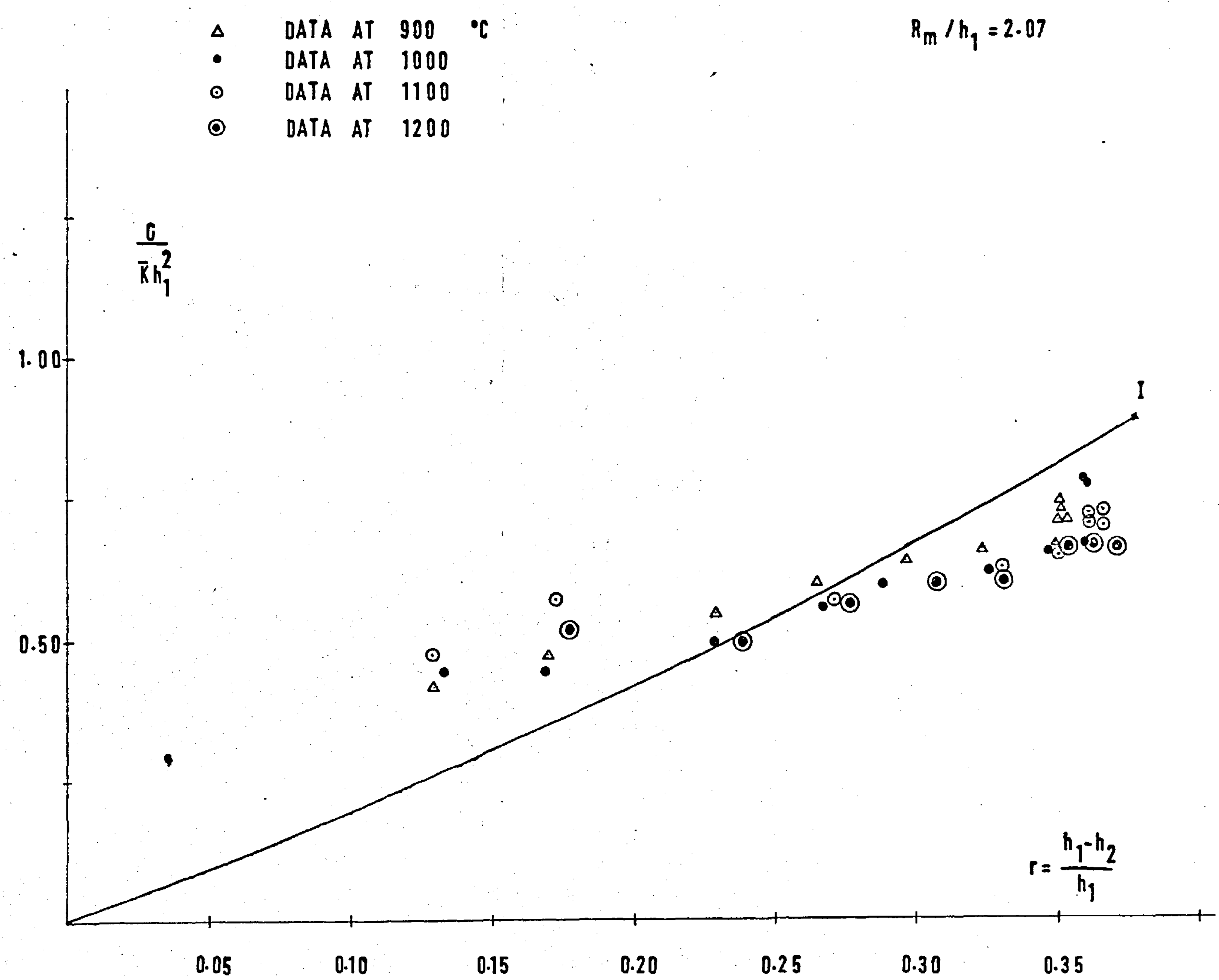


FIG(5-10) 5/8 SQUARE BAR
I CORRESPONDS TO OPTIMAL REDUCTION FOR
COMPLETE FILLING OF THE DIAMOND PASS

SPREAD AND DRAFT DATA FOR 1/4 SQARE BAR AT 900 °C

| NO. | VERTICAL DIAGONAL BEFORE ROLLING H1 IN | VERTICAL DIAGONAL AFTER ROLLING H2 IN | HORIZONTAL DIAGONAL BEFORE ROLLING D1 IN | HORIZONTAL DIAGONAL AFTER ROLLING D2 IN | DRAFT $\delta = H_1 - H_2$ INCHES | SPREAD S=D2-D1 INCHES $S_1$ | SPREAD BY NEW FORMULA $S_2$ | DIFFERENCE $S_1 - S_2$ INCHES | BAR ELONGATION |
|---|---|---|---|---|---|---|---|---|---|
| 1 | .3383 | .3095 | .3388 | .3423 | .0288 | .0035 | .0023 | .0012 | .8900 |
| 2 | .3447 | .2964 | .3413 | .3463 | .0483 | .0050 | .0074 | -.0024 | 2.4800 |
| 3 | .3382 | .2717 | .3389 | .3548 | .0665 | .0159 | .0146 | .0013 | 5.0600 |
| 4 | .3392 | .2592 | .3389 | .3609 | .0800 | .0220 | .0211 | .0009 | 9.2000 |
| 5 | .3442 | .2546 | .3400 | .3672 | .0896 | .0272 | .0261 | .0011 | 10.6400 |
| 6 | .3463 | .2478 | .3457 | .3750 | .0985 | .0293 | .0318 | -.0025 | 15.8100 |
| 7 | .3443 | .2410 | .3413 | .3768 | .1033 | .0355 | .0348 | .0007 | 17.9900 |
| 8 | .3381 | .2359 | .3390 | .3802 | .1022 | .0412 | .0346 | .0066 | 26.6400 |
| 9 | .3446 | .2296 | .3414 | .3903 | .1150 | .0489 | .0430 | .0059 | 0.0000 |
| 10 | .3423 | .2281 | .3408 | .3941 | .1142 | .0533 | .0427 | .0106 | 0.0000 |
| 11 | .3435 | .2288 | .3411 | .3922 | .1147 | .0511 | .0430 | .0081 | 0.0000 |

SPREAD AND DRAFT DATA FOR 3/8 SQARE BAR AT 900 °C

| NO. | VERTICAL DIAGONAL BEFORE ROLLING $H_1$ IN | VERTICAL DIAGONAL AFTER ROLLING $H_2$ IN | HORIZONTAL DIAGONAL BEFORE ROLLING $D_1$ IN | HORIZONTAL DIAGONAL AFTER ROLLING $D_2$ IN | DRAFT $\delta = H_1 - H_2$ INCHES | SPREAD $S = D_2 - D_1$ INCHES $S_1$ | SPREAD BY NEW FORMULA $S_2$ | DIFFERENCE $S_1 - S_2$ INCHES | BAR ELONGATION |
|---|---|---|---|---|---|---|---|---|---|
| 1 | .5162 | .4871 | .5182 | .5192 | .0291 | .0010 | .0006 | .0004 | .1200 |
| 2 | .5194 | .4337 | .5175 | .5280 | .0857 | .0105 | .0104 | .0001 | 3.5600 |
| 3 | .5196 | .4016 | .5189 | .5422 | .1180 | .0233 | .0213 | .0020 | 7.3600 |
| 4 | .5198 | .3812 | .5188 | .5508 | .1386 | .0320 | .0301 | .0019 | 11.8900 |
| 5 | .5203 | .3664 | .5186 | .5581 | .1539 | .0395 | .0376 | .0019 | 16.1900 |
| 6 | .5200 | .3544 | .5161 | .5620 | .1656 | .0459 | .0438 | .0021 | 21.1900 |
| 7 | .5200 | .3436 | .5189 | .5742 | .1764 | .0553 | .0504 | .0049 | 26.7000 |
| 8 | .5200 | .3394 | .5188 | .5819 | .1806 | .0631 | .0530 | .0101 | 28.3600 |
| 9 | .5188 | .3382 | .5190 | .5862 | .1806 | .0672 | .0532 | .0140 | 0.0000 |
| 10 | .5196 | .3374 | .5189 | .5864 | .1822 | .0675 | .0541 | .0134 | 0.0000 |
| 11 | .5200 | .3366 | .5180 | .5853 | .1834 | .0673 | .0547 | .0126 | 0.0000 |

SPREAD AND DRAFT DATA FOR 1/2 SQARE BAR AT 900 °C

| NO. | VERTICAL DIAGONAL BEFORE ROLLING $H_1$ IN | VERTICAL DIAGONAL AFTER ROLLING $H_2$ IN | HORIZONTAL DIAGONAL BEFORE ROLLING $D_1$ IN | HORIZONTAL DIAGONAL AFTER ROLLING $D_2$ IN | DRAFT $\delta = H_1 - H_2$ INCHES | SPREAD $S = D_2 - D_1$ INCHES $S_1$ | SPREAD BY NEW FORMULA $S_2$ | DIFFERENCE $S_1 - S_2$ INCHES | BAR ELONGATION |
|---|---|---|---|---|---|---|---|---|---|
| 1 | .6900 | .6459 | .6891 | .6903 | .0441 | .0012 | .0007 | .0005 | .0600 |
| 2 | .6900 | .6002 | .6894 | .6935 | .0898 | .0041 | .0054 | -.0013 | 2.5700 |
| 3 | .6902 | .5713 | .6894 | .6992 | .1189 | .0098 | .0110 | -.0012 | 3.6200 |
| 4 | .6893 | .5334 | .6900 | .7125 | .1559 | .0225 | .0211 | .0014 | 8.4800 |
| 5 | .6891 | .5073 | .6897 | .7200 | .1818 | .0303 | .0300 | .0003 | 12.7800 |
| 6 | .6890 | .4898 | .6900 | .7263 | .1992 | .0363 | .0369 | -.0006 | 17.2700 |
| 7 | .6902 | .4732 | .6892 | .7312 | .2170 | .0420 | .0446 | -.0026 | 21.7200 |
| 8 | .6893 | .4581 | .6901 | .7384 | .2312 | .0483 | .0516 | -.0033 | 26.5700 |
| 9 | .6894 | .4517 | .6896 | .7417 | .2377 | .0521 | .0549 | -.0028 | 0.0000 |
| 10 | .6894 | .4490 | .6896 | .7417 | .2404 | .0521 | .0563 | -.0042 | 0.0000 |
| 11 | .6894 | .4493 | .6896 | .7434 | .2401 | .0538 | .0561 | -.0023 | 0.0000 |

SPREAD AND DRAFT DATA FOR 5/8 SHAPE BAR AT 900 °C

| NO. | VERTICAL DIAGONAL BEFORE ROLLING $H_1$ IN | VERTICAL DIAGONAL AFTER ROLLING $H_2$ IN | HORIZONTAL DIAGONAL BEFORE ROLLING $D_1$ IN | HORIZONTAL DIAGONAL AFTER ROLLING $D_2$ IN | DRAFT $\delta = H_1 - H_2$ INCHES | SPREAD $S = D_2 - D_1$ INCHES $S_1$ | SPREAD BY NEW FORMULA $S_2$ | DIFFERENCE $S_1 - S_2$ INCHES | BAR ELONGATION |
|---|---|---|---|---|---|---|---|---|---|
| 1 | .8684 | .7655 | .8721 | .8750 | .1029 | .0029 | .0036 | -.0007 | 1.7600 |
| 2 | .8717 | .7243 | .8711 | .8812 | .1474 | .0101 | .0097 | .0004 | 4.6800 |
| 3 | .8704 | .6715 | .8687 | .8927 | .1989 | .0240 | .0208 | .0032 | 8.2500 |
| 4 | .8685 | .6394 | .8719 | .9058 | .2291 | .0339 | .0295 | .0044 | 12.8200 |
| 5 | .8686 | .6118 | .8717 | .9124 | .2568 | .0407 | .0387 | .0020 | 18.1300 |
| 6 | .8685 | .5895 | .8724 | .9190 | .2790 | .0466 | .0471 | -.0005 | 24.0000 |
| 7 | .8718 | .5687 | .8688 | .9225 | .3031 | .0537 | .0567 | -.0030 | 28.8400 |
| 8 | .8690 | .5625 | .8725 | .9281 | .3065 | .0556 | .0587 | -.0031 | 31.4300 |
| 9 | .8690 | .5644 | .8717 | .9240 | .3046 | .0523 | .0578 | -.0055 | 0.0000 |
| 10 | .8688 | .5649 | .8720 | .9247 | .3039 | .0527 | .0575 | -.0048 | 0.0000 |
| 11 | .8685 | .5648 | .8720 | .9295 | .3037 | .0575 | .0574 | .0001 | 0.0000 |

SPREAD AND DRAFT DATA FOR 1/4 SQARE BAR AT 1000 °C

| NO. | VERTICAL DIAGONAL BEFORE ROLLING H1 IN | VERTICAL DIAGONAL AFTER ROLLING H2 IN | HORIZONTAL DIAGONAL BEFORE ROLLING D1 IN | HORIZONTAL DIAGONAL AFTER ROLLING D2 IN | DRAFT $\delta$=H1-H2 INCHES | SPREAD $S_1$=D2-D1 INCHES $S_1$ | SPREAD BY NEW FORMULA $S_2$ | DIFFERENCE $S_1-S_2$ INCHES | BAR ELONGATION |
|---|---|---|---|---|---|---|---|---|---|
| 1 | .3440 | .3062 | .3440 | .3450 | .0378 | .0010 | .0043 | -.0033 | 1.0400 |
| 2 | .3430 | .2952 | .3434 | .3462 | .0478 | .0028 | .0073 | -.0045 | 2.5100 |
| 3 | .3451 | .2850 | .3450 | .3536 | .0601 | .0086 | .0118 | -.0032 | 4.1500 |
| 4 | .3434 | .2718 | .3423 | .3564 | .0716 | .0141 | .0168 | -.0027 | 5.9300 |
| 5 | .3440 | .2538 | .3436 | .3667 | .0902 | .0231 | .0267 | -.0036 | 10.7900 |
| 6 | .3439 | .2410 | .3444 | .3752 | .1029 | .0308 | .0349 | -.0041 | 17.1300 |
| 7 | .3441 | .2304 | .3447 | .3877 | .1137 | .0430 | .0426 | .0004 | 23.8600 |
| 8 | .3446 | .2290 | .3452 | .3900 | .1156 | .0448 | .0440 | .0008 | 24.9500 |
| 9 | .3446 | .2252 | .3417 | .3944 | .1194 | .0527 | .0465 | .0062 | 0.0000 |
| 10 | .3440 | .2247 | .3422 | .3930 | .1193 | .0508 | .0466 | .0042 | 0.0000 |
| 11 | .3465 | .2247 | .3442 | .3981 | .1218 | .0539 | .0484 | .0055 | 0.0000 |

SPREAD AND DRAFT DATA FOR 3/8 SQARE BAR AT 1000 °C

| NO. | VERTICAL DIAGONAL BEFORE ROLLING H1 IN | VERTICAL DIAGONAL AFTER ROLLING H2 IN | HORIZONTAL DIAGONAL BEFORE ROLLING D1 IN | HORIZONTAL DIAGONAL AFTER ROLLING D2 IN | DRAFT $\delta = H_1 - H_2$ INCHES | SPREAD $S = D2 - D1$ INCHES $S_1$ | SPREAD BY NEW FORMULA $S_2$ | DIFFERENCE $S_1 - S_2$ INCHES | BAR ELONGATION |
|---|---|---|---|---|---|---|---|---|---|
| 1 | .5191 | .4306 | .5200 | .5261 | .0885 | .0061 | .0113 | -.0052 | 3.7900 |
| 2 | .5187 | .4137 | .5197 | .5353 | .1050 | .0156 | .0165 | -.0009 | 4.4200 |
| 3 | .5190 | .3995 | .5195 | .5428 | .1195 | .0233 | .0219 | .0014 | 8.1200 |
| 4 | .5185 | .3796 | .5198 | .5502 | .1389 | .0304 | .0304 | -.0000 | 12.9300 |
| 5 | .5177 | .3635 | .5200 | .5572 | .1542 | .0372 | .0381 | -.0009 | 18.1900 |
| 6 | .5190 | .3524 | .5200 | .5644 | .1666 | .0444 | .0448 | -.0004 | 21.8500 |
| 7 | .5189 | .3459 | .5185 | .5685 | .1730 | .0500 | .0485 | .0015 | 25.1000 |
| 8 | .5184 | .3414 | .5191 | .5748 | .1770 | .0557 | .0510 | .0047 | 27.4000 |
| 9 | .5200 | .3350 | .5192 | .5811 | .1850 | .0619 | .0559 | .0060 | 0.0000 |
| 10 | .5200 | .3346 | .5198 | .5837 | .1854 | .0639 | .0562 | .0077 | 0.0000 |
| 11 | .5191 | .3350 | .5188 | .5886 | .1841 | .0698 | .0554 | .0144 | 0.0000 |

SPREAD AND DRAFT DATA FOR 1/2 SQARE BAR AT 1000 °C

| NO. | VERTICAL DIAGONAL BEFORE ROLLING H1 IN | VERTICAL DIAGONAL AFTER ROLLING H2 IN | HORIZONTAL DIAGONAL BEFORE ROLLING D1 IN | HORIZONTAL DIAGONAL AFTER ROLLING D2 IN | DRAFT $\delta$=H1-H2 INCHES | SPREAD S=D2-D1 INCHES $S_1$ | SPREAD BY NEW FORMULA $S_2$ | DIFFERENCE $S_1-S_2$ INCHES | BAR ELONGATION |
|---|---|---|---|---|---|---|---|---|---|
| 1 | .6892 | .5925 | .6877 | .6930 | .0967 | .0053 | .0066 | -.0013 | 3.6100 |
| 2 | .6899 | .5672 | .6890 | .7009 | .1227 | .0119 | .0119 | -.0000 | 5.7800 |
| 3 | .6892 | .5305 | .6890 | .7135 | .1587 | .0245 | .0219 | .0026 | 9.8300 |
| 4 | .6891 | .5062 | .6889 | .7212 | .1829 | .0323 | .0304 | .0019 | 14.3900 |
| 5 | .6892 | .4867 | .6890 | .7260 | .2025 | .0370 | .0383 | -.0013 | 18.8000 |
| 6 | .6893 | .4635 | .6886 | .7345 | .2258 | .0459 | .0488 | -.0029 | 26.0700 |
| 7 | .6898 | .4525 | .6888 | .7417 | .2373 | .0529 | .0546 | -.0017 | 30.2600 |
| 8 | .6892 | .4470 | .6889 | .7466 | .2422 | .0577 | .0572 | .0005 | 31.8400 |
| 9 | .6894 | .4488 | .6896 | .7444 | .2406 | .0548 | .0564 | -.0016 | 0.0000 |
| 10 | .6894 | .4457 | .6896 | .7455 | .2437 | .0559 | .0580 | -.0021 | 0.0000 |
| 11 | .6894 | .4415 | .6896 | .7493 | .2479 | .0597 | .0603 | -.0006 | 0.0000 |

SPREAD AND DRAFT DATA FOR 5/8 SQARE BAR AT 1000 °C

| NO. | VERTICAL DIAGONAL BEFORE ROLLING H1 IN | VERTICAL DIAGONAL AFTER ROLLING H2 IN | HORIZONTAL DIAGONAL BEFORE ROLLING D1 IN | HORIZONTAL DIAGONAL AFTER ROLLING D2 IN | DRAFT $\delta = H_1 - H_2$ INCHES | SPREAD $S = D_2 - D_1$ INCHES $S_1$ | SPREAD BY NEW FORMULA $S_2$ | DIFFERENCE $S_1 - S_2$ INCHES | BAR ELONGATION |
|---|---|---|---|---|---|---|---|---|---|
| 1 | .8683 | .7537 | .8710 | .8758 | .1146 | .0048 | .0049 | -.0001 | 2.4600 |
| 2 | .8688 | .7222 | .8705 | .8812 | .1466 | .0107 | .0096 | .0011 | 4.4900 |
| 3 | .8686 | .6702 | .8702 | .8966 | .1984 | .0264 | .0207 | .0057 | 8.9000 |
| 4 | .8686 | .6375 | .8704 | .9053 | .2311 | .0349 | .0300 | .0049 | 13.9400 |
| 5 | .8686 | .6192 | .8709 | .9126 | .2494 | .0417 | .0360 | .0057 | 19.1400 |
| 6 | .8682 | .5869 | .8703 | .9198 | .2813 | .0495 | .0479 | .0016 | 24.2000 |
| 7 | .8689 | .5682 | .8711 | .9260 | .3007 | .0549 | .0560 | -.0011 | 30.0400 |
| 8 | .8687 | .5572 | .8710 | .9331 | .3115 | .0621 | .0608 | .0013 | 33.6200 |
| 9 | .8684 | .5575 | .8720 | .9307 | .3109 | .0587 | .0607 | -.0020 | 0.0000 |
| 10 | .8684 | .5576 | .8716 | .9307 | .3108 | .0591 | .0606 | -.0015 | 0.0000 |
| 11 | .8682 | .5562 | .8712 | .9343 | .3120 | .0631 | .0611 | .0020 | 0.0000 |

SPREAD AND DRAFT DATA FOR 1/4 SQARE BAR AT 1100 °C

| NO. | VERTICAL DIAGONAL BEFORE ROLLING $H_1$ IN | VERTICAL DIAGONAL AFTER ROLLING $H_2$ IN | HORIZONTAL DIAGONAL BEFORE ROLLING $D_1$ IN | HORIZONTAL DIAGONAL AFTER ROLLING $D_2$ IN | DRAFT $\delta=H_1-H_2$ INCHES | SPREAD $S=D_2-D_1$ INCHES $S_1$ | SPREAD BY NEW FORMULA $S_2$ | DIFFERENCE $S_1-S_2$ INCHES | BAR ELONGATION |
|---|---|---|---|---|---|---|---|---|---|
| 1 | .3387 | .3030 | .3386 | .3397 | .0357 | .0011 | .0038 | -.0027 | 1.5800 |
| 2 | .3388 | .2901 | .3384 | .3413 | .0487 | .0029 | .0076 | -.0047 | 2.7700 |
| 3 | .3385 | .2807 | .3383 | .3472 | .0578 | .0089 | .0109 | -.0020 | 4.6100 |
| 4 | .3386 | .2706 | .3382 | .3541 | .0680 | .0159 | .0152 | .0007 | 6.5400 |
| 5 | .3387 | .2524 | .3388 | .3653 | .0863 | .0265 | .0246 | .0019 | 11.3100 |
| 6 | .3390 | .2394 | .3385 | .3705 | .0996 | .0320 | .0327 | -.0007 | 19.5700 |
| 7 | .3382 | .2344 | .3382 | .3796 | .1038 | .0414 | .0356 | .0058 | 23.0700 |
| 8 | .3382 | .2300 | .3386 | .3854 | .1082 | .0468 | .0387 | .0081 | 25.2200 |
| 9 | .3463 | .2256 | .3450 | .3943 | .1207 | .0493 | .0476 | .0017 | 0.0000 |
| 10 | .3464 | .2237 | .3450 | .3975 | .1227 | .0525 | .0492 | .0033 | 0.0000 |
| 11 | .3464 | .2247 | .3450 | .3960 | .1217 | .0510 | .0484 | .0026 | 0.0000 |

SPREAD AND DRAFT DATA FOR 3/8 SQARE BAR AT 1100 °C

| NO. | VERTICAL DIAGONAL BEFORE ROLLING $H_1$ IN | VERTICAL DIAGONAL AFTER ROLLING $H_2$ IN | HORIZONTAL DIAGONAL BEFORE ROLLING $D_1$ IN | HORIZONTAL DIAGONAL AFTER ROLLING $D_2$ IN | DRAFT $\delta=H_1-H_2$ INCHES | SPREAD $S=D_2-D_1$ INCHES $S_1$ | SPREAD BY NEW FORMULA $S_2$ | DIFFERENCE $S_1-S_2$ INCHES | BAR ELONGATION |
|---|---|---|---|---|---|---|---|---|---|
| 1 | .5162 | .4391 | .5183 | .5213 | .0771 | .0030 | .0082 | -.0052 | 3.2500 |
| 2 | .5165 | .4301 | .5177 | .5239 | .0864 | .0062 | .0107 | -.0045 | 3.7500 |
| 3 | .5157 | .3994 | .5180 | .5387 | .1163 | .0207 | .0208 | -.0001 | 8.7500 |
| 4 | .5160 | .3773 | .5173 | .5473 | .1387 | .0300 | .0304 | -.0004 | 14.0000 |
| 5 | .5161 | .3630 | .5171 | .5532 | .1531 | .0361 | .0375 | -.0014 | 18.8500 |
| 6 | .5165 | .3512 | .5173 | .5608 | .1653 | .0435 | .0441 | -.0006 | 24.7000 |
| 7 | .5169 | .3393 | .5183 | .5704 | .1776 | .0521 | .0515 | .0006 | 29.0500 |
| 8 | .5162 | .3358 | .5181 | .5764 | .1804 | .0583 | .0533 | .0050 | 33.5000 |
| 9 | .5172 | .3337 | .5186 | .5817 | .1835 | .0631 | .0552 | .0079 | 0.0000 |
| 10 | .5192 | .3343 | .5191 | .5767 | .1849 | .0576 | .0559 | .0017 | 0.0000 |
| 11 | .5194 | .3341 | .5191 | .5817 | .1853 | .0626 | .0561 | .0065 | 0.0000 |

SPREAD AND DRAFT DATA FOR 1/2 SQUARE BAR AT 1100 °C

| NO. | VERTICAL DIAGONAL BEFORE ROLLING $H_1$ IN | VERTICAL DIAGONAL AFTER ROLLING $H_2$ IN | HORIZONTAL DIAGONAL BEFORE ROLLING $D_1$ IN | HORIZONTAL DIAGONAL AFTER ROLLING $D_2$ IN | DRAFT $\delta = H_1 - H_2$ INCHES | SPREAD $S = D_2 - D_1$ INCHES $S_1$ | SPREAD BY NEW FORMULA $S_2$ | DIFFERENCE $S_1 - S_2$ INCHES | BAR ELONGATION |
|---|---|---|---|---|---|---|---|---|---|
| 1 | .6892 | .5903 | .6885 | .6929 | .0989 | .0044 | .0070 | -.0026 | 3.8700 |
| 2 | .6900 | .5568 | .6890 | .7011 | .1332 | .0121 | .0145 | -.0024 | 5.1400 |
| 3 | .6891 | .5271 | .6890 | .7144 | .1620 | .0254 | .0230 | .0024 | 9.8000 |
| 4 | .6900 | .5048 | .6889 | .7222 | .1852 | .0333 | .0312 | .0021 | 14.1300 |
| 5 | .6900 | .4846 | .6890 | .7281 | .2054 | .0391 | .0395 | -.0004 | 18.9000 |
| 6 | .6900 | .4615 | .6890 | .7375 | .2285 | .0485 | .0501 | -.0016 | 26.4300 |
| 7 | .6890 | .4515 | .6892 | .7473 | .2375 | .0581 | .0548 | .0033 | 29.8700 |
| 8 | .6890 | .4494 | .6890 | .7440 | .2396 | .0550 | .0559 | -.0009 | 30.6300 |
| 9 | .6901 | .4473 | .6890 | .7477 | .2428 | .0587 | .0574 | .0013 | 0.0000 |
| 10 | .6902 | .4431 | .6890 | .7498 | .2471 | .0608 | .0597 | .0011 | 0.0000 |
| 11 | .6901 | .4456 | .6893 | .7500 | .2445 | .0607 | .0584 | .0023 | 0.0000 |

SPREAD AND DRAFT DATA FOR 5/8 SQARE BAR AT 1100 °C

| NO. | VERTICAL DIAGONAL BEFORE ROLLING H1 IN | VERTICAL DIAGONAL AFTER ROLLING H2 IN | HORIZONTAL DIAGONAL BEFORE ROLLING D1 IN | HORIZONTAL DIAGONAL AFTER ROLLING D2 IN | DRAFT $\delta$ =H1-H2 INCHES | SPREAD S=D2-D1 INCHES $S_1$ | SPREAD BY NEW FORMULA $S_2$ | DIFFERENCE $S_1-S_2$ INCHES | BAR ELONGATION |
|---|---|---|---|---|---|---|---|---|---|
| 1 | .8720 | .7597 | .8720 | .8870 | .1123 | .0150 | .0047 | .0103 | 2.4100 |
| 2 | .8681 | .7195 | .8720 | .8811 | .1486 | .0091 | .0100 | -.0009 | 5.0400 |
| 3 | .8682 | .6652 | .8720 | .8944 | .2030 | .0224 | .0220 | .0004 | 10.4000 |
| 4 | .8682 | .6342 | .8720 | .9051 | .2340 | .0331 | .0310 | .0021 | 14.3200 |
| 5 | .8685 | .6067 | .8718 | .9125 | .2618 | .0407 | .0405 | .0002 | 19.5300 |
| 6 | .8684 | .5826 | .8720 | .9161 | .2858 | .0441 | .0498 | -.0057 | 25.2500 |
| 7 | .8680 | .5653 | .8719 | .9241 | .3027 | .0522 | .0570 | -.0048 | 31.2100 |
| 8 | .8682 | .5542 | .8717 | .9320 | .3140 | .0603 | .0621 | -.0018 | 34.8600 |
| 9 | .8706 | .5553 | .8686 | .9275 | .3153 | .0589 | .0623 | -.0034 | 0.0000 |
| 10 | .8720 | .5545 | .8689 | .9289 | .3175 | .0600 | .0632 | -.0032 | 0.0000 |
| 11 | .8720 | .5524 | .8689 | .9245 | .3196 | .0556 | .0641 | -.0085 | 0.0000 |

SPREAD AND DRAFT DATA FOR 5/8 SQARE BAR AT 1200 °C

| NO. | VERTICAL DIAGONAL BEFORE ROLLING $H_1$ IN | VERTICAL DIAGONAL AFTER ROLLING $H_2$ IN | HORIZONTAL DIAGONAL BEFORE ROLLING $D_1$ IN | HORIZONTAL DIAGONAL AFTER ROLLING $D_2$ IN | DRAFT $\delta = H_1 - H_2$ INCHES | SPREAD $S = D_2 - D_1$ INCHES $S_1$ | SPREAD BY NEW FORMULA $S_2$ | DIFFERENCE $S_1 - S_2$ INCHES |
|---|---|---|---|---|---|---|---|---|
| 1 | .8720 | .7189 | .8703 | .8792 | .1531 | .0089 | .0107 | -.0018 |
| 2 | .8723 | .6650 | .8686 | .8937 | .2073 | .0251 | .0231 | .0020 |
| 3 | .8720 | .6326 | .8683 | .9047 | .2394 | .0364 | .0326 | .0038 |
| 4 | .8719 | .6055 | .8686 | .9127 | .2664 | .0441 | .0420 | .0021 |
| 5 | .8720 | .5841 | .8680 | .9139 | .2879 | .0459 | .0505 | -.0046 |
| 6 | .8718 | .5645 | .8680 | .9213 | .3073 | .0533 | .0588 | -.0055 |
| 7 | .8718 | .5576 | .8684 | .9221 | .3142 | .0537 | .0619 | -.0082 |
| 8 | .8721 | .5510 | .8685 | .9232 | .3211 | .0547 | .0651 | -.0104 |

LOAD AND TORQUE DATA FOR 1/4 SQUARE BAR AT 900°C

| NO. | TOTAL MEASURED LOAD P IN KG | TOTAL MEASURED TORQUE G LB-IN | SHEAR YIELD STRES FROM COOK -MCRUM $\bar{K}$ TON/IN | LOAD PER UNIT WIDTH DEFORMING ZONE $P/\bar{W}$ | TORQ PER UNIT WIDTH DEFORMING ZONE $G/\bar{W}$ | EXPERIMENTAL $\frac{P}{\bar{W}\bar{K}H_1}$ | EXPERIMENTAL $\frac{G}{\bar{W}\bar{K}H_1^2}$ | THEORETICAL $\frac{P}{\bar{W}\bar{K}H_1}$ | THEORETICAL $\frac{G}{\bar{W}\bar{K}H_1^2}$ | $\frac{H_1-H_2}{H_1}$ | STRAIN RATE |
|---|---|---|---|---|---|---|---|---|---|---|---|
| 1 | 218.000 | 295.000 | 4.178 | 3093.270 | 4185.847 | 2.154 | 3.784 | .952 | .468 | .085 | 4.410 |
| 2 | 302.000 | 262.000 | 5.037 | 2567.731 | 2227.635 | 1.483 | 1.670 | 1.330 | .838 | .140 | 5.680 |
| 3 | 437.000 | 364.000 | 5.654 | 2602.084 | 2167.411 | 1.339 | 1.448 | 1.673 | 1.224 | .197 | 6.883 |
| 4 | 652.000 | 528.000 | 5.858 | 3196.852 | 2588.861 | 1.587 | 1.669 | 1.912 | 1.524 | .236 | 7.594 |
| 5 | 941.000 | 719.000 | 6.052 | 4088.968 | 3124.302 | 1.965 | 1.950 | 2.068 | 1.737 | .260 | 7.963 |
| 6 | 1223.000 | 848.000 | 6.120 | 4841.853 | 3357.229 | 2.301 | 2.072 | 2.217 | 1.944 | .284 | 8.341 |
| 7 | 1304.000 | 1080.000 | 6.310 | 4864.226 | 4028.654 | 2.242 | 2.411 | 2.307 | 2.065 | .300 | 8.620 |
| 8 | 1310.000 | 1141.000 | 6.331 | 4864.879 | 4237.273 | 2.235 | 2.528 | 2.308 | 2.054 | .302 | 8.735 |
| 9 | 1310.000 | 1150.000 | 6.485 | 4299.371 | 3774.257 | 1.928 | 2.198 | 2.511 | 2.357 | .334 | 9.150 |
| 10 | 1320.000 | 1165.000 | 6.503 | 4317.447 | 3810.474 | 1.931 | 2.213 | 2.505 | 2.343 | .334 | 9.179 |
| 11 | 1315.000 | 1160.000 | 6.494 | 4305.087 | 3797.643 | 1.928 | 2.209 | 2.510 | 2.352 | .334 | 9.168 |

LOAD AND TORQUE DATA FOR 3/8 SQUARE BAR AT 900°C

| NO. | TOTAL MEASURED LOAD P IN KG | TOTAL MEASURED TORQUE G LB-IN | SHEAR YIELD STRESS FROM COOK-MCRUM $\bar{K}$ TON/IN | LOAD PER UNIT WIDTH DEFORMING ZONE P /$\bar{W}$ | TORQ PER UNIT WIDTH DEFORMING ZONE G /$\bar{W}$ | EXPERIMENTAL $\frac{P}{\bar{W}\bar{K}H_1}$ | EXPERIMENTAL $\frac{G}{\bar{W}\bar{K}H_1^2}$ | THEORETICAL $\frac{P}{\bar{W}\bar{K}H_1}$ | THEORETICAL $\frac{G}{\bar{W}\bar{K}H_1^2}$ | $\frac{H_1-H_2}{H_1}$ | STRAIN RATE |
|---|---|---|---|---|---|---|---|---|---|---|---|
| 1 | 235.000 | 113.000 | 3.686 | 3380.384 | 1625.461 | 1.764 | .729 | .571 | .187 | .056 | 2.863 |
| 2 | 552.000 | 500.000 | 5.249 | 2631.447 | 2383.557 | .964 | .750 | 1.123 | .620 | .165 | 5.013 |
| 3 | 908.000 | 937.000 | 5.714 | 3080.815 | 3179.211 | 1.037 | .919 | 1.398 | .897 | .227 | 5.964 |
| 4 | 1179.000 | 1272.000 | 5.631 | 3375.633 | 3641.904 | 1.153 | 1.069 | 1.568 | 1.083 | .267 | 6.518 |
| 5 | 1582.000 | 1619.000 | 6.266 | 4051.544 | 4146.302 | 1.244 | 1.093 | 1.694 | 1.227 | .296 | 6.904 |
| 6 | 1926.000 | 1940.000 | 6.255 | 4559.466 | 4592.609 | 1.402 | 1.213 | 1.790 | 1.340 | .318 | 7.200 |
| 7 | 2324.000 | 2288.000 | 6.462 | 5116.262 | 5037.008 | 1.523 | 1.288 | 1.879 | 1.446 | .339 | 7.462 |
| 8 | 2560.000 | 2242.000 | 6.438 | 5454.058 | 4776.562 | 1.630 | 1.226 | 1.913 | 1.488 | .347 | 7.562 |
| 9 | 2700.000 | 2600.000 | 6.484 | 5719.023 | 5507.207 | 1.607 | 1.403 | 1.915 | 1.489 | .348 | 7.581 |
| 10 | 2650.000 | 2580.000 | 6.483 | 5566.124 | 5419.094 | 1.652 | 1.381 | 1.927 | 1.504 | .351 | 7.606 |
| 11 | 2627.000 | 2545.000 | 6.475 | 5486.631 | 5315.369 | 1.630 | 1.356 | 1.936 | 1.516 | .353 | 7.629 |

LOAD AND TORQUE DATA FOR 1/2 SQUARE BAR AT 900°C

| NO. | TOTAL MEASURED LOAD P IN KG | TOTAL MEASURED TORQUE G LB-IN | SHEAR YIELD STRES FROM COOK -MCRUM K TON/IN | LOAD PER UNIT WIDTH DEFORMING ZONE P/$\bar{W}$ | TORQ PER UNIT WIDTH DEFORMING ZONE G/$\bar{W}$ | EXPERIMENTAL $\frac{P}{\bar{W}KH_1}$ | EXPERIMENTAL $\frac{G}{\bar{W}KH_1^2}$ | THEORETICAL $\frac{P}{\bar{W}KH_1}$ | THEORETICAL $\frac{G}{\bar{W}KH_1^2}$ | $\frac{H_1-H_2}{H_1}$ | STRAIN RATE |
|---|---|---|---|---|---|---|---|---|---|---|---|
| 1 | 371.000 | 228.000 | 3.752 | 3528.534 | 2168.479 | 1.364 | .543 | .518 | .157 | .064 | 2.623 |
| 2 | 823.000 | 749.000 | 4.738 | 3824.267 | 3480.408 | 1.171 | .690 | .799 | .341 | .130 | 3.803 |
| 3 | 1247.000 | 1327.000 | 5.252 | 4332.017 | 4609.933 | 1.196 | .824 | .957 | .467 | .172 | 4.418 |
| 4 | 1887.000 | 2047.000 | 5.680 | 4915.763 | 5332.573 | 1.255 | .882 | 1.147 | .636 | .226 | 5.129 |
| 5 | 2069.000 | 2607.000 | 5.953 | 4594.226 | 5788.858 | 1.119 | .913 | 1.277 | .760 | .264 | 5.586 |
| 6 | 2427.000 | 3147.000 | 6.126 | 4897.913 | 6350.941 | 1.159 | .973 | 1.363 | .846 | .289 | 5.880 |
| 7 | 2831.000 | 3610.000 | 6.211 | 5228.719 | 6667.493 | 1.221 | 1.008 | 1.449 | .935 | .314 | 6.159 |
| 8 | 3342.000 | 4205.000 | 6.420 | 5769.721 | 7259.628 | 1.303 | 1.062 | 1.520 | 1.009 | .335 | 6.392 |
| 9 | 3704.000 | 4573.000 | 6.450 | 6202.865 | 7658.127 | 1.395 | 1.115 | 1.551 | 1.043 | .345 | 6.493 |
| 10 | 3699.000 | 4651.000 | 6.428 | 6128.924 | 7706.305 | 1.383 | 1.126 | 1.565 | 1.057 | .349 | 6.535 |
| 11 | 3603.000 | 4575.000 | 6.431 | 5965.674 | 7575.064 | 1.345 | 1.106 | 1.563 | 1.055 | .348 | 6.530 |

LOAD AND TORQUE DATA FOR 5/8 SQUARE BAR AT 900 °C

| NO. | TOTAL MEASURED LOAD P IN KG | TOTAL MEASURED TORQUE G LB-IN | SHEAR YIELD STRES FROM COOK -MCRUM K TON/IN | LOAD PER UNIT WIDTH DEFORMING ZONE P / $\overline{W}$ | TORQ PER UNIT WIDTH DEFORMING ZONE G / $\overline{W}$ | EXPERIMENTAL $\frac{P}{\overline{W}KH_1}$ | EXPERIMENTAL $\frac{G}{\overline{W}KH_1^2}$ | THEORETICAL $\frac{P}{\overline{W}KH_1}$ | THEORETICAL $\frac{G}{\overline{W}KH_1^2}$ | $\frac{H_1-H_2}{H_1}$ | STRAIN RATE |
|---|---|---|---|---|---|---|---|---|---|---|---|
| 1 | 979.000 | 808.000 | 4.661 | 3989.407 | 3292.585 | .985 | .418 | .649 | .235 | .118 | 3.202 |
| 2 | 1282.000 | 1488.000 | 5.227 | 3606.299 | 4185.782 | .794 | .474 | .812 | .349 | .169 | 3.864 |
| 3 | 1890.000 | 2543.000 | 5.706 | 3884.035 | 5225.979 | .784 | .542 | .988 | .490 | .229 | 4.557 |
| 4 | 2362.000 | 3391.000 | 5.953 | 4183.033 | 6005.362 | .809 | .597 | 1.088 | .576 | .264 | 4.940 |
| 5 | 2806.000 | 4128.000 | 6.083 | 4420.743 | 6503.502 | .837 | .633 | 1.178 | .657 | .296 | 5.265 |
| 6 | 3316.000 | 4748.000 | 6.236 | 4797.491 | 6869.266 | .886 | .652 | 1.250 | .724 | .321 | 5.518 |
| 7 | 3732.000 | 5388.000 | 6.331 | 4956.506 | 7155.856 | .901 | .669 | 1.326 | .797 | .348 | 5.760 |
| 8 | 4198.000 | 5830.000 | 6.399 | 5507.300 | 7648.299 | .991 | .707 | 1.338 | .808 | .353 | 5.816 |
| 9 | 4298.000 | 5873.000 | 6.373 | 5688.455 | 7772.986 | 1.028 | .722 | 1.332 | .802 | .351 | 5.796 |
| 10 | 4143.000 | 5892.000 | 6.385 | 5493.413 | 7812.501 | .990 | .724 | 1.330 | .800 | .350 | 5.789 |
| 11 | 4143.000 | 5778.000 | 6.386 | 5473.623 | 7633.742 | .987 | .707 | 1.330 | .800 | .350 | 5.789 |

LOAD AND TORQUE DATA FOR 1/4 SQUARE BAR AT 1000 °C

| NO. | TOTAL MEASURED LOAD P IN KG | TOTAL MEASURED TORQUE G LB-IN | SHEAR YIELD STRES FROM COOK -MCRUM $\bar{K}$ TON/IN | LOAD PER UNIT WIDTH DEFORMING ZONE P /$\bar{W}$ | TORQ PER UNIT WIDTH DEFORMING ZONE G /$\bar{W}$ | EXPERIMENTAL $\frac{P}{\bar{W}\bar{K}H_1}$ | EXPERIMENTAL $\frac{G}{\bar{W}\bar{K}H_1^2}$ | THEORETICAL $\frac{P}{\bar{W}\bar{K}H_1}$ | THEORETICAL $\frac{G}{\bar{W}\bar{K}H_1^2}$ | $\frac{H_1-H_2}{H_1}$ | STRAIN RATE |
|---|---|---|---|---|---|---|---|---|---|---|---|
| 1 | 67.000 | 69.000 | 3.896 | 743.590 | 765.787 | .555 | .742 | 1.130 | .633 | .110 | 4.999 |
| 2 | 168.000 | 148.000 | 4.259 | 1461.329 | 1287.361 | .908 | 1.142 | 1.322 | .829 | .139 | 5.677 |
| 3 | 243.000 | 204.000 | 4.529 | 1642.636 | 1379.003 | 1.055 | 1.150 | 1.545 | 1.079 | .174 | 6.379 |
| 4 | 349.000 | 283.000 | 4.775 | 1951.801 | 1582.693 | 1.189 | 1.252 | 1.754 | 1.329 | .209 | 7.053 |
| 5 | 538.000 | 436.000 | 5.084 | 2351.217 | 1905.447 | 1.345 | 1.416 | 2.079 | 1.752 | .262 | 7.997 |
| 6 | 850.000 | 652.000 | 5.251 | 3219.698 | 2469.698 | 1.783 | 1.776 | 2.301 | 2.057 | .299 | 8.612 |
| 7 | 1136.000 | 848.000 | 5.392 | 3816.094 | 2848.634 | 2.059 | 1.996 | 2.490 | 2.325 | .330 | 9.105 |
| 8 | 1170.000 | 899.000 | 5.361 | 3856.524 | 2963.260 | 2.092 | 2.088 | 2.521 | 2.372 | .335 | 9.177 |
| 9 | 1214.000 | 1020.000 | 5.427 | 3821.940 | 3211.185 | 2.048 | 2.235 | 2.588 | 2.469 | .346 | 9.347 |
| 10 | 1134.000 | 970.000 | 5.432 | 3587.059 | 3068.296 | 1.921 | 2.133 | 2.589 | 2.469 | .347 | 9.360 |
| 11 | 1235.000 | 1030.000 | 5.403 | 3810.338 | 3177.853 | 2.051 | 2.221 | 2.623 | 2.525 | .352 | 9.398 |

LOAD AND TORQUE DATA FOR 3/8 SQUARE BAR AT 1000°C

| NO. | TOTAL MEASURED LOAD P IN KG | TOTAL MEASURED TORQUE G LB-IN | SHEAR YIELD STRESS FROM COOK-MCRUM $\bar{K}$ TON/IN | LOAD PER UNIT WIDTH DEFORMING ZONE P /$\bar{W}$ | TORQ PER UNIT WIDTH DEFORMING ZONE G /$\bar{W}$ | EXPERIMENTAL $\frac{P}{\bar{W}KH_1}$ | EXPERIMENTAL $\frac{G}{\bar{W}KH_1^2}$ | THEORETICAL $\frac{P}{\bar{W}KH_1}$ | THEORETICAL $\frac{G}{\bar{W}KH_1^2}$ | $\frac{H_1-H_2}{H_1}$ | STRAIN RATE |
|---|---|---|---|---|---|---|---|---|---|---|---|
| 1 | 458.000 | 87.000 | 4.420 | 2145.580 | 407.567 | .934 | .152 | 1.147 | .643 | .170 | 5.103 |
| 2 | 562.000 | 384.000 | 4.642 | 2171.265 | 1483.569 | .900 | .528 | 1.289 | .783 | .202 | 5.604 |
| 3 | 707.000 | 706.000 | 4.865 | 2370.285 | 2366.933 | .937 | .804 | 1.411 | .910 | .230 | 6.013 |
| 4 | 889.000 | 953.000 | 5.015 | 2547.928 | 2731.355 | .977 | .900 | 1.572 | 1.087 | .268 | 6.543 |
| 5 | 1138.000 | 1233.000 | 5.075 | 2920.608 | 3164.420 | 1.107 | 1.030 | 1.700 | 1.232 | .298 | 6.949 |
| 6 | 1415.000 | 1431.000 | 5.270 | 3338.966 | 3376.721 | 1.219 | 1.059 | 1.800 | 1.350 | .321 | 7.239 |
| 7 | 1623.000 | 1665.000 | 5.374 | 3666.471 | 3761.352 | 1.313 | 1.157 | 1.853 | 1.413 | .333 | 7.397 |
| 8 | 1751.000 | 1799.000 | 5.395 | 3840.551 | 3945.831 | 1.369 | 1.208 | 1.886 | 1.454 | .341 | 7.501 |
| 9 | 2086.000 | 2093.000 | 5.411 | 4355.034 | 4369.648 | 1.548 | 1.334 | 1.950 | 1.532 | .356 | 7.666 |
| 10 | 2145.000 | 2178.000 | 5.406 | 4456.998 | 4525.567 | 1.586 | 1.383 | 1.953 | 1.536 | .357 | 7.676 |
| 11 | 2145.000 | 2151.000 | 5.418 | 4449.071 | 4461.516 | 1.580 | 1.361 | 1.944 | 1.524 | .355 | 7.659 |

LOAD AND TORQUE DATA FOR 1/2 SQUARE BAR AT 1000 °C

| NO. | TOTAL MEASURED LOAD P IN KG | TOTAL MEASURED TORQUE G LB-IN | SHEAR YIELD STRES FROM COOK -MCRUM $\bar{K}$ TON/IN | LOAD PER UNIT WIDTH DEFORMING ZONE P / $\bar{W}$ | TORQ PER UNIT WIDTH DEFORMING ZONE G / $\bar{W}$ | EXPERIMENTAL $\frac{P}{\bar{W}\bar{K}H_1}$ | EXPERIMENTAL $\frac{G}{\bar{W}\bar{K}H_1^2}$ | THEORETICAL $\frac{P}{\bar{W}\bar{K}H_1}$ | THEORETICAL $\frac{G}{\bar{W}\bar{K}H_1^2}$ | $\frac{H_1-H_2}{H_1}$ | STRAIN RATE |
|---|---|---|---|---|---|---|---|---|---|---|---|
| 1 | 627.000 | 590.000 | 4.081 | 2698.743 | 2539.487 | .959 | .584 | .838 | .370 | .140 | 3.960 |
| 2 | 823.000 | 911.000 | 4.428 | 2759.452 | 3054.508 | .904 | .648 | .977 | .484 | .178 | 4.496 |
| 3 | 1214.000 | 1438.000 | 4.785 | 3098.318 | 3670.001 | .939 | .720 | 1.161 | .650 | .230 | 5.180 |
| 4 | 1537.000 | 2004.000 | 4.952 | 3383.347 | 4411.339 | .991 | .836 | 1.282 | .766 | .265 | 5.605 |
| 5 | 1802.000 | 2325.000 | 5.098 | 3576.874 | 4615.002 | 1.018 | .850 | 1.379 | .863 | .294 | 5.933 |
| 6 | 2264.000 | 2870.000 | 5.195 | 4008.115 | 5080.958 | 1.119 | .918 | 1.493 | .981 | .328 | 6.307 |
| 7 | 2470.000 | 3062.000 | 5.240 | 4139.223 | 5131.296 | 1.146 | .920 | 1.549 | 1.041 | .344 | 6.482 |
| 8 | 2697.000 | 3403.000 | 5.265 | 4410.293 | 5564.786 | 1.215 | .993 | 1.574 | 1.067 | .351 | 6.564 |
| 9 | 2623.000 | 3430.000 | 5.280 | 4329.776 | 5661.888 | 1.189 | 1.007 | 1.566 | 1.058 | .349 | 6.538 |
| 10 | 2662.000 | 3492.000 | 5.287 | 4336.401 | 5688.473 | 1.190 | 1.010 | 1.581 | 1.074 | .353 | 6.585 |
| 11 | 2766.000 | 3519.000 | 5.285 | 4416.105 | 5618.320 | 1.212 | .998 | 1.601 | 1.097 | .360 | 6.650 |

LOAD AND TORQUE DATA FOR 5/8 SQUARE BAR AT 1000°C

| NO. | TOTAL MEASURED LOAD P IN KG | TOTAL MEASURED TORQUE G LB-IN | SHEAR YIELD STRES FROM COOK -MCRUM $\bar{K}$ TON/IN | LOAD PER UNIT WIDTH DEFORMING ZONE P / $\bar{W}$ | TORQ PER UNIT WIDTH DEFORMING ZONE G / $\bar{W}$ | EXPERIMENTAL $\frac{P}{\bar{W}\bar{K}H_1}$ | EXPERIMENTAL $\frac{G}{\bar{W}\bar{K}H_1^2}$ | THEORETICAL $\frac{P}{\bar{W}\bar{K}H_1}$ | THEORETICAL $\frac{G}{\bar{W}\bar{K}H_1^2}$ | $\frac{H_1-H_2}{H_1}$ | STRAIN RATE |
|---|---|---|---|---|---|---|---|---|---|---|---|
| 1 | 767.000 | 808.000 | 3.941 | 2795.706 | 2945.150 | .817 | .442 | .694 | .264 | .132 | 3.391 |
| 2 | 1037.000 | 1145.000 | 4.301 | 2929.409 | 3234.497 | .784 | .445 | .810 | .347 | .169 | 3.866 |
| 3 | 1503.000 | 1927.000 | 4.755 | 3086.088 | 3956.681 | .747 | .492 | .987 | .488 | .228 | 4.561 |
| 4 | 1948.000 | 2585.000 | 4.873 | 3417.179 | 4534.604 | .807 | .551 | 1.095 | .582 | .266 | 4.963 |
| 5 | 1145.000 | 3128.000 | 5.023 | 1853.072 | 5062.366 | .425 | .596 | 1.154 | .635 | .287 | 5.179 |
| 6 | 2609.000 | 3720.000 | 5.145 | 3734.773 | 5325.165 | .836 | .612 | 1.258 | .731 | .324 | 5.545 |
| 7 | 3015.000 | 4263.000 | 5.158 | 4030.365 | 5698.655 | .900 | .654 | 1.320 | .790 | .346 | 5.754 |
| 8 | 3211.000 | 4488.000 | 5.153 | 4124.998 | 5765.491 | .922 | .662 | 1.355 | .824 | .359 | 5.872 |
| 9 | 3264.000 | 4651.000 | 5.260 | 4213.036 | 6003.318 | .922 | .675 | 1.353 | .822 | .358 | 5.868 |
| 10 | 3211.000 | 4651.000 | 5.261 | 4144.465 | 6003.085 | .907 | .675 | 1.353 | .822 | .358 | 5.867 |
| 11 | 3211.000 | 4650.000 | 5.252 | 4115.220 | 5959.443 | .902 | .671 | 1.357 | .826 | .359 | 5.881 |

LOAD AND TORQUE DATA FOR 1/4 SQUARE BAR AT 1100 °C

| NO. | TOTAL MEASURED LOAD P IN KG | TOTAL MEASURED TORQUE G LB-IN | SHEAR YIELD STRES FROM COOK-MCRUM $\bar{K}$ TON/IN | LOAD PER UNIT WIDTH DEFORMING ZONE P / $\bar{W}$ | TORQ PER UNIT WIDTH DEFORMING ZONE G / $\bar{W}$ | EXPERIMENTAL $\frac{P}{\bar{W}\bar{K}H_1}$ | EXPERIMENTAL $\frac{G}{\bar{W}\bar{K}H_1^2}$ | THEORETICAL $\frac{P}{\bar{W}\bar{K}H_1}$ | THEORETICAL $\frac{G}{\bar{W}\bar{K}H_1^2}$ | $\frac{H_1-H_2}{H_1}$ | STRAIN RATE |
|---|---|---|---|---|---|---|---|---|---|---|---|
| 1 | 102.000 | 82.000 | 2.879 | 1197.165 | 962.426 | 1.210 | 1.263 | 1.093 | .596 | .105 | 4.928 |
| 2 | 168.000 | 146.000 | 3.201 | 1433.937 | 1246.159 | 1.303 | 1.470 | 1.345 | .850 | .144 | 5.807 |
| 3 | 251.000 | 208.000 | 3.366 | 1759.045 | 1457.695 | 1.520 | 1.635 | 1.514 | 1.038 | .171 | 6.373 |
| 4 | 336.000 | 270.000 | 3.630 | 1959.282 | 1574.423 | 1.570 | 1.638 | 1.699 | 1.256 | .201 | 6.958 |
| 5 | 485.000 | 414.000 | 3.853 | 2186.095 | 1866.069 | 1.650 | 1.829 | 2.025 | 1.670 | .255 | 7.932 |
| 6 | 774.000 | 617.000 | 4.026 | 3011.768 | 2400.854 | 2.176 | 2.252 | 2.259 | 1.988 | .294 | 8.585 |
| 7 | 891.000 | 627.000 | 4.005 | 3261.395 | 2295.056 | 2.368 | 2.164 | 2.336 | 2.093 | .307 | 8.809 |
| 8 | 1009.000 | 732.000 | 4.056 | 3513.150 | 2548.688 | 2.520 | 2.374 | 2.414 | 2.203 | .320 | 9.018 |
| 9 | 860.000 | 775.000 | 4.257 | 2700.590 | 2433.671 | 1.845 | 2.159 | 2.604 | 2.497 | .349 | 9.355 |
| 10 | 1024.000 | 845.000 | 4.247 | 3147.725 | 2597.488 | 2.156 | 2.310 | 2.639 | 2.549 | .354 | 9.440 |
| 11 | 962.000 | 775.000 | 4.261 | 2988.058 | 2407.219 | 2.040 | 2.134 | 2.622 | 2.523 | .351 | 9.396 |

LOAD AND TORQUE DATA FOR 3/8 SQUARE BAR AT 1100°C

| NO. | TOTAL MEASURED LOAD P IN KG | TOTAL MEASURED TORQUE G LB-IN | SHEAR YIELD STRES FROM COOK -MCRUM $\bar{K}$ TON/IN | LOAD PER UNIT WIDTH DEFORMING ZONE P / $\bar{W}$ | TORQ PER UNIT WIDTH DEFORMING ZONE G / $\bar{W}$ | EXPERIMENTAL $\frac{P}{\bar{W}\bar{K}H_1}$ | EXPERIMENTAL $\frac{G}{\bar{W}\bar{K}H_1^2}$ | THEORETICAL $\frac{P}{\bar{W}\bar{K}H_1}$ | THEORETICAL $\frac{G}{\bar{W}\bar{K}H_1^2}$ | $\frac{H_1-H_2}{H_1}$ | STRAIN RATE |
|---|---|---|---|---|---|---|---|---|---|---|---|
| 1 | 370.000 | 307.000 | 3.183 | 2006.263 | 1664.656 | 1.213 | .864 | 1.049 | .550 | .149 | 4.766 |
| 2 | 485.000 | 416.000 | 3.252 | 2325.469 | 1994.629 | 1.376 | 1.013 | 1.131 | .627 | .167 | 5.064 |
| 3 | 741.000 | 732.000 | 3.657 | 2564.266 | 2533.121 | 1.349 | 1.145 | 1.387 | .884 | .226 | 5.963 |
| 4 | 977.000 | 1002.000 | 3.720 | 2806.091 | 2877.895 | 1.451 | 1.278 | 1.574 | 1.087 | .269 | 6.571 |
| 5 | 1179.000 | 1233.000 | 3.867 | 3051.962 | 3191.746 | 1.518 | 1.364 | 1.693 | 1.223 | .297 | 6.943 |
| 6 | 1349.000 | 1439.000 | 4.019 | 3211.079 | 3425.309 | 1.537 | 1.408 | 1.793 | 1.340 | .320 | 7.244 |
| 7 | 1752.000 | 1697.000 | 4.019 | 3851.025 | 3730.131 | 1.843 | 1.533 | 1.894 | 1.461 | .344 | 7.539 |
| 8 | 1988.000 | 1879.000 | 4.027 | 4268.823 | 4034.768 | 2.039 | 1.655 | 1.918 | 1.490 | .349 | 7.617 |
| 9 | 1513.000 | 1627.000 | 4.106 | 3176.991 | 3416.367 | 1.489 | 1.375 | 1.942 | 1.520 | .355 | 7.675 |
| 10 | 1534.000 | 1588.000 | 4.100 | 3223.484 | 3336.957 | 1.513 | 1.345 | 1.950 | 1.532 | .356 | 7.677 |
| 11 | 1530.000 | 1580.000 | 4.097 | 3186.422 | 3290.553 | 1.496 | 1.327 | 1.953 | 1.536 | .357 | 7.683 |

LOAD AND TORQUE DATA FOR 1/2 SQUARE BAR AT 1100 °C

| NO. | TOTAL MEASURED LOAD P IN KG | TOTAL MEASURED TORQUE G LB-IN | SHEAR YIELD STRES FROM COOK -MCRUM $\bar{K}$ TON/IN | LOAD PER UNIT WIDTH DEFORMING ZONE P /$\bar{W}$ | TORQ PER UNIT WIDTH DEFORMING ZONE G /$\bar{W}$ | EXPERIMENTAL $\frac{P}{\bar{W}\bar{K}H_1}$ | EXPERIMENTAL $\frac{G}{\bar{W}\bar{K}H_1^2}$ | THEORETICAL $\frac{P}{\bar{W}\bar{K}H_1}$ | THEORETICAL $\frac{G}{\bar{W}\bar{K}H_1^2}$ | $\frac{H_1-H_2}{H_1}$ | STRAIN RATE |
|---|---|---|---|---|---|---|---|---|---|---|---|
| 1 | 607.000 | 525.000 | 3.072 | 2561.877 | 2215.791 | 1.209 | .677 | .850 | .380 | .143 | 4.008 |
| 2 | 776.000 | 821.000 | 3.372 | 2400.808 | 2540.030 | 1.033 | .707 | 1.031 | .531 | .193 | 4.700 |
| 3 | 1147.000 | 1297.000 | 3.620 | 2865.828 | 3240.609 | 1.148 | .841 | 1.178 | .665 | .235 | 5.240 |
| 4 | 1430.000 | 1644.000 | 3.721 | 3106.046 | 3570.866 | 1.211 | .901 | 1.293 | .777 | .268 | 5.636 |
| 5 | 1618.000 | 1991.000 | 3.862 | 3159.827 | 3888.267 | 1.187 | .945 | 1.392 | .877 | .298 | 5.973 |
| 6 | 1687.000 | 1440.000 | 3.969 | 2944.278 | 2513.195 | 1.076 | .595 | 1.506 | .995 | .331 | 6.343 |
| 7 | 2360.000 | 2827.000 | 4.014 | 3928.945 | 4706.410 | 1.420 | 1.101 | 1.551 | 1.042 | .345 | 6.494 |
| 8 | 2441.000 | 2956.000 | 4.035 | 4044.255 | 4897.508 | 1.454 | 1.140 | 1.561 | 1.053 | .348 | 6.526 |
| 9 | 2034.000 | 2674.000 | 4.033 | 3314.808 | 4357.815 | 1.192 | 1.015 | 1.576 | 1.069 | .352 | 6.564 |
| 10 | 2108.000 | 2751.000 | 4.022 | 3371.806 | 4400.303 | 1.216 | 1.027 | 1.597 | 1.092 | .358 | 6.629 |
| 11 | 2055.000 | 2674.000 | 4.032 | 3320.054 | 4320.109 | 1.194 | 1.006 | 1.584 | 1.078 | .354 | 6.590 |

LOAD AND TORQUE DATA FOR 5/8 SQUARE BAR AT 1100°c

| NO. | TOTAL MEASURED LOAD P IN KG | TOTAL MEASURED TORQUE G LB-IN | SHEAR YIELD STRES FROM COOK -MCRUM $\bar{K}$ TON/IN | LOAD PER UNIT WIDTH DEFORMING ZONE P / $\bar{W}$ | TORQ PER UNIT WIDTH DEFORMING ZONE G / $\bar{W}$ | EXPERIMENTAL $\frac{P}{\bar{W}\bar{K}H_1}$ | EXPERIMENTAL $\frac{G}{\bar{W}\bar{K}H_1^2}$ | THEORETICAL $\frac{P}{\bar{W}\bar{K}H_1}$ | THEORETICAL $\frac{G}{\bar{W}\bar{K}H_1^2}$ | $\frac{H_1-H_2}{H_1}$ | STRAIN RATE |
|---|---|---|---|---|---|---|---|---|---|---|---|
| 1 | 642.000 | 640.000 | 2.899 | 2328.555 | 2321.301 | .925 | .474 | .684 | .258 | .129 | 3.340 |
| 2 | 945.000 | 1103.000 | 3.197 | 2642.162 | 3083.920 | .952 | .571 | .817 | .353 | .171 | 3.898 |
| 3 | 1269.000 | 1515.000 | 3.546 | 2562.386 | 3059.114 | .832 | .510 | 1.003 | .501 | .234 | 4.621 |
| 4 | 1451.000 | 2042.000 | 3.717 | 2520.312 | 3546.848 | .781 | .565 | 1.105 | .590 | .270 | 5.000 |
| 5 | 1836.000 | 2518.000 | 3.810 | 2839.621 | 3894.425 | .868 | .605 | 1.195 | .672 | .301 | 5.323 |
| 6 | 1984.000 | 2903.000 | 3.943 | 2811.723 | 4114.129 | .821 | .617 | 1.272 | .745 | .329 | 5.594 |
| 7 | 2295.000 | 3242.000 | 3.996 | 3055.912 | 4316.892 | .881 | .639 | 1.327 | .797 | .349 | 5.782 |
| 8 | 2531.000 | 3662.000 | 3.971 | 3231.863 | 4676.049 | .937 | .697 | 1.363 | .832 | .362 | 5.902 |
| 9 | 2538.000 | 3729.000 | 3.969 | 3231.959 | 4748.611 | .938 | .708 | 1.366 | .835 | .362 | 5.899 |
| 10 | 2507.000 | 3798.000 | 3.977 | 3168.521 | 4800.177 | .917 | .714 | 1.372 | .842 | .364 | 5.912 |
| 11 | 2643.000 | 3721.000 | 3.983 | 3331.836 | 4690.792 | .963 | .697 | 1.379 | .848 | .367 | 5.934 |

LOAD AND TORQUE DATA FOR 5/8 SQUARE BAR AT 1200 °C

| NO. | TOTAL MEASURED LOAD P IN KG | TOTAL MEASURED TORQUE G LB-IN | SHEAR YIELD STRESS FROM COOK -MCRUM $\bar{K}$ TON/IN | LOAD PER UNIT WIDTH DEFORMING ZONE P / $\bar{W}$ | TORQ PER UNIT WIDTH DEFORMING ZONE G / $\bar{W}$ | EXPERIMENTAL $\frac{P}{\bar{W}\bar{K}H_1}$ | EXPERIMENTAL $\frac{G}{\bar{W}\bar{K}H_1^2}$ | THEORETICAL $\frac{P}{\bar{W}\bar{K}H_1}$ | THEORETICAL $\frac{G}{\bar{W}\bar{K}H_1^2}$ | $\frac{H_1-H_2}{H_1}$ | STRAIN RATE |
|---|---|---|---|---|---|---|---|---|---|---|---|
| 1 | 698.000 | 921.000 | 2.512 | 1895.835 | 2501.524 | .865 | .585 | .836 | .367 | .176 | 3.971 |
| 2 | 863.000 | 1281.000 | 2.708 | 1701.446 | 2525.554 | .720 | .547 | 1.020 | .517 | .238 | 4.685 |
| 3 | 1133.000 | 1727.000 | 2.829 | 1918.066 | 2923.655 | .777 | .607 | 1.127 | .610 | .275 | 5.077 |
| 4 | 1265.000 | 2167.000 | 2.954 | 1917.493 | 3284.748 | .745 | .653 | 1.215 | .691 | .306 | 5.392 |
| 5 | 1449.000 | 2403.000 | 3.002 | 2035.725 | 3376.016 | .778 | .660 | 1.284 | .757 | .330 | 5.633 |
| 6 | 1864.000 | 2791.000 | 3.010 | 2444.204 | 3659.750 | .931 | .714 | 1.347 | .817 | .352 | 5.847 |
| 7 | 1864.000 | 2896.000 | 2.996 | 2392.157 | 3716.571 | .916 | .729 | 1.369 | .839 | .360 | 5.921 |
| 8 | 1708.000 | 2907.000 | 2.990 | 2145.175 | 3651.068 | .823 | .717 | 1.391 | .860 | .368 | 5.992 |